Worcester Polytechnic Institute
Digital WPI

Doctoral Dissertations (All Dissertations, All Years) | Electronic Theses and Dissertations

2003-10-10

Ultrasonic Technique in Determination of Grid-Generated Turbulent Flow Characteristics

Tatiana A. Andreeva
Worcester Polytechnic Institute

Follow this and additional works at: https://digitalcommons.wpi.edu/etd-dissertations

Repository Citation
Andreeva, T. A. (2003). *Ultrasonic Technique in Determination of Grid-Generated Turbulent Flow Characteristics*. Retrieved from https://digitalcommons.wpi.edu/etd-dissertations/392

This dissertation is brought to you for free and open access by Digital WPI. It has been accepted for inclusion in Doctoral Dissertations (All Dissertations, All Years) by an authorized administrator of Digital WPI. For more information, please contact wpi-etd@wpi.edu.

ULTRASONIC TECHNIQUE IN DETERMINATION OF GRID-GENERATED TURBULENT FLOW CHARACTERISTICS

by

Tatiana A. Andreeva

A Dissertation

submitted to the Faculty of the

WORCESTER POLYTECHNIC INSTITUTE

in partial fulfillment of the requirements for the

Degree of Doctor of Philosophy

in

Mechanical Engineering

by

_____

Tatiana A. Andreeva

October, 2003

Approved:

_____

Dr. William W. Durgin, Advisor

_____

Dr. Mikhail F. Dimentberg, Committee Member

_____

Dr. Zhikun Hou, Graduate Committee Representative

_____

Dr. David J. Olinger, Committee Member

_____

Dr. Suzanne L. Weekes, Committee Member

Abstract

The present study utilizes the ultrasonic travel-time technique to diagnose grid-generated turbulence. The statistics of the travel-time variations of ultrasonic wave propagation along a path are used to determine some metrics of the turbulence. The motivation for this work stems from the observation of substantial delta-t variation in ultrasonic measuring devices like flow meters and circulation meters. Typically, averaging can be used to extract mean values from such time series. The corollary is that the fluctuations contain information about the turbulence.

Experimental data were obtained for ultrasonic wave propagation downstream of a heated grid in a wind tunnel. Such grid-generated turbulence is well characterized and features a mean flow with superimposed velocity and temperature fluctuations. The ultrasonic path could be perpendicular or oblique to the mean flow direction. Path lengths were of the order of 0.3 m and the transducers were of 100 kHz working frequency. The data acquisition and control system featured a very high-speed analog to digital conversion card that enabled excellent resolution of ultrasonic signals.

Experimental data for the travel-time variance were validated using ray acoustic theory along with the Kolmogorov "2/3" law. It is demonstrated that the ultrasonic technique, together with theoretical models, provides a basis for turbulent flow diagnostics. As a result, the structure constant appearing in the Kolmogorov "2/3" law is determined based on the experimental data.

The effect of turbulence on acoustic waves, in terms of the travel time, was studied for various mean velocities and for different angular orientations of the acoustic waves

with respect to the mean flow. Average travel time in the presence of turbulence was shorter then in the undisturbed media. The effect of the time shift between the travel times in turbulent and undisturbed media is associated with Fermat's principle.

The travel time and log-amplitude variance of acoustic waves were investigated as functions of travel distance and mean velocity over a range of Reynolds number varying from 4000 to 20000. Experimental data are interpreted using classical ray acoustic approach and the parabolic acoustic equation approach together with the perturbation method. It was experimentally demonstrated that there is a strong dependence of the travel time on the mean velocity even in the case where the propagation of acoustic waves is perpendicular to the mean velocity. The effect of thermal fluctuations, which result in fluctuations of sound speed, was studied for two temperatures of the grid: $59^{\circ}F$ (no grid heating) and $159^{\circ}F$. A semi analytical acoustic propagation model that allows determination of the spacial correlation functions of flow field is developed based on the classical flow meter equation and statistics of the travel time of acoustic waves traveling through the velocity and the thermal turbulence. The basic flow meter equation is reconsidered in order to take into account sound speed fluctuations and turbulent velocity. The resulting equation is written in terms of correlation functions of travel time, sound speed fluctuation and turbulent velocity fluctuations. Experimentally measured travel time statistics data with and without grid heating are approximated by Gaussian function and used to solve the integral flow meter equation in terms of correlation functions analytically.

Acknowledgements

I would like to express my deepest gratitude to my advisor, Professor William W. Durgin. His knowledge and guidance inspired me to continue my education and try to reach far beyond the level that I have now and had before. I would like to thank him for his personal support, trust, and understanding throughout these years. Financial support that he provided is deeply appreciated.

I would like to thank my entire committee Professor Zhikun Hou, Professor David J. Olinger, Professor Suzanne L. Weekes, and especially Professor Mikhail F. Dimentberg, who provided invaluable feedback during this work.

I would like to thank Professor Vladimir Palmov for his contribution to this work.

I would like to thank the following people for their assistance and support: Barbara Furhman, Janice Dresser, Pam St. Louis, Gail Hayes, Nancy Hickman, Siamak Najafi, Frank Weber.

I would like to express my admiration to Barbara Edilberti for her friendship and moral support.

My thanks are extended to all my friends outside the school.

My special gratitude to my mother. Her love and belief in me lit the path for me throughout my life.

And lastly, my very special thanks to my husband, Daniil, for his profound and unconditional love. I would not have been able to complete this work without his support.

Table of Contents

List of Figures

List of Tables

Nomenclature

B(u)	Probability density function
c	Speed of sound
C_{eff}	Effective structure parameter
C_u^2	Structure function parameter
c_v, c_p	Specific heats at constant volume and constant pressure
$D(t_1, t_2)$	Structure function of a random process
D	Rod diameter
e	Internal energy
E_t	Specific energy
k	Wave number
K	Correlation function
L	Travel distance
L_0	Integral length scale
l_ε	Characteristic inhomogenuity size
l	Current length scale
l_G	Gaussian length scale
l_v	Von Karman scale
M	Grid size
$M(t_1, t_2)$	Joint moment
r	Distance between the observation points
$\overline{\overline{\mathbf{P}}}$	Pressure tensor

p_{ij}	Components of stress tensor
Pr	Prandtl number
$\mathbf{q}$	Heat addition per unit mass
R	Gas constant
Re	Reynolds number
s	Distance along a beam
S	Entropy
t	Travel time
T	Mean temperature
$\overline{\overline{\mathbf{T}}}$	Stress tensor
U	$x-$component of mean velocity
$u(t)$	$x-$component of velocity at a fixed instant of time
$v(x,\mathbf{r})$	Complex wave amplitude
V_f	Phase velocity of a wave
v_K	Kolmogorov velocity scale
Vol	Specific volume
w	Enthalpy
W	Eikonal
α	Mean dissipation rate of turbulent kinetic energy
β	Coefficient of thermal expansion of air
$\left\langle \chi^2 \right\rangle$	Variance of the log-amplitude of a wave
ε	Index of refraction of sound waves
x,y,z	Components of Cartesian position vector

$\langle \phi^2 \rangle$	Variance of phase fluctuations of a wave
$\Phi(\omega)$	Spectral density
Φ_{eff}	3-D spectral density of a random field or an effective function
Π	Velocity potential
γ	Ratio of specific heats c_p / c_v
η	Kolmogorov microscale
λ	Wave length
λ_T	Taylor microscale
μ_v	Viscosity coefficient
ν	Kinematic viscousity
$\nu(x, y, z)$	Complex wave amplitude
κ	Thermal diffusivity
Æ	Thermal conductivity
ρ	Density
τ_{ij}	Components of viscous stress tensor
τ_k	Kolmogorov time scale
σ^2	Variance
ω	Frequency of the sound wave

Superscripts

'	Turbulent fluctuations

Subscripts

0	Ambient, undisturbed state of the medium

Chapter 1. Introduction

This research investigates the influence of heated and non-heated grid-generated turbulent flow on acoustic wave propagation. An acoustic wave carries some structural information of the turbulent medium as a result of interaction with the medium so thus it is possible to use some statistical characteristics of the acoustic wave as a diagnostic tool to obtain some statistical information about the medium. Our interest in studying the acoustic waves moving in a turbulent media is predicated on the fact that this problem is found in many practical problems of atmospheric and oceanic acoustics and aeroacoustics. Among these problems are noise pollution near highways, airports and factories; acoustic remote sensing and tomography of the atmosphere and ocean; detection, ranging and recognition of helicopters, aeroplanes, rockets and explosive sources; and the study of noise emitted by nozzles and exhaust pipes.

The motivation of this study is recognition of the fact that ultrasonic technology is evolving rapidly and technical advances offering great potential for performing experimental investigations of statistical characteristics of turbulence in laboratory conditions with high precision and non-invasively. Measuring flow parameters in turbulent medium non-invasively and rapidly by means of ultrasound dating back to experiments performed by Schmidt in 1970; demonstrated that ultrasonic flowmeters provide many potential advantages over traditional techniques. The transit-time method is the most widely used technique for ultrasonic flow metering. The principle is based on modification of the time of flight of the ultrasound by the fluid velocity along the line of

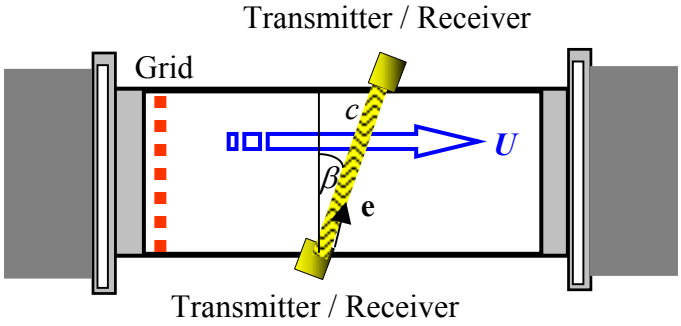

Figure 1.1 Ultrasonic flowmeter.

the flight path between the two ultrasonic transducers as shown in Figure 1. The basic flowmeter equation is

$$\int_R^T dt = \int_R^T \frac{ds}{c + \mathbf{u}\cdot\mathbf{e}} = \int_R^T \frac{ds}{c+u} \quad \text{where } u = U\sin\beta + u'. \qquad (1.1)$$

The transit times and the differential time of flight are functions of the fluid velocity. Therefore this method results in measurement of very short time delays of about a few nanoseconds. Advances in computing capabilities offer prospects for utilizing the ultrasonic technique in turbulent flow diagnostics in laboratory conditions.

The first objective of the work is to apply travel-time ultrasonic technique for data acquisition in the grid-generated turbulence produced in a wind tunnel. This work expands the previous experimental work by *Weber* [1994] that utilized the ray trace method to examine the effect of flow turbulence on sound waves propagation across a velocity field.

The second objective is to implement two basic approaches of theory of sound wave propagation in moving inhomogeneous media for data interpretation, the classical ray acoustic approach, and modern, parabolic equation approach. Using these two approaches

for interpretation of experimental measurements of travel time and wave amplitude an investigation of the effect of turbulence on ultrasound wave propagation was conducted. The work also demonstrates that combination of ultrasonic technique with one of the theoretical models can be used to perform flow diagnostics.

Despite the advances in computing technology and consequently improvements in measuring travel-time, ultrasonic flowmeter accuracy has not improved very much at all. The explanation may lay in the effect of turbulence on ultrasound waves, namely velocity and density fluctuations. To examine this possibility, the basic ultrasonic flowmeter equation is reconsidered, where the effects of turbulent velocity and sound speed fluctuations are included. The result is an integral equation in terms of correlation functions of travel time, turbulent velocity and sound speed fluctuations. The third objective is to develop an acoustic propagation model that allows determination of the spatial correlation functions of travel time, turbulent velocity, sound speed fluctuations and their spectra based on measured experimentally travel-time, thus identifying the effect of sound speed fluctuations.

The intention to utilize ultrasonic methodology for turbulent flow diagnostics is also motivated by the difficulty of obtaining laboratory measurements of time-of-flight variance indicated by the dearth of data. Although a large number of atmospheric measurements were made, they suffered from a lack of reliability and accuracy in addition to poor characterization of the turbulence. The problem of travel-time fluctuations is equivalent to the problem of finding the auto-correlation functions of these fluctuations, which involves enormous amounts of experimental data and a large amount of computational work. From the point of view of repeatability of experiments, it is much

more complicated and time-consuming to conduct outdoor experiments as compared to those performed under convenient laboratory conditions. On the other hand, current ultrasonic flow metering technology benefits from simple design and ease of operation assuring high measurement precision.

1.1 Theoretical, Computational and Experimental Issues in a Theory of Sound Propagation in a Moving Random Media

Our interest is concentrated on the effect of turbulence on sound wave propagation. The random changes of velocity and temperature produced by turbulence are very rapid and affect the sound propagation. This area of research lies on the boundary between acoustics and aerodynamics. The present research is a result of experimental and theoretical approaches. The literature review presents both classical and new results of the theory of sound propagation in media with random inhomogeneities of sound speed, density and medium velocity.

1.1.1 Review of Theoretical Investigations

The classical theory of wave propagation in turbulent media considers wave propagation in isotropic or locally isotropic and homogeneous random media and based on statistical representation of the turbulence [*Chernov*, 1960; *Tatrskii*, 1961, 1971; *Ishimaru*, 1978]. The statistical moments of phase and log-amplitude fluctuations of a sound wave propagating in the turbulent atmosphere have been calculated by *Tatarskii* [1961] using the ray approximation and the Rytov method [*Monin and Yaglom*, 1981; *Brown and Hall*, 1978]. Ray acoustics have been a standard approach for rigorous consideration of sound wave parameters for outdoor experiments. The main advantages

of the ray theory of wave propagation are the clarity of its physics and relative simplicity. The main results of geometrical acoustics were obtained before the mid-1940s and summarized in the book by *Blokhintzev* [1953]. Nevertheless, until recently there was no detailed treatment of geometrical acoustics in an inhomogeneous moving medium. The main ideas are systematically reviewed in monograph by *Ostashev* [1997]. However, in most cases, all scales of heterogeneities must be considered and mathematical conditions for ray solutions are seldom met outdoors. Moreover, for example, in statistical tomography in seismic media, all scales of heterogeneities are present so that scattering occurs rapidly and geometrical optics fails [*Samuelides*, 1998; *Iooss*, 2000].

The modern theory of sound propagation in a moving random medium has been developing intensively since mid-1980s. The governing system of linearized system of equations of fluid dynamics, which allows description of the propagation of sound waves in moving media, is rather complicated. Scientists have been trying to reduce it to a single equation using various approximations and assumptions about a moving medium. The most widely used single equation approaches in atmospheric acoustics are: Monin's equation [*Tatarskii*, 1961], Pierce's equation [*Pierce*, 1990], parabolic equation [*Rytov et al.*, 1978]. The statistical characteristics of sound waves propagating in a moving random medium with an arbitrary state equation have been calculated by the ray acoustics method, Rytov and parabolic-equation methods. Efforts focusing on the stochastic Helmholtz equation and its parabolic approximation are especially of interest.

The parabolic equation method is a very powerful method in the theory of wave propagation. In certain cases it allows significant simplification of an analytical or numerical solution of the problem. For describing acoustics in a moving medium, several

parabolic wave equations have been obtained [*Godin*, 1987; *Nghiem-Phu and Tappert*, 1985, *Ostashev*, 1987, *Robertson et al.*, 1985]. In this approach the small perturbation method is the most used solution to the parabolic approximation [*Rytov et al.*, 1978; *Ostashev*, 1997; *Samueldis*, 1998]. *Clifford and Lataitis* [1983] used the Rytov method to calculate phase and log-amplitude fluctuations of the direct and ground-reflected waves due to refractive index fluctuations. They followed *Tatarskii*, who considered the case, when refractive index fluctuations are caused by temperature fluctuations. Furthermore, *Clifford and Lataitis* calculated mean squared sound pressure by an energy conserving approach. They presented a formula for mean squared sound pressure for a Gaussian correlation function of refractive index fluctuations. These results made a significant contribution to the development of atmospheric acoustics. Since the publication by *Clifford and Lataitis* paper, the theory of atmospheric acoustics has been developed significantly.

The effect of wind velocity and temperature fluctuations on the statistical moments of a sound field was studied by numerous authors: *Ostashev* [1997, and references therein], *Ostashev and Wilson* [1999]; *Ostashev et al.* [2001], *Blanc-Benon et al*. [1991], *Wilson* [2000, and references therein]. Generalization of the theory by *Clifford and Lataitis* was found in *Ostashev and Goedecke* [1998]; *Ostashev et al*. [2001]. The Rytov approximation permits one to deal with log-amplitude and travel time fluctuations. Lately, two effects of random heterogeneities have been investigated. First, the velocity shift, which states, that the apparent velocity of the wave is greater than the average sound velocity of the non-turbulent medium. This is in accordance with Fermat's principle, which states that the wave path minimizes the travel time of the wave [*Landau*

and Lifshitz, 1959]. This effect was discovered in the late 1980's. The particular interest to this effect lies in the area of surface seismic deterministic methods [*Boyse*, 1986, 1994; *Roth*, 1993; *Wielandt*, 1987; *Iooss and Galli*, 2000]. Theoretical methods are based on small perturbations in geometrical optics [*Snieder and Aldridg*, 1995 *Boyse and Keller*, 1994]. The results showed that if the magnitude of the heterogeneities is sufficiently small, the relative velocity shift increases linearly with the propagation distance. In seismology the determination of travel time is an important issue. Hence, the second effect is the linear increase of the first-order travel-time variance with the propagation distance [*Chernov*, 1960]. However, nonlinear effects appear at certain propagation distances [*Karweit et al*., 1991; *Iooss*, 2000]. Overall, since the mid 1980s the rigorous theory of line-of sight sound propagation through media with random inhomogeneities of medium velocity, temperature has been developed; the statistical characteristics of the sound wave have been calculated using the Born approximation, by ray, Rytov and parabolic-equation methods, by the theory of multiple scattering and the diagram technique [*Ostashev*, 1997]. Statistical characteristics are obtained for different models of the random fields of velocity and temperature; homogeneous turbulence, homogeneous and isotropic turbulence, turbulence with the Kolmogorov spectrum and Gaussian correlation functions [*Ostashev*, 1997].

Further extension of our knowledge of sound propagation in the turbulent atmosphere requires the validation of theory by experiments carried out outdoors and in wind tunnels. Until recently, although a large number of atmospheric measurements were made, they suffered a lack of reliability and accuracy in addition to poor characterization of the turbulence. Laboratory experiments, despite there crucial importance, are

extremely rare. The objective in this dissertation is to demonstrate that ultrasonic technology can be effectively utilized for data acquisition and flow diagnostics in laboratory conditions.

1.1.2 Review of Experimental Issues in Waves Propagation in Random Media

We consider a locally isotropic, passive temperature field coupled with a locally isotropic velocity field, which is realized by introducing a heated grid in a uniform flow [*Yeh and Van Atta*, 1973 and references therein]. If temperature fluctuations are sufficiently small then density is effectively constant and buoyancy forces are negligible. Statistical turbulence data from hot and cold wire anemometry that describe the temperature and velocity field downstream of a heated grid in a low speed wind tunnel are typically given in the form of downstream decay of turbulence intensities, energy spectra, autocorrelations, spatially separated cross correlations, phase, coherence [*Comte-Bellot and Corrsin*, 1971; *Yeh and Van Atta*, 1973; *Sepri*, 1976; *Warhaft and Lumley*, 1978; *Sreenivasan et al*, 1980; *Van Atta*, 1991; *Nelkin*, 1991; *Sreenivasan and Antonia*, 1997; *Warhaft* (and references therein), 2000].

The influence of turbulence on sound wave propagation has been studied by a number of authors, who conducted a variety of experiments and provided a wide range of experimental and analytical results in this area for the last fifty years. The book by *Tatarskii* [1971] and paper by *Brawn and Hall* [1978] present a detailed review of the research into sound propagation in turbulent atmosphere prior to the mid 1970. Recently outdoor sound propagation in a turbulent medium has received serious attention. Measurements of the intensity fluctuations in the atmosphere or ocean have been obtained by *Daigle et al.* [1978, 1983, 1986]; *Ewart et al.* [1986]. Experimental

measurements of sound propagation through the atmosphere with particular emphasis on amplitude and phase fluctuations due to atmospheric turbulence were performed by *Bass et al*, [1991 and references therein]. Particular interest to large-scale turbulence was paid by *Chessel*, [1976]; *Roth* [1983], *Wilken*, [1986]. *Noble et al*.[1992] provided experimental evidences that large eddies cause phase fluctuations over a broad range of frequencies. The acoustic propagation model that incorporates the current state of understanding of a large-scale atmospheric turbulence structure was developed by *Wilson and Thompson* [1994, references therein].

It has been emphasized that sound propagation is sensitive to random variations in the effective refractive index, which is a function of temperature and medium velocity fluctuations. *Di Iorio and Farmer* [1996] showed that the velocity fluctuations can be dominant source of acoustic scattering and in their 1998 paper they showed that the random variations in temperature also contribute to the total scattered signal. Although a large number of atmospheric measurements were made, the uncertainties with regard to relevant environmental parameters, namely velocity and temperature variations, make it difficult to assess their individual influence on acoustic wave propagation. Moreover, outdoor experiments suffered a lack of reliability and accuracy in addition to poor characterization of the turbulence. The problem of phase fluctuations is equivalent to the problem of finding the auto-correlation functions of these fluctuations, which involves enormous amounts of experimental data and a large amount of computational work. From the repeatability of experiments point of view, it is much more complicated and time-consuming to conduct outdoor experiments compared to those performed under convenient laboratory conditions. The challenge in conducting laboratory experiment is

first the fact that there is a dearth of reliable data collected in well-controlled experimental conditions. Secondly, to demonstrate that rapidly evolving computational technology and ultrasonic technique provide great potential for conducting acoustic experiments in laboratory conditions that will lead to further extension of knowledge of sound propagation in the turbulent atmosphere. The propagation of sound waves through turbulent velocity fields has been previously investigated under laboratory conditions. *Ho and Kovasznay* [1974] made such measurements across an air jet over an extremely short propagation distance. *Blanc Benon* in his work in 1981 generated an approximately plane acoustic wave with a pistonlike sound source and aimed it across jet-generated air flows. In his later work, in 1993 together with *Juve* he presented experimental results for the variance of the normalized intensity fluctuations and for the probability functions of acoustic waves that propagate through thermal grid-generated turbulence. Experimental data were obtained by varying both the frequency of the wave and the distance of propagation. Although review of the literature reveals a substantial improvement in the understanding of the sound propagation in the turbulent atmosphere, it is obvious that experimental investigations performed in laboratory conditions are very rare.

1.1.3 Review of Experimental Issues in Ultrasonic Technique

The breakthrough in the problem of measuring flow parameters in a turbulent medium using sound was made by *Schmidt* [1970, 1975], who discovered the possibility of measuring flow parameters non-invasively and without perturbation by means of ultrasound. His concern was in connection with his efforts to measure the circulation associated with aerodynamic surfaces in a wind tunnel. *Johari and Durgin* [1998] reported a number of applications that extended *Schmidt's* initial work. Specifically, they

investigated unsteady flow about an airfoil, the trailing vortex from a delta wing, and swirling free-surface flows.

During the past twenty five years ultrasonic technology has progressed very rapidly and has been used to improve flow measurement accuracy, specifically the development of the equipment capable of measuring the very small time differences associated with changes in the ultrasound wave propagation time resulted in measuring devices with accuracy of the order of 0.25%. An exhaustive review of recent works on theory, techniques and applications of ultrasonic measurements is presented in the book by *Lynnworth* [1989]. The study of the transmission and attenuation of the signal and noise mechanism performed by *Brassier et al.* [2001] gives us a preferred choice of the frequency at which ultrasonic transducers can be operated. In their work authors presented an innovative prototype of the ultrasonic flow meter using optimal choice of ultrasonic frequency, the design and the "echo process". With improved technology we are now able to measure volumetric flow rate and other flow parameters in pipes and conduits reliably and accurately in laboratory scale apparatus.

The intention to utilize the principles of the ultrasonic flowmeter for turbulent flow diagnostics is motivated first by its advantages over traditional methods. The principle advantages include noninvasiveness, relatively simple operation/installation, fast response, high date rate, maintenance of long term accuracy be maintained, low production cost, unit-to –unit interchangeability. Secondly, our interest in the ultrasonic technique is substantiated by its broad range of applications in many engineering and scientific fields. Potential applications include, but not limited to marine aviation, meteorological and industrial areas [*Kits van Heyningen*, 1987]. Other potential

applications are: high accuracy sensors as part of a wind shear warning system for airports and for meteorological stations where maintenance and/or environmental considerations make mechanical devices impractical [*Lynnworth*, 1989]. The National Institute of Standards and Technology investigates ways to reduce the uncertainty and improve the operational capability of flow calibration facilities. As understanding of ultrasonic metering methods spreads through the flow metering community, these methods may evolve into primary flow standards [*Mattingly and Yeh*, 2000]. There are fundamental theoretical and computational issues related to the ultrasonic flowmeter technique that must be understood and in some instances resolved. Industrial flowmeters are designed for idealized flows: usually a mean velocity profile while turbulence including velocity and temperature fluctuations is ignored. The presence of secondary flows is known to cause significant metering inaccuracies, so it is clear that non-ideal flows are of concern for accurate measurements. *Yeh* and his colleagues [*Yeh and Espina*, 2001; *Yeh et al.*, 2001] have been working to develop an intelligent ultrasonic flow meter that can identify swirl and cross flow characteristics and appropriately influence volumetric flow rate calculations. The objective in this thesis is to account for some of the aforementioned shortcomings by identifying the effect of turbulence on ultrasound wave propagation including the effect of velocity and density fluctuations on travel time of ultrasound wave. Our theoretical formulation of the basic ultrasonic flowmeter includes sound speed fluctuations and velocity fluctuations terms.

1.1.4 Review of Numerical Works in Modeling of Sound Propagation in Moving Random Media

Another rapidly developing approach, besides analytical and experimental, is the numerical one. Calculation of sound propagation in atmosphere requires accurate representation of turbulence spectrum. The complexity of the turbulence dynamics, however, makes development of turbulence models for propagation calculations difficult. Another practical difficulty is that turbulence modeling is associated with fully three-dimensional spatial models of the turbulence. Structure along the direction of propagation, as well as in the direction transverse, must be known. Some initial efforts in multidimensional modeling of sound propagation in atmosphere have been made by *Kristensen et al.* [1989]; *Mann*, [1994]; *Peltier et al*. [1996]; and *Wilson* [2000]. Recognition of the fact that large eddies, belonging to the energy-containing subrange, play a significant role in acoustic scattering favors a Gaussian model over the Kolmogorov one [*Wilson and Thomson*, 1994; *Daigle et al*., 1983; *Jojnson et al*.]. To reconcile the Kolmogorov and Gaussian approaches, recent investigators used a von Karman model for the turbulence spectrum (*Wilson*, 2000 and references therein). The effect of turbulence on sound propagation through numerical simulations was investigated in works by *Karweit et al.* [1991 and references therein], *Ph. Blanc-Benon et al.* [1991,1995], *Chevret* [1996], *Ioos et al* [2000] analytically and numerically studied the high frequency propagation of acoustic plane and spherical waves in random media. Using ray acoustics and a perturbation approach they obtained the travel time variance at the second order and demonstrated nonlinear behavior of travel time variance at large propagation distances.

1.2 Objectives and Approach

The primary goal of this work is to determine turbulent flow characteristics from the statistics of travel-time variations. The thesis includes theoretical modeling, experimental measurements, and comparison (interpretation) of experimental data with known theoretical, numerical and experimental data.

The theoretical modeling includes:

1. Development of an acoustical propagation model that allows determination of the spatial correlation functions of travel time, turbulent velocity, sound speed fluctuations and their spectra based on measured experimentally travel time.

2. Derivation of the flowmeter equation in terms of cross correlations of travel time, turbulent velocity and sound speed fluctuations.

3. Application of the spectral analysis as a technique in obtaining integral solutions for the correlation functions, which are of interest in themselves.

4. Development of a methodology for spectral analysis of isotropic homogeneous turbulence.

The experimental investigation is primarily concerned with application of the travel time ultrasonic technique for data acquisition in the grid-generated turbulence produced in a wind tunnel. The ultrasonic technique implementation includes two different experimental setups for both heated and non-heated grid-generated turbulence:

1. Travel time versus travel distance (downstream and upstream propagation of ultrasound with respect to the mean velocity vector);

2. Travel time versus mean flow velocity (perpendicular propagation of ultrasound waves with respect to the mean velocity vector).

The experimental data validation is based on well-known Kolmogorov law, derived purely from the dimensional analysis. The interpretation of experimental data includes:

a) Ray acoustics approach for travel time interpretation and determination of structure constant.

b) Stochastic Helmholtz equation, its parabolic approximation and the small perturbation method as a solution to the parabolic approximation for log-amplitude, travel-time variations interpretations.

c) Demonstration of Fermat's principle.

d) A Gaussian turbulent spectra model for travel-time sound propagation.

The thesis is organized as follows. In Chapter 2 we review several topics from the theory of random fields and turbulence theory. In Chapter 3 we present the fundamental equations of the acoustics of a moving inhomogeneous medium with its further two approximations: ray acoustics and stochastic Helmholtz equation along with Rytov approach. In Chapter 3 we also review some physical and mathematical issues of the theory of sound propagation in a random media. In Chapter 4 we present description of experimental apparatus, generation of grid-generated turbulence using grids, ultrasonic system, data acquisition and analysis system. Chapter 5 is devoted to the analysis of experimental data, discussion of results and comparisons with theoretical and numerical data. Conclusions and recommendations are presented in Chapter 6.

Chapter 2. Isotropic Turbulence

In this chapter we give a brief exposition of some topics from the theory of random fields and turbulence theory, which are necessary in the following experimental and theoretical analysis. We give special attention to the representation of isotropic turbulence by means of correlation functions, spectral expansions based on the wavelength scale. Review of isotropic, homogeneous turbulence characteristics is followed by the outline of length scales in turbulent flows and corresponding turbulence spectrum models. The second part of the chapter is devoted to the generation of approximately isotropic homogeneous turbulence in a wind tunnel by means of a grid. The relations for decay of velocity, temperature fluctuations, integral length scale downstream of a grid are presented.

2.1 Statistical Characteristics of the Medium

In what follows we repeatedly need basic information about the statistical properties of developed turbulent flow. In this chapter we present only those results of statistical theory of random functions and fields, which are important for our purposes, and refer to the original sources [*Kolmogorov*, 1941, 1963; *Obukhov*, 1941; *Loitsyanskii*, 1939, *Batchelor*, 1953; *Tatarskii*, 1961, 1971; *Monin and Yaglom*, 1981; *Landau and Lifshitz*, 1959; *Stratonovich*, 1961] for more detailed information.

2.1.1 Stationary Random Functions

The curve shown in Figure 2.1 serves as an example of realizations of random functions. The value of any such function at a fixed instant of time is a random variable, which can be decomposed into mean value and fluctuation

$$u(t)=U+u' \qquad (2.1)$$

The probability density function *B(u)* defines probability of finding *u(t)* between *u* and $u+\Delta u$ [*Tennekes and Lumley*, 1972]

$$B(u)\Delta u \equiv \lim_{T\to\infty}\frac{1}{T}\Sigma(\Delta t) \qquad (2.2)$$

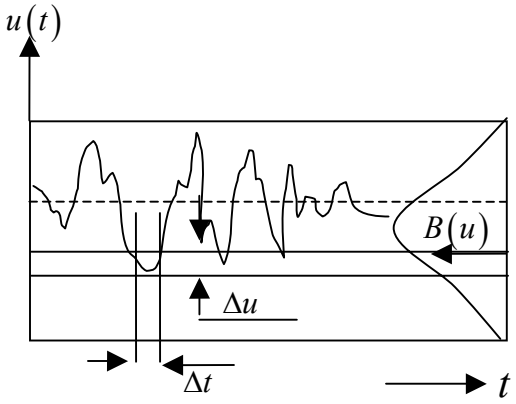

Figure 2.1 Example of realizations of random function u(t).

The basic features of Probability density function are $B(u)\geq 0$, $\int_{-\infty}^{+\infty} B(u)du = 1$. But to completely specify the random function u(t) it is not enough to know only the probability density function, B(t,u); one must know all possible multidimensional probability distributions, i.e. all the probabilities $B(t_1,t_2,...,t_N;u_1,u_2,...,u_N)$ [Tatarskii, 1971]. However, in applications it is

difficult to determine all the functions. It is customary used simpler characteristics of the random field. They are called moments. The first moment is the mean value

$$\mathrm{U} \equiv \int_{-\infty}^{+\infty} uB(u)du \,. \qquad (2.3)$$

The second moment is a variance – mean square departure from the mean

$$K(t_1,t_1) = \sigma^2 \equiv \overline{u'^2} = \left\langle \left[u(t_1) - \langle u(t_1) \rangle \right]^2 \right\rangle = \int_{-\infty}^{+\infty} u'^2 B(u)du \,. \qquad (2.4)$$

The square root of variance is called standard deviation or rms amplitude. The joint moment is

$$M(t_1,t_2) \equiv \langle u(t_1)u(t_2) \rangle = \int_{-\infty}^{+\infty}\int_{-\infty}^{+\infty} u_1 u_2 B(u_1,u_2)\,du_1 du_2 \,. \qquad (2.5).$$

The most important characteristic of a random function is its correlation function [*Tatarskii*, 1961]

$$K(t_1,t_2) \equiv \langle u'(t_1)u'(t_2) \rangle = \int_{-\infty}^{+\infty}\int_{-\infty}^{+\infty} (u_1 - \langle u_1 \rangle)(u_2 - \langle u_2 \rangle) B(u_1,u_2)\,du_1 du_2 = \\ = M(t_1,t_2) - \langle u(t_1) \rangle \langle u(t_2) \rangle \,. \qquad (2.6)$$

A random function *u(t)* is called stationary if its mean value does not depend on the time and if its correlation function $K(t_1,t_2)$ depends only on a difference $t_1 - t_2$ [*Tatarskii*, 1961], i.e.

$$K_u(t_1,t_2) = K_u(t_1 - t_2) \qquad (2.7).$$

For stationary random functions u(t) there exist expansions in Fourier integrals, namely a stationary random function can be represented in the form of a stochastic Fourier-Stieltjes

integral with random complex amplitudes $\varphi(\omega)$, where ω is the frequency of the wave [*Tatarskii*, 1961]

$$u(t) = \int_{-\infty}^{+\infty} \varphi e^{i\omega t} d\omega . \qquad (2.8)$$

Using the inverse Fourier transform, the function $\varphi(\omega)$ can be expressed as follows:

$$\varphi(\omega) = \frac{1}{2\pi} \int_{-\infty}^{+\infty} u(t) e^{-i\omega t} dt . \qquad (2.9)$$

The spectral density of the stationary random function *u(t)* by definition is [*Rytov et al*., 1978] is

$$\Phi_u(\omega) = \frac{1}{(2\pi)} \int_{-\infty}^{+\infty} K_u(t) e^{-i\omega t} dt . \qquad (2.10)$$

In its turn, a correlation function $K_u(t)$ can be written as

$$K_u(t) = \int_{-\infty}^{+\infty} \Phi_u(\omega) e^{i\omega t} d\omega . \qquad (2.11)$$

Hence, $K_u(t)$ and $\Phi_u(t)$ are Fourier transforms of each other.

2.1.2 Random Functions with Stationary Increments

In order to describe random functions that are more general then stationary random functions, in turbulence theory a so-called structure function can be used instead of correlation function [*Kolmogorov*, 1941; *Obukhov*, 1941]. The basic idea consists of the following. In the case when *u(t)* represents a non-stationary random function, the difference $f_u(t) = u(t+\tau) - u(t)$ can be considered instead of the random function *u(t)*. The advantage of this technique is in the fact that for values of τ , which are not too

large, slow changes in the function *u(t)* do not affect the value of this difference, and it can be a stationary random function at least approximately. In the case where *f(t)* is a stationary random function, the function *u(t)* is called a random function with stationary increments. The function of arguments t_1, t_2 where t_1 and t_2 take the values $t_1+\tau, t_1, t_2, t_2+\tau$ is called the structure function of a random process and has the following form

$$D_u(t_1,t_2)=\left\langle\left[u(t_1)-u(t_2)\right]^2\right\rangle. \qquad (2.12)$$

2.1.3 Homogeneous and Isotropic Random Fields

For a random field *u(r)* (random function of three variables) a correlation function can be defined as [*Tatarskii*, 1961]

$$K_u(\mathbf{r}_1,\mathbf{r}_2)=\left\langle\left[u(\mathbf{r}_1)-\left\langle u(\mathbf{r}_1)\right\rangle\right]\left[u(\mathbf{r}_2)-\left\langle u(\mathbf{r}_2)\right\rangle\right]\right\rangle. \qquad (2.13)$$

In the case of random fields the concept of stationarity generalizes to the concept of homogeneity. A random field is called homogeneous if its mean value is a constant and if its correlation function satisfies the relation

$$K_u(\mathbf{r}_1,\mathbf{r}_2)=K_u(\mathbf{r}_1+\mathbf{r}_0,\mathbf{r}_2+\mathbf{r}_0). \qquad (2.14)$$

Hence, the correlation function of a homogeneous random field depends only on $\mathbf{r}_1-\mathbf{r}_2$.

The spectral density function in a case of homogeneous random field is

$$\Phi_u(\mathbf{k})=\frac{1}{(2\pi)^3}\int_{-\infty}^{+\infty}K_u(\mathbf{r})e^{-i\omega\mathbf{r}}d^3r. \qquad (2.15)$$

For even correlation functions $K_u(-\mathbf{r})=K_u(\mathbf{r})$, in particular, for correlation functions of a real or isotropic field, spectral density is also even, $\Phi_u(-\mathbf{r})=\Phi_u(\mathbf{r})$. In this case, the

correlation function and spectral density can be expressed through cosine Fourier transform:

$$\Phi_u(\mathbf{k}) = \frac{1}{(2\pi)^3} \int_{-\infty}^{+\infty} \iint \cos(\mathbf{k}\cdot\mathbf{r}) K_u(\mathbf{r}) d\mathbf{r} . \qquad (2.16)$$

A homogeneous random field is called isotropic if the correlation function $K_u(\mathbf{r})$ depends only on $r = |\mathbf{r}|$, i.e. only on the distance between the observation points. In order to derive an expression for the spectral density function in isotropic random field in the integral (2.16) the spherical coordinates can be introduced and the angular integration carried out. As a result we obtain an expression

$$\Phi_u(k) = \frac{1}{2\pi^2 k} \int_0^{\infty} r K_u(r) \sin(kr) dr . \qquad (2.17)$$

2.1.4 Locally Homogeneous and Isotropic Random Fields

A very rough approximation for the spatial structure of atmospheric turbulence may be obtained by applying the method of structure functions [*Kolmogorov*, 1941, *Tatarskii*, 1961]. The advantage of this approximation is in the fact that the difference between the values of the field *u(r)* at two points $\mathbf{r}_1, \mathbf{r}_2$ is mainly affected by inhomogeneities of the field ***u*** with characteristic size less than distance $|\mathbf{r}_1 - \mathbf{r}_2|$. If the distance is not too large, the largest inhomogeneities have no effect on $u(\mathbf{r}_1) - u(\mathbf{r}_2)$, and therefore the structure function depends only on the difference $\mathbf{r}_1 - \mathbf{r}_2$:

$$D_u(\mathbf{r}_1, \mathbf{r}_2) = \left\langle \left[u(\mathbf{r}_1) - u(\mathbf{r}_2) \right]^2 \right\rangle = D_u(\mathbf{r}_1 - \mathbf{r}_2) . \qquad (2.18)$$

This local dependence is the basis of the concept of local homogeneity [*Kolmogorov*, 1941, *Tatarskii*, 1961]. A random field *u(r)* is said to be locally homogeneous in the region *G* if the distribution functions of the random variable $u(\mathbf{r}_1)-u(\mathbf{r}_2)$ are invariant with respect to shifts of the pair of points $\mathbf{r}_1,\mathbf{r}_2$, as long as these points are located in the region *G*. Thus, the mean value and the structure function (2.15) of locally homogeneous random field depend only on $\mathbf{r}_1-\mathbf{r}_2$ [*Kolmogorov*, 1941, *Tatarskii*, 1961]. The relationship between the spectral density function and the structure function can be obtained as

$$D_u(\mathbf{r}) = 2\int_{-\infty}^{+\infty}\iint\left(1-\cos\mathbf{k}\cdot\mathbf{r}\right)\Phi_u(\mathbf{k})d\mathbf{k}\,. \qquad (2.19)$$

A locally homogeneous random field is said to be locally isotropic in the region *G* if the distribution functions of the quantity $u(\mathbf{r}_1)-u(\mathbf{r}_2)$ are invariant with respect to rotations and mirror reflections of the vector $\mathbf{r}_1-\mathbf{r}_2$, as long as the points $\mathbf{r}_1,\mathbf{r}_2$ are located in *G* [*Kolmogorov*, 1941, *Tatarskii*, 1961]. The structure function of a locally isotropic random field depends only on $|\mathbf{r}_1-\mathbf{r}_2|$:

$$D_u(\mathbf{r}) = \left\langle\left[u(\mathbf{r}+\mathbf{r}_1)-u(\mathbf{r}_1)\right]^2\right\rangle = D_u(r). \qquad (2.20)$$

In the case where the field is locally isotropic, equation (2.19) is

$$D_u(r) = 8\pi\int_{-\infty}^{+\infty}\left(1-\frac{\sin kr}{kr}\right)\Phi_u(k)k^2dk\,. \qquad (2.21)$$

2.1.5 Frozen Turbulence Hypothesis

Under some conditions, sound passes through the turbulence in a time that is short compared to the timescales characteristic of the evolution of the turbulence. In such cases

the turbulence can be imagined as "frozen" during passage of the acoustic wave. If a real field *u(t,r)* is stationary in time and homogeneous in space, it is described by means of space-time correlation function

$$K_u(\mathbf{r},\ t) = \left\langle u(\mathbf{r}+\mathbf{r_1}, t+t_1)u(\mathbf{r},t)\right\rangle, \qquad (2.22)$$

assuming $\left\langle u(\mathbf{r})\right\rangle = 0$. *G. Tylor's* hypothesis [*Tennekes and Lumley*, 1972] states that the entire spatial pattern of a random field is transported with the mean wind velocity *U*,

$$K_u(\mathbf{r},\ t+t') = K_u(\mathbf{r}-Ut',\ t). \qquad (2.23).$$

2.2 Turbulence Spectral Models for Sound Propagation in Inhomogeneous Media

In this subsection, isotropic models for the turbulence spectrum are presented on the basis of the turbulence scales.

2.2.1 Length Scales in Turbulent Flows

No one model exists to accurately describe the entire turbulence spectrum in all flows. It is important to know, which portion of the spectrum contributes significantly in a given problem. There are three primary spectral subranges: the energy containing subrange, the inertial subrange and the dissipation subrange, that are characterized by their own length scales: Integral, Taylor and Kolmogorov respectively [*Tennekes and Lumley*, 1972]. These subranges are schematically demonstrated in Figure 2.2. Whereas the integral length scale L_0 is a characteristic length scale of the largest, most energetic, and least dissipative motions, the Kolmogorov microscale η is the characteristic of the

smallest, most dissipative, and least energetic motions. The integral length scale is defined by

$$L_0 = \frac{1}{\sigma^2}\int_0^\infty K_u(r)dr\,. \qquad (2.24)$$

where $\sigma^2 = \langle u'^2 \rangle$, K_u are the variance and autocorrelation of a velocity component (or temperature), and r is the spatial displacement. By definition, the Kolmogorov microscale is

$$\eta = \left(\nu^3/\varepsilon\right)^{1/4}, \qquad (2.25)$$

where ε is a mean dissipation rate of turbulent kinetic energy. For velocity fluctuations, for example, $\varepsilon_u = -1.5d\langle u^2 \rangle/dt$. In atmospheric turbulence, η is of order 1 to 10 mm, many orders of magnitude smaller than L_0. The inertial subrange consists of turbulent motions having scales L between L_0 and η. The Taylor microscale λ_T falls within the inertial subrange and is given in the isotropic turbulence by [*Tennekes and Lumley*, 1972]

$$\lambda_T^2 = 15\nu\frac{\sigma_u^2}{\varepsilon}. \qquad (2.26)$$

The dissipation subrange can generally be ignored [*Wilson et al*, 1999] for the prediction of acoustic propagation. For most frequencies the motions in the dissipation subrange are very small compared to the acoustical wavelength and hence unimportant. Therefore, the energy-containing and inertial subranges of atmospheric turbulence play the primary role. It was demonstrated [*Lawrence and Strohbehn*, 1970; *Wilson and Thompson*, 1994] that large scale energetic motions are responsible for phase fluctuations, while smaller scale motions derive the amplitude fluctuations. However, the interplay between the

propagation geometry, refraction, scattering, and frequency complicates the idealized picture.

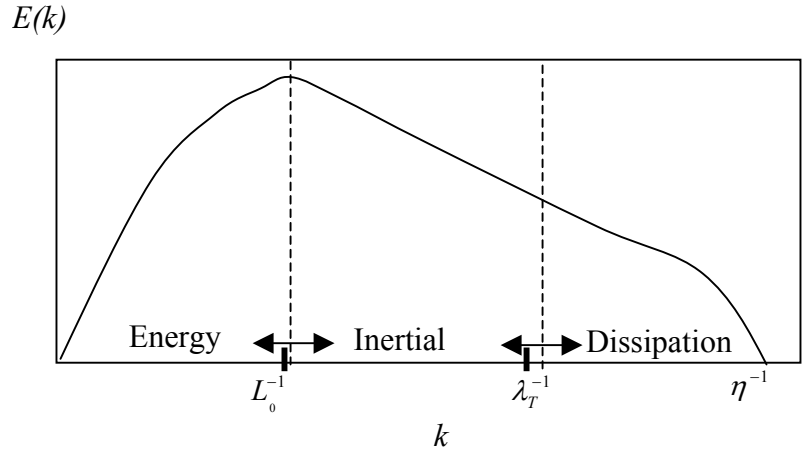

Figure 2.2 Spectral view of three subranges of turbulence and corresponding length scales.

2.2.2 Isotropic Turbulence Spectrum Models

Inertial Subrange Model

Kolmogorov's original hypothesis [*Kolmogorov*, 1941] implies that the structure function, defined as $D_u(L)=\left\langle\left[u(L)-u(0)\right]^2\right\rangle$, is proportional to $L^{2/3}$. Specifically,

$$D_{u'}(r)=C_u^2 r^{2/3},\ r>>l_0, \qquad (2.27)$$

where C_u^2 is the structure-function parameter for the longitudinal velocity fluctuations. The equation (2.27) is so called the Kolmogorov "2/3" law and is valid in the inertial subrange. Based on *Tatarskii*, [1961], a general function

$$D(r)=C^2 r^{\mu}, 0<\mu<2, \qquad (2.28)$$

corresponds to the 3-D spectral density function

$$\Phi(k) = \frac{\Gamma(\mu+2)}{4\pi^2}\sin\left(\frac{\pi\mu}{2}\right)C^2 k^{-(\mu+3)}. \qquad (2.29)$$

Consequently, the 1-D density for the inertial part of the spectrum is

$$\Phi_u(k) = \frac{\alpha}{2}\varepsilon_u^{2/3}k^{-5/3}, \qquad (2.30)$$

where α is a constant, whose value for atmosphere is approximately 0.52 [*Högström*, 1996].

For $r << l_0$, structure function has a following form [*Rytov et al.*, 1978]

$$D_{u'}(r) = C_u^2 l_0^{-4/3} r^2,\ r << l_0, \qquad (2.31)$$

Finally, at $r >> L_0$ the structure function approaches the asymptotic value

$$D_{u'}(r) = C_u^2 L_0^{2/3},\ r >> L_0, \qquad (2.32)$$

Figure 2.3 depicts a real structure function along with three approximations expressed by equations (2.27, 2.31, 2.32) [*Rytov et al*., 1978].

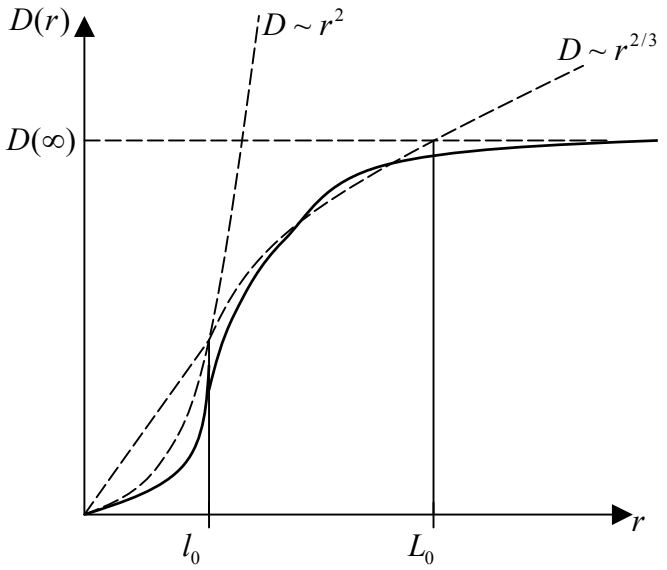

Figure 2.3 Structure function with three limit approximations.

Gaussian Model

The starting point for the Gaussian model is the longitudinal velocity correlation function

$$K_{\mathrm{G}u} = \sigma^2 \exp\left(-\frac{r^2}{l_{\mathrm{G}}^2}\right), \qquad (2.33)$$

where l_G is the Gaussian length scale parameter. Fourier transformation yields the spectrum

$$\Phi_{\mathrm{G}}(k) = \frac{\sigma^2 l_{\mathrm{G}}}{2\sqrt{\pi}} \exp\left(-\frac{k^2 l_{\mathrm{G}}^2}{4}\right). \qquad (2.34)$$

The Gaussian spectrum of inhomogeneities of the medium is very convenient for analytical studies of wave propagation in random media. It allows accounting of the effects of the largest inhomogeneities in a medium on the statistical moments of a sound field [*Rytov et al*, 1978; *Ostashev*, 1997]. The Gaussian model is best suited for the energy containing subrange. The Gaussian length scale parameter is the scale of the largest inhomogeneities in a turbulent medium that affect the statistical moments of a sound field [*Ostashev*, 1997]. In many practical cases l_G is of the order of L_0, however, l_G can be less than L_0. More advanced procedures for determination of the length scale are described in *Wilson* [2000].

Von Karman Model

The von Karman model incorporates both the energy-containing and inertial subranges [*Ostashev*, 1997]. The model is presented in many different, and not always

equivalent, forms in the literature. The correlation function for spatial separation parallel to the direction of the velocity fluctuations, based on *Wilson* [2000] is

$$K_{v^u} = \frac{2\sigma^2}{\Gamma\left(\frac{1}{3}\right)}\left(\frac{L}{l_v}\right)^{1/3} . \qquad (2.35)$$

The 1-D Fourier transform of the above correlation function is

$$\Phi_v(k) = \frac{\Gamma(5/6)}{\sqrt{\pi}\Gamma(1/3)}\frac{\sigma^2 l_v}{\left(1+k^2 l_v^2\right)^{5/6}} . \qquad (2.36)$$

A reasonable approach for determining the parameters in the von Karman model is to set σ^2 to the actual variance of the field and then choose l_V to match the Kolmogorov model in the inertial subrange. The von Karman model reduces, by design, to the inertial subrange model. Qualitative comparison of three primary turbulence spectra is sketched in Figure 2.4 [*Wilson*, 1999].

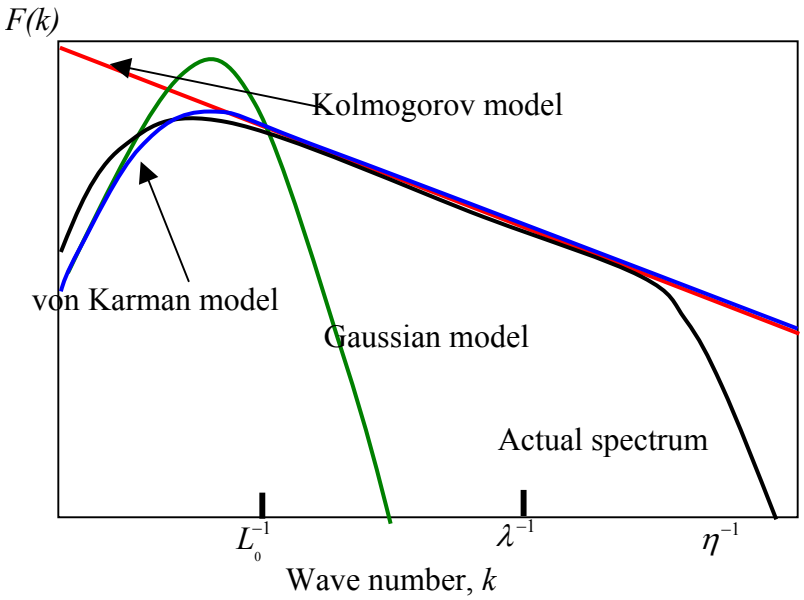

Figure 2.4. Comparison of three 1-D primary turbulence spectra $F(k)$ and the corresponding length scales

2.3 Wind Tunnel Turbulence

The following section is devoted to the description of the turbulence that may be generated experimentally by the insertion of a grid into a low speed wind tunnel. The actual experimental procedure is described in Chapter 5, while the theoretical issues are considered here. Homogeneous, isotropic turbulence is considered an idealization that, at most, can be achieved approximately in laboratory experiments.

2.3.1 Description of Ideal Grid Turbulence

The traditional method of generating, approximately, isotropic turbulence is by means of a grid: a rectangular array of bars placed at the entrance of the test section [*Batchelor*, 1953; *Comte-Bellot and Corrsin*, 1966]. In practice the flow in a wind tunnel is constrained by walls forming a finite boundary to the fluid motion. Boundary layer effects are almost negligible for measurements made near the centerline of the tunnel. We consider a fluid flow of infinite extent in its three spatial directions and being unconfined by any boundaries. In the plane $x = x_0$ a uniform grid is inserted. The grid is characterized by two parameters: mesh size *M* and rod diameter *D*. The grid is imagined to be of infinite extent in the plane such that the origin for the *x*-axis would be indiscernible. The mean flow velocity is normal to the grid and is constant in time and space (except in the immediate neighborhood of the grid). Sufficiently downstream of the grid, the statistics of turbulence shall be assumed to be independent of *(t,y,z)* the cellular flow generated by the grid having been consumed by the overall turbulent field. The turbulence thus produced is statistically stationary, homogeneous with respect to translations in the planes normal to the *x*-axis, and it decays in the downstream direction of the grid. The above model shall be called ideal grid turbulence. For the generation of

thermal turbulence, the grid should be considered as being uniformly heated. Although the thermal turbulence generated by heating the grid may exhibit large fluctuations, the heat addition is small, so that there is no transfer of energy from thermal turbulence to mean temperature. The thermal turbulence thus behaves like a passive scalar convected by the mean velocity and is dissipated by conduction to the ultimate state of uniform mean temperature [*Sepri*, 1976, *Mydlarskii and Warhaft*, 1998]. Since our research work is not focused on investigation of turbulence characteristics, and the statistics of isotropic turbulence are well known, we do not intend to go any further into representation of equations of turbulence and statistics of turbulent flow. We limit ourselves to the definitions and references.

2.3.2 The Decay of Flow Parameters Downstream of the Grid.

The Decay of Velocity Fluctuations

The downstream decay of the mean-squared streamwise turbulent velocity behind the unheated grid is a relation of the type (*Sreenivasan et al*, 1980; *Comte-Bellot & Corrsin*, 1966; *Kistler et al.*, 1954; *Mills et al.*, 1958; *Yeh & Van Atta*, 1973; *Warhaft & Lumley*, 1978 (a,b))

$$\frac{\overline{u^2}}{U^2} = \alpha_1 \left(\frac{x}{M} - \frac{x_0}{M} \right)^{-n}, \qquad (2.37)$$

where $\alpha_1 = 0.04, x_0 / M = 3, n = 1.2$ are constants chosen to give the maximum possible straight line fit to the experimental data in logarithmic co-ordinates [*Sreenivasan et al*, 1980].

The Decay of Temperature Fluctuations

The downstream decay of $\overline{T'^2}$ behind the heated grid is described by the relation of the type

$$\frac{\overline{T'^2}}{(\Delta T)^2} = \beta\left(\frac{x}{M} - \frac{x_0}{M}\right)^{-m}, \beta = 0.124, m = 1.4, \qquad (2.38)$$

where β, m were chosen as a best fit for experimental data [*Sreenivasan et al*, 1980]

The downstream development of the integral length scale

The expression for downstream decay of the integral length scale is

$$\frac{L}{M} = 0.13\left(\frac{x}{M} - \frac{x_0}{M}\right)^{-0.4}. \qquad (2.39)$$

The constants are chosen based on the best fit to the experimental data obtained by *Sreenivasan et al*, [1980], *Kistler et al*, [1954], *Mills et al*, [1958], *Yeh & Van Atta*, [1973].

Chapter 3. Sound Propagation in a Moving Random Media

In this chapter, we present a derivation of the equations describing the propagation of acoustical waves in inhomogeneous moving media. The main equations were obtained in the literature by the mid forties [*Blokhintzev*, 1953; *Kolmogorov*, 1941; *Chernov*, 1960; *Tatarskii*, 1961, 1967, 1971] while some of them have been derived just recently [*Rytov et al*, 1978; *Ostashev*, 1997; *Wilson*, 1999, 2000]. The propagation of a sound wave in an inhomogeneous moving medium is completely described by the system of linearized equations of fluid dynamics. Then, starting from the general system of equations using several assumptions with defined ranges of applicability, two well known approximate theories of wave propagation, namely ray acoustics and the Rytov method are developed. The statistical moments of a sound fields are calculated using these two approaches, mainly following the reviews of published works [*Tatarskii*, 1967, 1971; *Rytov*, 1978; *Ostashev*, 1997]. The eikonal equation and Fermat's principle [*Blokhintzev*, 1953; *Landau and Lifshitz*, 1959; *Wilson*, 1992] are discussed in application to the stationary, inhomogeneous moving medium. The theory of travel-time fluctuations of sound waves due to turbulence in the atmosphere based on a law, established by *Obukhov* [1941] and *Kolmogorov* [1941], known as "2/3" law, is developed and the physical and mathematical issues related to basic flowmeter equation are addressed. In subchapter 3.6 the classical flowmeter equation is reconsidered in a form that includes turbulent velocity and sound

speed fluctuations. The result is an integral equation in terms of correlation functions for travel time, turbulent velocity and sound speed fluctuations. Hence, the effect of velocity and temperature fluctuations on acoustic wave propagation will be investigated. The effect of these two factors in application to the flowmeter equation as well as a new formulation of the classical flowmeter equation that has not been studied previously in the literature will be shown.

3.1 The Aerodynamic Equations of a Compressible Gas

Any medium, in which sound is propagated, whether it is a gas, a liquid, or a solid, has an atomic structure. However, it has been shown [*Leontovich*, 1936; *Blokhintzev*, 1953] that for a gas, if $f << 1/\tau_c$ (where f is the sound frequency and τ_c is the mean time between collisions) the gas can be regarded as a continuous medium, which is characterized by certain constants. Such a method of analysis is used in the theory of aerodynamics [*Blokhintzev*, 1953]. The aerodynamic equations of a compressible gas are taken as a basis of the theoretical analysis of the problem of the acoustics of a moving medium. The aerodynamic equations of a compressible gas are expressed in three fundamental conservation laws.

Continuity Equation

Assuming that there are no chemical reactions, the continuity equation is

$$\frac{\partial \rho}{\partial t} + \nabla \cdot (\rho \mathbf{V}) = 0 . \tag{3.1}$$

Momentum Equation

The general form of the momentum equation of is:

$$\frac{\partial}{\partial t}(\rho \mathbf{V}) + \nabla \cdot (\rho \mathbf{V}\mathbf{V}) = \nabla \cdot \overline{\overline{\mathbf{P}}} + \mathbf{F}_g . \tag{3.2}$$

The pressure tensor is:

$$\overline{\overline{\mathbf{P}}} = \{p_{ij}\}, \text{where } p_{ij} = -p\delta_{ij} + \tau_{ij}, i, j = 1,2,3., \tag{3.3}$$

where

$$\delta_{ij} = \begin{cases} 0 \text{ if } i \neq j \\ 1 \text{ if } i = j \end{cases} .$$

The term p_{ij} is the ij th components of the stress tensor acting on the area perpendicular to e_j with the direction given by e_i. The term τ_{ij} is the ij th components of the viscous stress tensor $\overline{\overline{\mathbf{T}}}$ in accordance with Stokes theory, expressed for Newtonian fluids as

$$\overline{\overline{\mathbf{T}}} = \mu_v \left\{ \left(\frac{\partial V_i}{\partial x_j} + \frac{\partial V_j}{\partial x_i} \right) - \frac{2}{3} \frac{\partial V_k}{\partial x_k} \delta_{ij} \right\}, i, j, k = 1,2,3., \tag{3.4}$$

where μ_v is a viscosity coefficient.

Energy Equation

$$\frac{\partial}{\partial t}(\rho E_t) + \nabla \cdot (\rho E_t \mathbf{V}) = -\nabla \cdot (p\mathbf{V}) + \nabla \left(\overline{\overline{\mathbf{T}}} \cdot \mathbf{V} \right) + \nabla \cdot \mathbf{q} . \tag{3.5}$$

The total specific energy E_t is obtained as a sum of the specific internal energy e and the specific kinetic energy

$$E_t = e + \frac{V^2}{2} . \tag{3.6}$$

The heat transfer by conduction per unit mass is given by Fourier's Law as

$$\mathbf{q} = -æ\nabla T , \tag{3.7}$$

where the thermal conductivity æ is given by $æ = \rho c_0 \kappa$, and κ is thermal diffusivity and c_p is specific heat at constant pressure. To the three basic laws of hydrodynamics there must be added a constitutive equation such as the equation of state of the gas, which connects the pressure, the density and the temperature:

$$p = Z(\rho, T). \qquad (3.8)$$

From the first law of thermodynamics we have for the energy per unit mass

$$de = TdS - pdVol, \qquad (3.9)$$

where S is the entropy, and Vol is a specific volume ($Vol = 1/\rho$). Then

$$\frac{de}{dt} = T\frac{dS}{dt} - p\frac{dVol}{dt} = T\frac{dS}{dt} + \frac{p}{\rho^2}\frac{d\rho}{dt}. \qquad (3.10)$$

On the other hand,

$$\frac{d\rho}{dt} = \frac{\partial\rho}{\partial t} + (\mathbf{V}\cdot\nabla)\rho = -\rho\nabla\cdot\mathbf{V} \Rightarrow p\frac{\nabla\cdot\mathbf{V}}{\rho} = -\frac{p}{\rho^2}\frac{d\rho}{dt}. \qquad (3.11)$$

The effect produced by viscosity and heat conduction in general energy balance usually appears as small corrections [*Blokhintzev*, 1953] thus the process of sound propagation in air is considered adiabatic. Consequently, for adiabatic processes we have

$$\frac{de}{dt} = \frac{p}{\rho^2}\frac{d\rho}{dt} \Rightarrow e = \int^p \frac{dp}{\rho} - \frac{p}{\rho}, \qquad (3.12)$$

The quantity $\frac{de}{dt} = \frac{p}{\rho^2}\frac{d\rho}{dt} \Rightarrow w = e + \frac{p}{\rho} = \int^p \frac{dp}{\rho}$ is known as enthalpy. If the process is non-adiabatic, then equation (3.10) must be used. Then we get from equations (3.5) and (3.10)

$$T\frac{dS}{dt}=\frac{1}{\rho}\nabla\cdot\mathbf{q}+\frac{1}{\rho}\nabla\left(\overline{\overline{\mathbf{T}}}\cdot\mathbf{V}\right). \qquad (3.13)$$

If we neglect æ and μ, since the effect produced by them in the general energy balance usually negligible, we have

$$\frac{dS}{dt}=\frac{\partial S}{\partial t}+\mathbf{V}\cdot\nabla S=0, \qquad (3.14)$$

i.e., the motion of fluid is adiabatic. If the motion is also irrotational, $\nabla\times\mathbf{V}=0$ then the Bernouilli theorem holds. It is convenient to introduce the velocity potential by putting $\mathbf{V}=-grad\Pi$, momentum and energy equation (3.5) leads to

$$\nabla\left[-\frac{\partial\Pi}{\partial t}+0.5(\nabla\Pi)^2\right]=-\frac{\nabla p}{\rho}. \qquad (3.15)$$

Taking into consideration that $\frac{\nabla p}{\rho}=\nabla w$, integration of equation (3.15) yields

$$w=\int_p\frac{p}{\rho}=\frac{\partial\Pi}{\partial t}-0.5(\nabla\Pi)^2. \qquad (3.16)$$

If the compressibility of the fluid is also neglected, then $w=\frac{p}{\rho_0}+const$, consequently,

$$p=\rho_0\frac{\partial\Pi}{\partial t}-\frac{\rho_0}{2}(\nabla\Pi)^2+const, \qquad (3.17$$

and for stationary flow,

$$p=const-\frac{\rho_0}{2}(\nabla\Pi)^2=const-\frac{\rho_0 V^2}{2}. \qquad (3.18).$$

The fact that the entropy of an ideal fluid $(æ=\mu=0)$ undergoing motion remains a constant, makes it expedient to replace the variables (ρ,T) in the equation of state (3.8)

by variables (ρ, S).

3.2 The Acoustic Equations in the Absence of Wind

An oscillatory motion with small amplitude in a compressible fluid is called a sound wave. The vibrations of the medium can be represented as acoustic vibrations under the following assumptions:

1. Vibrations are small, so that any changes of state of the gas in an arbitrary small volume can be neglected.
2. Frequencies under consideration are in the audible range (classical acoustics), or near it (ultrasonic).

Based on aforementioned assumptions the terms of the second order can be neglected. The relative changes in the fluid density and pressure are assumed to be small, namely

$$p = p_0 + p_a, \rho = \rho_0 + \rho_a, \tag{3.19}$$

where p_a is the excess pressure, ρ_0 is the density at $p = p_0$, $T = T_0$ and $\mathbf{V} = \mathbf{V}_a$ ($\mathbf{V}_a$ is a small velocity). In a similar fashion, we have for the temperature, entropy and energy

$$T = T_0 + T_a, S = S_0 + S_a, e = e_0 + e_a. \tag{3.20}$$

We then get from equations (3.1, 3.2)

Continuity Equation

$$\frac{\partial \rho_a}{\partial t} + \rho_0 \nabla \cdot \mathbf{V}_a = 0. \tag{3.21}$$

Momentum Equation

$$\rho_0 \frac{\partial \mathbf{V}_a}{\partial t} = -\nabla p_a + \mu \nabla^2 \mathbf{V}_a + \frac{1}{3} \mu \nabla \nabla \cdot \mathbf{V}_a = 0. \tag{3.22}$$

The closure relation for an ideal gas is $p = \rho RT$, where R is the gas constant per unit mass. In terms of (ρ, S) this becomes

$$p = \rho^{\gamma} \frac{p_0}{\rho_0^{\gamma}} \exp\left(\frac{S - S_0}{c_v} \right), \qquad (3.23)$$

where c_v is the specific heat at constant volume and $\gamma = c_p / c_v$ is the ratio of the specific heats. The condition that the linearized equations of motion (3.21, 3.22) should be applicable to the propagation of sound waves is that the velocity of the fluid particles in the wave should be small compared with the velocity of sound: $V << c$. This condition can be obtained, for example, from the requirement that $\rho_a << \rho_0$.

Energy Equation

For small changes in the state, equation (3.23) leads to [*Blokhintzev*, 1953]

$$p_a = \gamma \frac{p_0}{\rho_0} \rho_a + \frac{p_0}{c_v} \rho_a + ... = c^2 \rho_a + h S_a + ...; h = \frac{p_0}{c_v}. \qquad (3.24)$$

For $S_a = 0$, the only term left is the one, which represents the small change in pressure for small adiabatic expansions or compressions. The quantity $c = \sqrt{\frac{\gamma p_0}{\rho_0}}$ is adiabatic sound velocity. The second term represents the change in pressure produced by the influx or outflow of heat. The entropy changes satisfy equation (3.14), which, neglecting quantities of second order, may be written in the form

$$T_0 \frac{\partial S_a}{\partial t} = \frac{æ}{\rho_0} \nabla^2 T_a. \qquad (3.25)$$

Temperature changes T_a can be expressed in terms of the changes in the density and entropy. Consequently, from equation (3.9)

$$T = \left(\frac{\partial e}{\partial S}\right)_{\rho} . \qquad (3.26)$$

The energy of an ideal gas is given by

$$e = c_v T = \frac{p}{(\gamma - 1)\rho} = \frac{p_0 \rho^{\gamma - 1}}{(\gamma - 1)\rho_0^{\gamma}} \exp(S_a / c_v). \qquad (3.27)$$

Since $\frac{\partial e}{\partial S} = \frac{\partial e}{\partial S_a}$, equation (3.26) can be written in the form

$$T = \frac{p_0 \rho^{\gamma - 1}}{(\gamma - 1)c_v \rho_0^{\gamma}} \exp(S_a / c_v) = \frac{p}{(\gamma - 1)c_v \rho}, \qquad (3.28)$$

i.e. for small changes of density and entropy

$$T_a = \frac{p_0 \rho_a}{c_v \rho_0^2} + \frac{p_0 \rho_a}{(\gamma - 1)c_v^2 \rho_0} + \ldots . \qquad (3.29)$$

Here the first term represents the change in temperature, which follows from the adiabatic expansion or compression of gas, while the second represents the change in temperature due to a change in the entropy Substituting in equation (3.25) leads to

$$\frac{\partial S_a}{\partial t} = \kappa \nabla^2 S_a + \kappa_1 \nabla^2 \rho_a, \kappa_1 = \kappa \ \frac{(\gamma - 1)}{\rho_0} c_v . \qquad (3.30)$$

Equations (3.21, 3.22, 3.30) together with the equation of state (3.24) govern the propagation of sound in a medium at rest, taking viscosity and heat conduction into account. In all instances, in which sound absorption is not a matter of concern the viscosity and thermal conductivity of the air can be ignored. Putting $(æ = \mu = 0)$ leads to $S_a = 0$, i.e. adiabatic sound propagation, and the governing equations are

$$\frac{\partial \rho_a}{\partial t} + \rho_0 \nabla \cdot \mathbf{V}_a = 0 , \qquad (3.31)$$

$$\rho_0 \frac{\partial V_a}{\partial t} = -\nabla p_a, \qquad (3.32)$$

$$p_a = c^2 \rho_a. \qquad (3.33)$$

These equations can be solved using the velocity potential. Setting

$$p_a = \rho_0 \frac{\partial \Pi_a}{\partial t}; \mathbf{V}_a = -\nabla \Pi_a \qquad (3.34)$$

satisfies the equation (3.31). Then from equations (3.32, 3.33) the wave equation for the potential is obtained

$$\nabla^2 \Pi_a - \frac{1}{c^2} \frac{\partial^2 \Pi_a}{\partial t^2} = 0. \qquad (3.35)$$

The wave is called plane wave if all its quantities depend only on one coordinate, for example *x*-coordinate. That is, the flow is homogeneous in the *yz*-plane. The wave equation (3.35) becomes

$$\frac{\partial^2 \Pi_a}{\partial x^2} - \frac{1}{c^2} \frac{\partial^2 \Pi_a}{\partial t^2} = 0. \qquad (3.36)$$

The solution of the equation (3.36) has the following form

$$\Pi_a = f_1(x - ct) + f_2(x + ct). \qquad (3.37)$$

The distribution of the other quantities p_a, ρ_a, V_a in a plane wave is given by functions having the same form. If $f_2 = 0$ then, for density $\rho_a = f_1(x - ct)$. Expression $f_1(x - ct)$ represents a traveling plane wave. Since only $V_x = \partial \Pi_a / \partial x$ is non-zero component of fluid velocity in a sound wave, sound wave in a fluid are longitudinal. In the case of monochromatic waves all quantities are periodic (harmonic) functions of the time. For example, velocity potential has the following form

$$\Pi_a = re\left[\Pi_{a0}(x,y,z)\exp(-i\omega t)\right], \tag{3.38}$$

where ω is the frequency of the wave. The function ϕ_0 satisfies the equation

$$\Delta\Pi_{a0} + \left(\omega^2 / c^2\right)\Pi_{a0} = 0\,, \tag{3.39}$$

which is obtained by substitution of equation (3.38) into the wave equation. In the case of a monochromatic traveling plane wave, propagating in a positive direction of *x*-axis is considered, the potential is of the form

$$\Pi_a = re\left[A\exp(-i\omega(t - x/c))\right], \tag{3.40}$$

where A is a constant called the complex amplitude. Writing this as $A = ae^{i\alpha}$ with real constants a and α

$$\Pi_a = a\cos\left[\omega x/c - \omega t + \alpha\right], \tag{3.41}$$

where a is called amplitude of the wave, and the argument of the cosine is called the phase. If $\mathbf{n}$ is a unit vector in the direction of propagation, then the vector

$$\mathbf{k} = \left(\omega/c\right)\mathbf{n} = \left(2\pi/\lambda\right)\mathbf{n} \tag{3.42}$$

is called the wave vector, and its magnitude k the wave number. In terms of this vector equation (3.40) can be written as

$$\Pi_a = re\left[A\exp(-i(\mathbf{k}\cdot\mathbf{r} - \omega t))\right]. \tag{3.43}$$

Any wave can be represented as a sum of superimposed monochromatic waves with various wave vectors and frequencies. The decomposition of a wave into monochromatic waves is an expansion as a Fourier series or integral.

3.3 Fundamental Acoustic Equations of the Moving Medium

Acoustic phenomena become more complicated in the presence of airflow. In the general case, strictly speaking, it is not possible to distinguish acoustic phenomena from the non-linear processes, which take place in a moving medium. For example, a current of pulsating velocity acts on a microphone placed in the flow as if it were sound of the corresponding frequency (provided that the frequency of these pulsations is sufficiently high) although the velocity of propagation of these pulsations is different from the velocity of sound. The relation between the pressure of these pulsations and their velocity is non-linear and fundamentally different from the relation between the pressure and velocity of sound wave. In order to distinguish sound propagation in a medium from acoustic phenomena arising in the same medium as a result of motion of the medium, the motion is considered to be frozen, i.e. it is assumed that motions in the flow are sufficiently slow that

$$\tau >> 1/f \qquad (3.44),$$

where τ is the time for an appreciable change in the state of flow [*Tatarskii*, 1961]. Supposing sound is propagated in the medium, the state of which is described by the variables V, p, ρ, S. The original state of the medium is considered as steady state and the sound is regarded as a small perturbation, so that all the variables under consideration have small fluctuations: p_a, ρ_a, V_a, S_a. In order to obtain the equations of the sound wave, the following replacements are introduced [*Blokhintzev*, 1953]

$$V = V + V_a, p = p_0 + p_a, \rho = \rho_0 + \rho_a, S = S + S_a \qquad (3.45)$$

Limiting ourselves to the linear approximations, the terms of higher order of the relatively small quantities p_a, ρ_a, V_a, S_a. In addition, the irreversible processes, which take place in sound propagation, are neglected. This means that in linear equations for p_a, ρ_a, V_a, S_a the terms that are proportional to viscosity and thermal conductivity are neglected. Under the listed assumptions the fundamental acoustic equations of the moving medium are [*Blokhintzev*, 1953]

$$\frac{\partial \rho_a}{\partial t} + \mathbf{V} \cdot \nabla \rho_a + \mathbf{V}_a \cdot \nabla \rho + \rho \nabla \cdot \mathbf{V}_a + \rho_a \nabla \cdot \mathbf{V} = 0, \qquad (3.46)$$

$$\frac{\partial V_a}{\partial t} + (\nabla \times \mathbf{V}) \times \mathbf{V}_a + (\nabla \times \mathbf{V}_a) \times \mathbf{V} + \nabla(\mathbf{V} \cdot \mathbf{V}_a) = -\frac{\nabla p_a}{\rho} + \frac{(\nabla p)\rho_a}{\rho^2}, \qquad (3.47)$$

$$\frac{\partial S_a}{\partial t} + \mathbf{V} \cdot \nabla S_a + \mathbf{V}_a \cdot \nabla S = 0. \qquad (3.48)$$

The equations of state are

$$p_a = c^2 \rho_a + h S_a ; c^2 = \left(\frac{\partial p}{\partial \rho} \right)_s ; h = \left(\frac{\partial p}{\partial \rho} \right)_\rho . \qquad (3.49)$$

The linear character of the system of equations (3.46-3.49) requires small disturbances to remain small in time, i.e. initial state is stable. The choice of thermodynamic variables ρ, S is extremely useful for general theoretical considerations. For final numerical calculations, however, the variables ρ, T are more convenient. The quantities $\left(\frac{\partial p}{\partial \rho} \right)_S, \nabla S$ in terms of the variables p and T can be found in the following way.

The closed system of the linearized equations of fluid dynamics (3.46-3.49) gives the starting equations for describing sound propagation in a moving medium. The first two equations of this system were used in the first papers on acoustics in a moving medium.

All equations of this system were derived and used for the study of sound propagation by *Blokhintzev*. In the system of fundamental equations (3.46-3.49) there are five unknown even if one variable is eliminated by means of equation (3.49). The system therefore is exceedingly complicated. The fundamental difficulty lies in the fact that as soon as the pressure in the medium appears as a function of two coordinates ρ, S or ρ, T, then even in a quiescent medium, where there are no vortices and no current at all, the right hand side of equation (3.46) will still not be a total differential and therefore sound will be rotational. Important simplifications are obtained in the case when the changes in p_a, ρ_a, V_a, S_a are small over one wavelength of the sound. This approach is called ray acoustics [*Kolmogorov*, 1941].

3.4 Ray Acoustics Approach

The basic characteristics of sound propagation in the atmosphere are determined by slow changes in the state of the medium, for example, wind force, temperature and density of the air. Under these conditions it is expedient to make use of the methods of ray acoustics. In the following, the basic equations of ray acoustics are introduced in the form that Blochintzev derived them. Starting with the system of equations (3.46-3.49), it is assumed that flow parameters undergo only small changes within a single wavelength. In order to make use of this fact in an approximate theory of sound propagation, it is assumed that

$$\begin{aligned} &V_a = V_{a0}\exp(i\Phi);\ p_a = p_{a0}\exp(i\Phi); \\ &\rho_a = \rho_{a0}\exp(i\Phi);\ S_a = S_{a0}\exp(i\Phi);, \\ &\Phi = \omega t - k_0 W,\ k_0 = \omega_0 / c_0 = 2\pi / \lambda_0 \end{aligned} \qquad (3.50).$$

where ω is a sound frequency, $k_0 = \omega_0 / c_0 = 2\pi / \lambda_0$ is the wave number in the undisturbed state of the medium, W is called the eikonal. The following assumptions are made in order to derive the system of ray acoustic equations [*Blokhintzev*, 1953]. The quantities $V_{a0}, p_{a0}, \rho_{a0}, S_{a0}$ are considered to be slow changing functions of the coordinated and time. The value of k_0 is considered to be large, so that the phase $k_0 W$ changes very rapidly. The solutions for fluctuations of ambient flow parameters p_a, ρ_a, V_a, S_a will be sought in the form of a series of inverse powers of the large parameter ik_0

$$
\begin{aligned}
V_{a0} &= V'_{a0} + \frac{V''_{a0}}{ik_0} + \ldots; \; p_{a0} = p'_{a0} + \frac{p''_{a0}}{ik_0} + \ldots; \\
\rho_{a0} &= \rho'_{a0} + \frac{\rho''_{a0}}{ik_0} + \ldots; \; S_{a0} = S'_{a0} + \frac{S''_{a0}}{ik_0} + \ldots;
\end{aligned}
\qquad (3.51)
$$

Substituting (3.50) in equations (3.46-3.49) leads to the following system

$$
\begin{aligned}
& ik_0 \left\{ q\mathbf{V}_{a0} - \nabla W \frac{p_{a0}}{\rho} \right\} = b_1, \\
& b_1 = -\frac{\partial \mathbf{V}_{a0}}{\partial t} - \mathbf{V}_{a0} \times (\nabla \times \mathbf{V}) + \mathbf{V} \times (\nabla \times \mathbf{V}_{a0}) - \nabla(\mathbf{V} \cdot \mathbf{V}_{a0}) - \frac{\nabla p_{a0}}{\rho} + \frac{\nabla p}{\rho^2} \left(\frac{p_{a0} - hS_{a0}}{c^2} \right)
\end{aligned}
\qquad (3.52)
$$

$$
\begin{aligned}
& ik_0 \left\{ \frac{q}{c^2} p_{a0} - \frac{hq}{c^2} S'_{a0} - \rho \mathbf{V}'_{a0} \nabla W \right\} = b_2, \\
& b_2 = -\frac{1}{c^2} \frac{\partial p'_{a0}}{\partial t} + \frac{1}{c^2} \frac{\partial S'_{a0}}{\partial t} - \left(\mathbf{V} \cdot \nabla \frac{1}{c^2} \right) (p_{a0} - hS_{a0}) - \\
& \frac{1}{c^2} [\mathbf{V} \cdot (p_{a0} - hS_{a0})] - \rho \nabla \cdot \mathbf{V}_{a0} - (\nabla \rho) \cdot \mathbf{V}_{a0} - \frac{1}{c^2} (p_{a0} - hS_{a0}) \nabla \cdot \mathbf{V}
\end{aligned}
\qquad (3.53)
$$

$$ik_0 qS_{a0} = b_3, b_3 = -\frac{\partial S_{a0}}{\partial t} - (\mathbf{V}\cdot\nabla S_{a0}) - (\mathbf{V}_{a0}\cdot\nabla S),$$
$$\text{where } q = c_0 - \mathbf{V}\cdot\nabla W; \frac{q}{c} - \text{index of refraction} \quad (3.54).$$

Substituting (3.51) into system of equations (3.52-3.54) and collecting coefficients for like powers ik_0 the following two system of equations for zero and first power of ik_0 were obtained

For $(ik_0)^0$:

$$q\mathbf{V}'_{a0} - \nabla W\left(\frac{p'_{a0}}{\rho}\right) = 0, \quad (3.55)$$

$$\frac{q}{c^2}(p'_{a0} - hS'_{a0}) - \rho\mathbf{V}'_{a0}\cdot\nabla W = 0, \quad (3.56)$$

$$qS'_{a0} = 0 \quad (3.57).$$

For $(ik_0)^1$:

$$q\mathbf{V}''_{a0} - \nabla W\left(\frac{p''_{a0}}{\rho}\right) = b_1', \quad (3.58)$$

$$\frac{q}{c^2}(p''_{a0} - hS''_{a0}) - \rho\mathbf{V}''_{a0}\cdot\nabla W = b_2', \quad (3.59)$$

$$qS''_{a0} = b_3', \quad (3.60)$$

Here b_1', b_2', b_3' are the values of b_1, b_2, b_3 obtained upon substitution in them zero approximations for $V_{a0}, p_{a0}, \rho_{a0}, S_{a0}$ from equations (3.55-3.57). Solution of the system of ray acoustic equations (3.55-3.57) leads to the eikonal equation and consequently to the flowmeter equation. From the system of ray acoustic equations (3.58-3.60) an equation for determination of sound pressure can be obtained. We conclude this

subchapter with a list of assumptions that define the range of applicability of the ray acoustic approach [Rytov et al, 1978]:

$l_\varepsilon >> \lambda,$ where l_ε is a characteristic inhomogenuity size

$l_\varepsilon >> \sqrt{\lambda L},$ where L is a travel distance; $\sqrt{\lambda L}$ is a first Frenel zone

3.4.1 Eikonal Equation

We are concerned with a derivation of eikonal and flowmeter equations. In the following, the derivation obtained by *Blokhintzev* is reproduced. Solution of the equations (3.55-3.57) leads to the equation that connects particle velocity with pressure

$$\mathbf{V}'_{a0} = \frac{(\nabla W)}{q} \frac{p'_{a0}}{\rho}. \qquad (3.61)$$

By simultaneous solution of equations (3.56, 3.57) the equation of surface of constant phase ($W = const$) is obtained

$$|\nabla W|^2 = \frac{q^2}{c^2}. \qquad (3.62)$$

For $V = 0$ it follows from equation (3.54) that

$$\frac{q^2}{c^2} = \frac{c_0^2}{c^2} = \varepsilon^2, \qquad (3.63),$$

where ε is the index of refraction of sound waves. The expression known as the eikonal equation is

$$|\nabla W|^2 = \varepsilon^2. \qquad (3.64)$$

Substituting q from (3.54) into equation (3.62) and solving (3.62) for $|\nabla W| = \frac{\partial W}{\partial n}$, where $\frac{\partial W}{\partial n}$ denotes differentiation in the direction of the normal to the surface of constant phase, we get

$$|\nabla W| = \frac{\partial W}{\partial n} = \frac{c_0}{c + V_n}, \qquad (3.65)$$

where V_n is the projection of the wind velocity on the normal to the wave front, shown in Figure 3.1

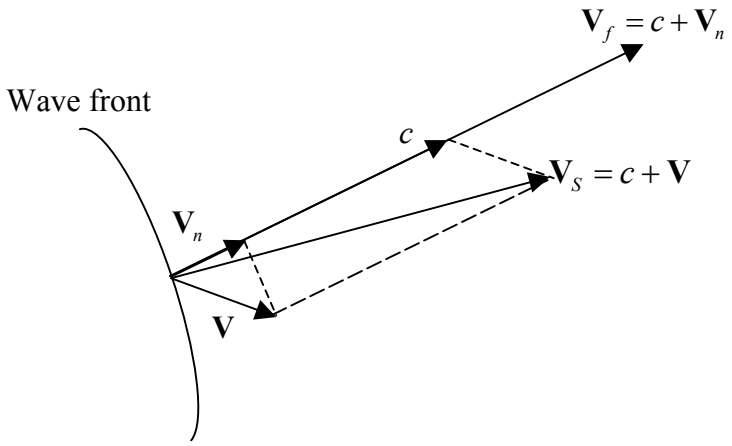

Figure 3.1. Kinematic relations in a geometrical theory of sound propagation.

Knowing $\frac{\partial W}{\partial n}$, we can determine the phase velocity of the wave V_f. The equation of the moving phase surface is

$$\Phi = \omega t - k_0 W = const\,. \qquad (3.66)$$

If we differentiate equation (3.66) with respect to time we find $\omega - k_0 \frac{\partial W}{\partial n}\frac{dt}{dn} = \omega - k_0 \frac{\partial W}{\partial n} V_f = 0$. On the basis of equation (3.65) we will obtain equation for the phase velocity of the wave

$$\mathbf{V}_f = c + \mathbf{V}_n, \qquad (3.67)$$

i.e. the phase velocity of the wave is equal to the local sound velocity plus the normal component of the flow velocity. Kinematic relation is shown in Figure 3.1. Formula (3.66) is one of the original assumptions in a geometrical theory of sound propagation.

3.4.2 Fermat's Principle

Surfaces of constant phase are given by $W = const$, and therefore define the wave fronts defined by equation (3.66) and shown in Figure 3.2 [*Bergmann and Schaefer*, 1999]. The direction of propagation $\mathbf{n}$ is normal to the phase surfaces. It is the gradient of the phase surfaces

$$\mathbf{n} = \frac{gradW}{|gradW|} \tag{3.68}$$

or, with equation (3.64)

$$\varepsilon \mathbf{n} = |gradW|. \tag{3.69}$$

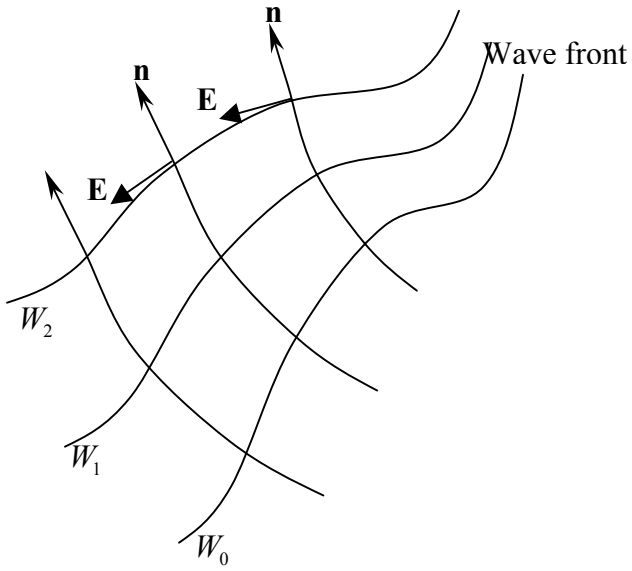

Figure 3.2. Surfaces of constant phase in an inhomogeneous medium. The rays are the curves perpendicular to the surfaces $W = const$.

The beam propagation is in the direction of $\mathbf{n}$. The curves, orthogonal to the phase surfaces are called beams or rays, $\mathbf{n}$ is the tangential vector to the beams. The difference of two adjoining eikonals dW, whose distance along a beam is ds, is $dW = \mathbf{n} \cdot \left| gradW \right| ds$, or with equation (3.69)

$$dW = \varepsilon ds \,. \qquad (3.70)$$

The integral is the length of the optical path between a transmitter (T) and a receiver (R)

$$\text{travel path} = \int_R^T \varepsilon \text{ds} = W(T) - W(R) \,. \qquad (3.71)$$

Fermat's principle is a principle of extremum and says that the travel path between transmitter and receiver always is an extremum [*Bergmann and Schaefer*, 1999]. The length of the travel path, measured along a ray is always shorter then any other path

$$\int_{\substack{R \\ rayS}}^{T} \varepsilon ds \le \int_{\substack{R \\ curveC}}^{T} \varepsilon ds \,, \qquad (3.72)$$

where *curve C* is an arbitrary path. In terms of the travel time equation (3.72) has the following form

$$\left(t_2 - t_1\right)_{rayS} < \left(t_2 - t_1\right)_{curveC} . \qquad (3.73).$$

3.5 Turbulence of the Atmosphere, Travel-time Fluctuations, Kolmogorov's "2/3" law.

In the preceding section we considered the propagation of sound in a slowly changing medium state. In a real atmosphere such characteristics give very general characteristics of sound propagation. In fact, in addition to the slow changes of the state

of the atmosphere, there take place much more rapid changes, which are produced by random fluctuations of the ambient temperature and wind velocity, i.e. by the turbulence of the atmosphere. These changes are very rapid and their effect on sound propagation cannot be treated by the methods of ray acoustics, since the dimensions of the region under consideration can be comparable with the wavelength. As the waves propagate through the medium, there occur scattering of the waves, fluctuations of amplitude, phase, frequency and other wave parameters [*Tatarskii*, 1961]. In this subsection we are interested in the phase or travel-time fluctuations. Since ray acoustics theory is not sufficient, the theory of wave propagation in turbulent media is founded on the statistical representation of isotropic and homogeneous turbulence together with Kolmogorov's "2/3" law, which states that the velocity fluctuations at two different points are proportional to the distance between these points to the power 2/3, and therefore sometimes it is called "2/3 law" [*Kolmogorov*, 1941, 1963; *Obukhov*, 1941]. For small time intervals it is expedient to consider turbulence to be superimposed on the mean wind, i.e. the change in the mean wind will fall outside of small units of time of the observation [*Blokhintzev*, 1953]. The sound propagates a distance L across the turbulent flow from a speaker to microphone, as shown in Figure 3.3. The flowmeter equation may be used to derive an expression for a travel time of a wave, traveling from a speaker to a microphone t_1 and in opposite direction t_2 [*Krasil'nikov*, 1949]. Flowmeter equation follows directly from eikonal equation (3.65). Travel times may be written as

$$t_1 = \int_0^L \frac{dy}{c - u_1} \approx t_0 + \frac{1}{c^2}\int_0^L u_1\, dy,\ u_1 = U\sin\beta + u_1'$$
$$t_2 = \int_0^L \frac{dy}{c + u_2} \approx t_0 - \frac{1}{c^2}\int_0^L u_2 dy,\ u_2 = U\sin\beta + u_2' \quad , \qquad (3.74)$$

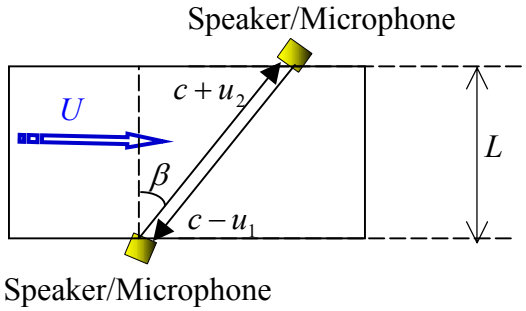

Figure 3.3 Sketch of experimental setup.

where t_0 is a travel time in the undisturbed media, U is a mean velocity, c is a sound speed, u' are fluctuations along the sound path. In Equation (3.74) we neglected the terms of order $U/c,\ U^2/c^2$. Then, for the time difference we find:

$$\Delta t = t_2 + t_1 - 2t_0 \approx \frac{1}{c^2}\int_0^L \left(u_1' - u_2'\right)dy = \frac{1}{c^2}\int_0^L \Delta u dy\,. \qquad (3.75)$$

However, the turbulent velocity fluctuations on which travel time of the wave depends appear as a random function of time and position. Then, from Equation (3.75)

$$\overline{\Delta t^2} = \frac{1}{c^4}\int_0^L dy' \int_0^L dy''\, \overline{\Delta u(y')\Delta u(y'')}\,. \qquad (3.76)$$

where the overscore indicates time averaging. The principal change in the total velocity u is due to the drift of the turbulence in the mean flow, so that the change in the velocity

u in the time t can be represented as the result of a displacement of the turbulence in a small distance $\delta(\vartheta) = ut$ as shown in Figure 3.4 for the case of perpendicular direction of the sound wave [*Krasil'nikov*, 1949, 1963]. The under integral term in Equation (3.76) is:

$$\overline{\Delta u(y')\Delta u(y'')} = \overline{\left[u(y',0) - u(y',\delta)\right]\left[u(y'',0) - u(y'',\delta)\right]} = \\ = \overline{u(y',0)u(y'',0)} + \overline{u(y',\delta)u(y'',\delta)} - \overline{u(y',\delta)u(y'',0)} - \overline{u(y',0)u(y'',\delta)} \quad . \qquad (3.77)$$

To take into account the correlation of fluctuations at different points of the flow we use the "2/3" law obtained independently by Kolmogorov [1941] and Obukhov [1941]. Following this law, one may get:

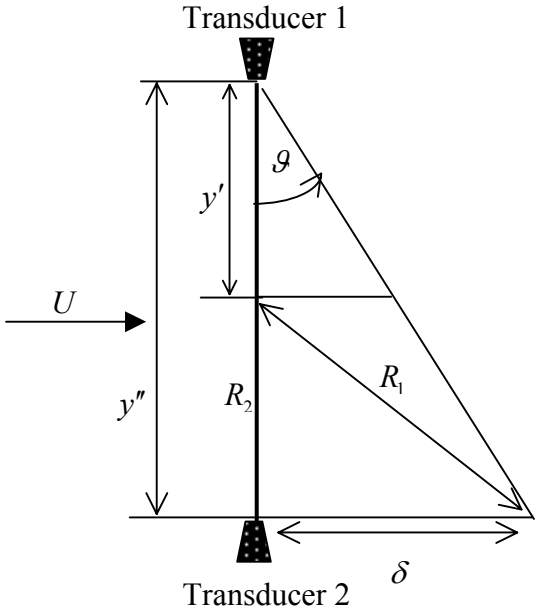

Figure 3.4. Sketch for the basic relations for the ultrasound measurement.

$$\overline{\left[u(y') - u(y'')\right]^2} = C^2 R^{2/3}, \qquad (3.78)$$

where constant C is the characteristic of turbulence having a dimension of $1cm^{2/3} \times s^{-1}$ and R is a distance between the points y' and y''. However, based on the hypotheses of isotropy of the turbulence the left side of Eq. (3.78) may be written as following

$$C^2 R^{2/3} = \overline{\left[u(y') - u(y'')\right]^2} = 2\overline{\left[\left(u(y')\right)^2 - u(y')u(y'')\right]}. \quad (3.79)$$

Based on the Figure 3.4 it is seen that

$$R_1 = R\left((y', \delta), (y'', 0)\right) = R\left((y', 0), (y'', \delta)\right), \quad (3.80)$$

$$R_2 = R\left((y', 0), (y'', 0)\right) = R\left((y', \delta), (y'', \delta)\right), \quad (3.81)$$

Simple geometry for small ϑ gives the following:

$$R_1^2 = \delta^2 + (y' - y'')^2, \quad (3.82)$$

$$R_2^2 = (y'' - y')^2. \quad (3.83)$$

Now making use of the 2/3 law and equations (3.82), (3.83), one obtains for equation (3.77):

$$\overline{\Delta u(y') \Delta u(y'')} = C^2 \left\{R_1^{2/3} - R_2^{2/3}\right\} = -0.5C^2 \left\{2(y' - y'')^{2/3} - 2\left((y' - y'')^2 + \delta^2\right)^{1/3}\right\}. \quad (3.84)$$

Substitution of the Equation (3.84) into Equation (3.76), and integration yields the following result:

$$\overline{\Delta t^2} = C^2 L \left(\frac{1}{c^2}\right)^2 \delta^{5/3} const. \quad (3.85)$$

in which the *const* was determined experimentally in the works by *Obukhov* [1951] to be equal to 3. Then, for the standard deviation the following expression takes place [*Krasil'nikov*, 1949]

$$\sigma = \sqrt{\overline{\Delta t^2}} = \sqrt{3} C L^{1/2} \left(\frac{1}{c^2} \right) (\delta)^{5/6} . \qquad (3.86)$$

Limits of Applicability of Geometrical Optics and Kolmogorov's law

The theory of travel-time fluctuation, which we have just considered was based on the equations of geometrical optics, statistical description of the turbulence and Kolmogorov's "2/3" law. The area of validity is defined by the following limits [*Rytov et al*, 1978]

1. $\lambda << l_\varepsilon$

If there is a geometrical object with dimension l_ε is located on the propagation path of a plane wave. At a distance L from the obstacle we obtain its image with the same dimension l_ε. At the same time diffraction of the wave by the obstacle will occur. The angle of divergence o the diffracted wave by the obstacle will be of order $\alpha \sim \lambda / l$. At a distance L from the obstacle the size of the distracted bundle will be of order $\alpha L \sim \lambda L / l$. In order to neglect by diffraction effects it is necessary for the relation $\lambda L / l_\varepsilon << l_\varepsilon$ to hold. Consequently, the second condition is

2. $\sqrt{\lambda L} << l_\varepsilon$

Parameter $\sqrt{\lambda L}$ is called the first Fresnel zone. The second condition applies restrictions on the length of the travel path, i.e. $L << L_{critical} = l_\varepsilon^2 / \lambda$. In the Chapter 4 it will be shown based on our experimental data and supported by theoretical evidences [*Rytov et al*, 1978] that for travel time variances in the presence of small diffraction effects, the ray acoustic analytical approach may be considered as valid one for prediction of the travel time

variance. Consequently, the area of applicability of the ray acoustic approach for calculation of travel time can be broader than the rigorous sufficient conditions define.

3.6 Travel-time Statistics of Acoustic Waves as an Experimental Tool for Diagnostic of Turbulent Medium.

The fact that an acoustic wave carries some structural information regarding the turbulent medium, after interaction, makes it possible to use the statistical characteristics of the acoustic wave as a diagnostic tool to obtain some statistical information about the medium. We consider isotropic homogeneous turbulence. The original goal of the following theoretical derivations was firstly, to develop a methodology for determination of correlation functions of turbulent velocity and sound speed fluctuations. Secondly, to demonstrate quantitatively that effect of thermal fluctuations is as important as the effect of velocity fluctuations on acoustic wave propagation. The ultrasonic flowmeter equation is reconsidered, where the effects of turbulent velocity and sound speed fluctuations are included [*Andreeva and Durgin*, 2001, 2002, 2003]. The result is an integral equation in terms of correlation functions for travel time, turbulent velocity and sound speed fluctuations.

We start with a classical equation for the flowmeter in the form it was derived in equation (3.74) applied to waves traveling downstream shown in Figure 3.5

$$t = \int_s \frac{dy}{c-u} \approx t_0 + \frac{1}{c^2}\int_s \left(U\sin\beta + u'\right)dy; u = U\sin\beta + u'. \qquad (3.87)$$

In the experiment the only parameter that is measured is the travel time of ultrasound pulses $t(s)$. Our intention is to construct a correlation function of the travel time using

experimental data. The data from experiments performed for a finite number of different lengths s, s', s'' etc are collected. For each of these lengths 700 realizations were completed, in other words, ultrasonic pulse traveled 700 times from the transmitter to the receiver. For instance, for two lengths s, s' we have two columns of travel times, $t(s)$ and $t(s')$. We multiply corresponding elements from $t(s)$ and $t(s')$, average it over 700 realizations to get the product $\langle t(s)t(s')\rangle$. Proceeding with the described operation for the rest of the travel path lengths we obtain a correlation function of travel time t as follows

$$K_t(s,s') = \frac{\sum_N t(s)t(s')}{N}, \tag{3.88}$$

where N is a number of realizations. Our objective here, then, is to construct spatial correlation functions for turbulent velocity u' and sound speed fluctuations c'.

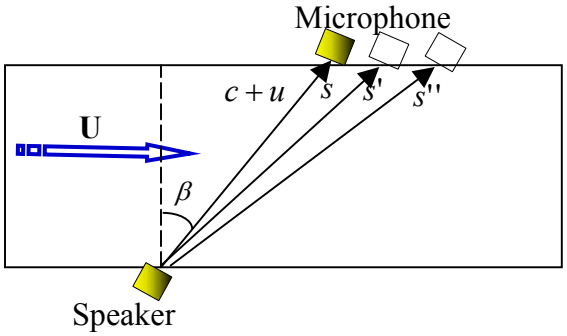

Figure 3.5. Scheme of experimental setup.

Perturbation analysis applied to (3.87) leads to the following expression:

$$t(s) = \int_s \frac{dx}{U\sin\beta + u' + \bar{c} + c'} = \frac{1}{\bar{c}}\int_s \frac{dx}{1 + \frac{U\sin\beta}{\bar{c}} + \frac{u'}{\bar{c}} + \frac{c'}{\bar{c}}} \cong$$
$$\cong \frac{1}{\bar{c}}\int_s \left(1 - \frac{U\sin\beta}{\bar{c}} - \frac{u'}{\bar{c}} - \frac{c'}{\bar{c}}\right)dx = \frac{s}{\bar{c}} - \frac{U\sin\beta}{\bar{c}^2} - \frac{1}{\bar{c}^2}\int_s (u' + c')dx \tag{3.89}$$

Here we assumed that terms $u'/\bar{c}$ and $c'/\bar{c}$ are the same order infinitesimal compare to unity. In order to construct the correlation function we introduce new variable:

$$t^0(s) = t(s) - \langle t(s) \rangle . \tag{3.90}$$

where angular brackets mean an operation of time averaging. Consequently,

$$t^0(s) = -\frac{1}{\bar{c}^2}\int_s (u' + c')\,dx; \;\; t^0(s') = -\frac{1}{\bar{c}^2}\int_{s'} (u' + c')\,dx' \;\; . \tag{3.91}$$

Then,

$$\begin{aligned} t^0(s)t^0(s') = \frac{1}{\bar{c}^4}\left[\int_s\int_{s'} \{u'(x)u'(x') + c'(x)c'(x')\}\,dxdx'\right] + \\ + \frac{1}{\bar{c}^4}\left[\int_s\int_{s'} \{c'(x)u'(x') + u'(x)c'(x')\}\,dxdx'\right] \end{aligned} \;\; . \tag{3.92}$$

In the Equation (3.92) the first two terms represent the auto correlation functions of turbulent velocity and sound speed fluctuations respectively. The second two terms are cross correlation functions of turbulent velocity and sound speed fluctuations. In the classical theory of isotropic, homogeneous turbulence cross correlation between velocity and temperature, and, consequently between velocity and sound speed must necessarily vanish everywhere. For the velocity measurement used here, the data were collected in the isotropic region of flow, so that u' and c' are not correlated. Consequently, the space correlation function of time can be defined from the following equation

$$\left\langle t^0(s)t^0(s') \right\rangle = K_t(s,s') = \frac{1}{\bar{c}^4}\left[\int_s\int_{s'} \left(K_{u'}(x,x') + K_{c'}(x,x')\right)dxdx'\right]. \tag{3.93}$$

It was observed experimentally [*Sepri*, 1976] that the velocity statistics were identical within experimental limits with and without grid heating. It is important to emphasize that the space correlation function $K_u(x,x')$ alone can be defined based on data from

room temperature experiments. Then, data from heated air experiments can be used to identify $K_c(x,x')$ knowing $K_u(x,x')$ that is taken unchanged from the room temperature experiment and $K_t(s,s')$.

3.7 Parabolic Equation Approximation

As it was mentioned in section 3.2 the closed system of linearized equations (3.46-3.49) is rather complicated. One of the simplifications, the ray acoustics approach, was discussed and applied in the previous subsection. Nevertheless, scientists have been trying to reduce the system to a single equation, which would be simpler then for analysis then the starting system. There are various approximations or assumptions about a moving medium in use, such as the Andreev-Rusakov-Blokhintzev equation for irrotational flow, Monin's equation for dry air, Goldstein equation for sound waves in parallel shear flow, equation for acoustical and internal gravity waves in a stratified moving medium, derived by *Ostashev* [1997], parabolic equation method approximation. These are only a few approximations existing up to date. Because of the specifics of our research work, namely, when limits of applicability of ray acoustics theory are violated, i.e.

1. $l_\varepsilon >> \lambda$
2. $l_\varepsilon << \sqrt{\lambda L}$
3. $l_0^2/\lambda < L < L_0^2/\lambda$ – Diffraction region

If this is the case, then effects of small diffractions must be taken into account. The parabolic equation exhibits a perfect fit for this situation. The parabolic equation method

is very powerful method in the theory of wave propagation. We do not intend to rederive the parabolic equations, but rather reproduce it in the form it was derived by *Rytov* [1978] from the Helmholtz equation

$$\Delta u + k^2\left(1+\tilde{\varepsilon}(r)\right)u = 0 \qquad (3.94)$$

where u is the wave field, k is the wave number and $\tilde{\varepsilon} = \left[\varepsilon(\mathbf{r}) - \bar{\varepsilon}\right]/\bar{\varepsilon}$ reflects the relative fluctuations of dielectric permeability [*Rytov*, 1978]. We consider a plane wave propagating along the direction x. Let u be such that $u = A_0 \exp(ikx)$. We assume that l is the smallest correlation length. We study only the high-frequency propagation, $kl > 1$. This condition allows us to neglect, explicitly, the backscattered parts of the wave in the Helmholtz equation. It is useful to express the solution of equation (3.94) in the following form:

$$u(x,\mathbf{r}) = v(x,\mathbf{r})\exp(ikx), \mathbf{r} = (y,z) \qquad (3.95)$$

Here $v(x,\mathbf{r})$ is complex wave amplitude. Substitution of the equation (3.95) in (3.94) leads to the parabolic wave equation [*Rytov*, 1978]

$$2ik\frac{\partial v}{\partial x} + \frac{\partial^2 v}{\partial y^2} + \frac{\partial^2 v}{\partial z^2} + k^2\tilde{\varepsilon}(x,\mathbf{r})v = 0\,. \qquad (3.96)$$

In a turbulent medium there are inhomogeneities with different scales, which are greater than the inner scale of turbulence, l_0, and smaller than the outer scale, L_0: $L_0 > l > l_0$. It has been shown, [*Ostashev*, 1997] that in a turbulent medium the range of applicability of the parabolic equation is given by inequality $L_0 >> \lambda$. The parabolic equation cannot be solved exactly in a general case. As the velocity fluctuations are small ($\sigma_\varepsilon << 1$, where $\sigma_\varepsilon = \sqrt{\langle \varepsilon^2 \rangle}$), the parabolic equation can be solved using a perturbation

method or, so called, the first order Rytov approximation. The method of perturbations is perfectly suited for investigating such wave parameters as the phase difference and the log-amplitude. Introducing the complex amplitude $v(x,\mathbf{r})$ as follows

$$v(x,\mathbf{r}) = A_0 \exp\left[(i\phi(x,\mathbf{r}) + \ln\frac{A(x,\mathbf{r})}{A_0} \right] = A_0 \exp(\Phi(x,\mathbf{r}). \tag{3.97}$$

It follows from equation (3.97) that $\Phi = \ln(v/A_0)$. Here $\phi = W - kx$ - phase difference, and $\ln(A/A_0) \equiv \chi$ - log-amplitude. Substitution (3.97) into (3.96) leads to the equation for the complex phase.

$$2ik\frac{\partial\Phi}{\partial x} + \Delta_\perp\Phi + (\nabla_\perp\Phi)^2 + k^2\tilde{\varepsilon}(x,\mathbf{r}) = 0,\ \nabla_\perp = \frac{\partial}{\partial y} + \frac{\partial}{\partial z},\ \Delta_\perp = \frac{\partial^2}{\partial y^2} + \frac{\partial^2}{\partial z^2}. \tag{3.98}$$

Solution can be expressed as a power series

$$\Phi = \sigma_\varepsilon\Phi_1 + \sigma_\varepsilon{}^2\Phi_2 + \ldots. \tag{3.99}$$

Substituting into the parabolic equation and keeping terms up to second order gives:

$$\begin{aligned} 2ik\frac{\partial\Phi_1}{\partial x} + \Delta_\perp\Phi_1 &= -k^2\tilde{\varepsilon}(x,\mathbf{r}) \\ 2ik\frac{\partial\Phi_2}{\partial x} + \Delta_\perp\Phi_2 &= -(\nabla_\perp\Phi_1)^2 \end{aligned}. \tag{3.100}$$

The problem of phase and log-amplitude fluctuations is considered using these equations. Equations (3.100) are solvable and valid only when the small fluctuations regime holds [*Rytov*, 1997] i.e.

$$\overline{|\nabla_\perp\Phi_1|^2} << k^2\sigma_\varepsilon \text{ or } \overline{|\lambda\nabla_\perp\Phi_1|^2} << \sigma_\varepsilon. \tag{3.101}$$

Consequently, the parabolic approximation neglects the backscattered part of the wave. Rytov's approximation says that the wave field u is not different from the

monochromatic wave $\exp(ikx)$, which propagates in the background homogeneous medium. Using the Rytov approximation, explicit equations for the phase Φ of a sound wave and its log-amplitude χ are obtained.

The equations for the variances of the log-amplitude and phase fluctuations of a plane wave in a moving random medium derived by means of Rytov method, have the following form [*Ostashev*, 1997]

$$\left\langle \chi^2 \right\rangle = \frac{\pi^2 k^2 x}{2} \int_0^\infty K \left[1 - \frac{K_F^2}{K^2} \sin \frac{K^2}{K_F^2} \right] \Phi_{eff}(0, K) dK \,, \tag{3.102}$$

$$\left\langle \phi^2 \right\rangle = \frac{\pi^2 k^2 x}{2} \int_0^\infty K \left[1 + \frac{K_F^2}{K^2} \sin \frac{K^2}{K_F^2} \right] \Phi_{eff}(0, K) dK \,. \tag{3.103}$$

Here $K_F^2 = k / x,$ where k is a wave number. Note, that $K_F = \sqrt{2\pi} / L_F,$ where $L_F = \sqrt{\lambda x}$ is the scale of the first Fresnel zone. Φ_{eff} is the three-dimensional spectral density of the random field ε and is called an effective function. The equations for statistical moments of ϕ and χ are valid for an arbitrary spectra of inhomogeneities in moving random medium. For our purpose we use Kolmogorov and Gaussian spectra of medium inhomogeneities. The Markov approximation for the effective spectral density is [*Ostashev*, 1997]

$$\Phi_{eff}(0, K) = A C_{eff}^2 K^{-11/3}, \tag{3.104}$$

where A is a numerical coefficient, and C_{eff}^2 is, so called, effective structure parameter, given by

$$C_{eff}^2 = C_\varepsilon^2 + \frac{22}{3} \frac{C_v^2}{c_\varepsilon^2}. \tag{3.105}$$

Here C_ε^2 and C_v^2 are the structure parameters of the random field [Ostashev, 1997]. Substituting (3.104) into (3.102) results into formula for the variance of the log-amplitude fluctuations for a plane wave:

$$\left\langle \chi^2 \right\rangle = 0.077\left(C_\varepsilon^2 + \frac{22}{3}\frac{C_v^2}{c_\varepsilon^2} \right) k^{7/6} x^{11/6} . \tag{3.106}$$

Substitution of (3.104) for the Kolmogorov spectrum into the integral for phase fluctuations results in a divergent integral. Therefore, $\left\langle \phi^2 \right\rangle$ can be determined neither for a plane nor for a spherical wave [*Ostashev*, 1997]. The formula for an effective spectral density for the Gaussian spectrum is

$$\Phi_{eff}(0,K) = \frac{l^3}{8\pi^{3/2}}\left(\sigma_\varepsilon^2 + \frac{\sigma_v^2 K^2 l^2}{c_{0\varepsilon}^2} \right) \exp\left(-K^2 l^2 / 4 \right). \tag{3.107}$$

For plane wave propagation, the variances of the log-amplitude and phase fluctuations are [Ostashev , 1997]

$$\left\langle \chi^2 \right\rangle = \frac{\pi^2 k^2 l x}{8}\left[\left(1 - \frac{\arctan D}{D} \right)\sigma_\varepsilon^2 + \left(1 - \frac{\arctan D}{D} \right)\frac{4\sigma_v^2}{c_0^2} \right], \tag{3.108}$$

$$\left\langle \phi^2 \right\rangle = \frac{\pi^2 k^2 l x}{8}\left[\left(1 + \frac{\arctan D}{D} \right)\sigma_\varepsilon^2 + \left(1 + \frac{\arctan D}{D} \right)\frac{4\sigma_v^2}{c_0^2} \right]. \tag{3.109}$$

In equations. (3.108) and (3.109) $D = 4x/\left(kl^2 \right)$ is the wave parameter used in the theory of waves in random media [*Chernov*, 1961] and σ_v is a sound scattering cross section due to the velocity fluctuations. Equations (3.108) and (3.109) in their original version were given for $\sigma_v^2 = 0$ [*Rytov*, 1978].

Chapter 4. Experimental Apparatus

The experiment was performed in a low-speed tunnel. The turbulence was produced by a grid. The ultrasonic technique was employed for diagnostic and determination of the statistics of grid-generated turbulence. The following chapter is devoted to the description of the experimental apparatus: wind tunnel, grid, ultrasonic system and data acquisition and analysis system. The major steps of the performance of ultrasonic measurement system with a discussion of each component of the system, namely, ultrasonic flowmeter, Data Acquisition Cards, LabVIEW software and characteristics of each component are summarized in this chapter. This chapter is concluded with description of LabVIEW Vi - the block diagram of the OSCOPE module, responsible for driving data acquisition cards, and analyzing acquired.

4.1 Wind Tunnel

The experiments were carried out in a wind tunnel of 45.25″ length with a 11.75″x 11.62″ rectangular test section. The AEROLAB low turbulence, low speed, research tunnel is of the Eiffel or Open Circuit type. The airspeed is infinitely variable from 0 to 80 mph. The tunnel achieves a high energy ratio through its large contraction ratio, 16:1, its small angle diffuser and efficient fan system. The high energy ratio is

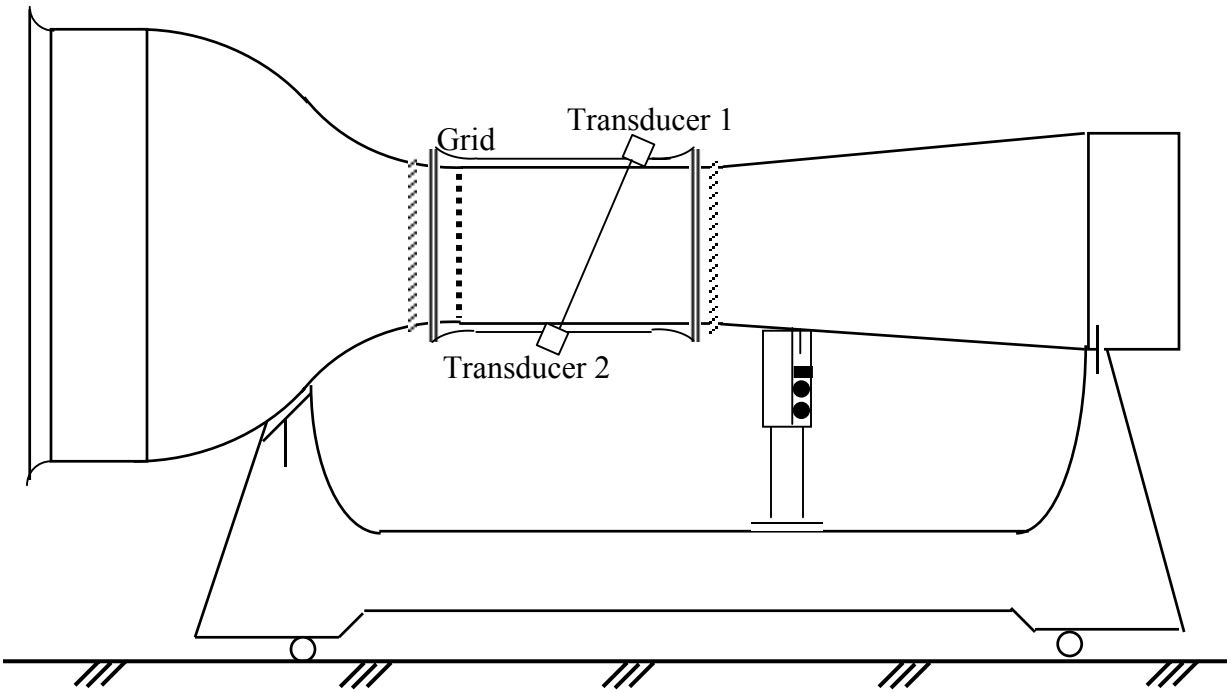

Figure 4.1. Sketch of the low turbulence, low speed research tunnel together with experimental setup.

important in indicating low aerodynamic losses, which are associated with intermittency and unsteadiness. The fan operated in an acoustically treated section to reduce the noise level. The tunnel is equipped with an aluminum honeycomb and four turbulence management screens, which can be removed through the entrance section. An orifice ring encircles the contraction and the upstream end of the test section to provide the differential pressure used to measure airspeed.

4.1.1 Boundary Layer

Air flowing into a test section forms a boundary layer on the walls of the tunnel. It is determined that for this flow the boundary layer displacement thickness is given by

$$\delta^* \sim 0.0033x^{1/2} \qquad (4.1),$$

where x is a distance downstream the tunnel. It can be estimated that the maximum displacement thickness $\delta^* \sim 0.0031m$ corresponding to the measurements taken at $x = 0.89m$ downstream the grid. Consequently, the effect of boundary layer results in 7% change in mean velocity U and in 0.05% in the total velocity which is a sum of the velocity of a sound wave and a mean velocity.

4.2 The Grid

The turbulent velocity and turbulent temperature fluctuations are simultaneously generated by a bi-planar grid composed of 18 round chromalox heating rods, model TSSM 14XX [*Sreenivasan*, 1980], placed at the entrance of the test section. To insure uniformity of the grid, the heating rods were inserted in hollow aluminum rods with diameter of 0.25″ positioned 1″ between centers. The mesh, M, was therefore 1″ and the grid solidity was 0.64. The rods are all heated evenly; hence the thermal mesh size is equal to that of the momentum. The grid power was regulated by variable transformator. The heated grid surface temperature was measured by thermocouple, while mean air temperature of the tunnel flow is measured by thermometer. Overall, the grid structure resembles the features of the grid used by Sreenivasan, who performed measurements of turbulence decay in the wind tunnel with similar geometry. It has been experimentally verified [*Sreenivasan*, 1980; *Yeh and van Atta*, 1973; *Sepri*, 1976; *Mohammed and LaRue,* 1990] that this particular choice of the grid geometry together with geometry of the tunnel, insures that in the region $25" - 40"$ the turbulence can be considered approximately isotropic.

4.3 Description of the Ultrasonic System

4.3.1 Transit Time Flowmeters

Measurements were performed by means of an ultrasonic system. The transducer is one of the most critical components of any ultrasonic system. A transducer is any device that converts one form of energy to another. An ultrasonic transducer converts electrical energy to mechanical energy, in the form of sound, and vice versa. The main components are the active element, backing, and wear plate as shown in Figure 4.2. The active element, which is piezo or ferroelectric material, converts electrical energy such as an excitation pulse from a flaw detector into ultrasonic energy. The backing is usually a highly attenuative, high density material that is used to control the vibration of the transducer by absorbing the energy radiating from the back face of the active element. The basic purpose of the transducer wear plate is to protect the transducer element from the testing environment. In the case of contact transducers, the wear plate must be a durable and corrosion resistant material in order to withstand the wear caused by use on materials such as steel. For our application we use Low Frequency Narrowband Transducers, meant for use in pairs for through transmission in materials with working frequency of 100KHz. The ultrasonic flowmeter utilizes two transducers functioning both as a transmitter and as a receiver, as shown in Figure 4.3. The principle is based on modification of the time of flight of the ultrasound by the fluid velocity along the line of the flight path between the two transducers. The method results in measurement of very short time delays of about a few nanoseconds.

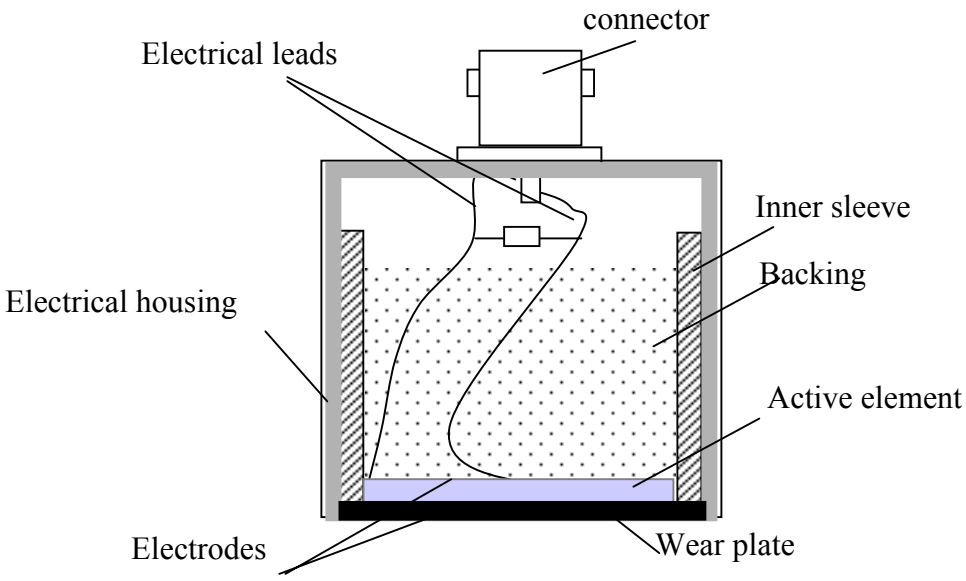

Figure 4.2. Design characteristics of an ultrasonic transducer

A great deal of attention should be paid to selecting the proper transducer for the application. The optimal choice of ultrasonic frequency depends on two factors. Consistent with absorption factor and minor fluid turbulence the highest practical frequency should be used. The lower limit is related to the vortex size, which, in turn, is related to the size of the vortex-generating strut [Lynnworth, 1989]

$$k = 1/L;\ ck = c/\lambda = f, f(Hz) = 2\pi\omega \qquad (4.2).$$

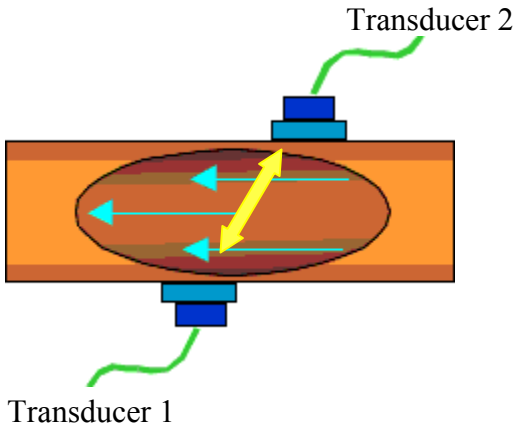

Figure 4.3. Transit-time ultrasonic flowmeter.

4.3.2 Data Acquisition and Analysis System

Measurement devices, such as general-purpose data acquisition (DAQ) devices and special-purpose instruments, are concerned with the acquisition, analysis, and presentation of measurements and other data you acquire. Acquisition is the means by which physical signals, such as voltage, current, pressure, and temperature, are converted into digital formats and brought into the computer. Popular methods for acquiring data include plug-in DAQ and instrument devices. Data analysis transforms raw data into meaningful information. This can involve such things as curve fitting, statistical analysis, frequency response, or other numerical operations. DAQ devices are devices that connect to the computer allowing the user to retrieve digitized data values. These devices typically connect directly to the computer's internal bus through a plug-in slot. With DAQ devices, the hardware only converts the incoming signal into a digital signal that is sent to the computer as shown in Figure 4.4. The DAQ device does not compute or calculate the final measurement. That task is left to the software that resides in the computer. The same device can perform a multitude of measurements by simply changing the software application that is reading the data. Before a computer-based system can measure a physical signal, a sensor or signal conditioning must convert the physical signal into an electrical one, such as voltage or current. The software controls the DAQ system by acquiring the raw data, analyzing the data, and presenting the results. The role of software is crucial. Software takes the raw data and presents it in a form of a graph, chart etc. The software controls the DAQ system, telling the DAQ device when to acquire data. DAQ software includes drivers and application software. Drivers are unique to the type of the device and include the set of commands the device accepts.

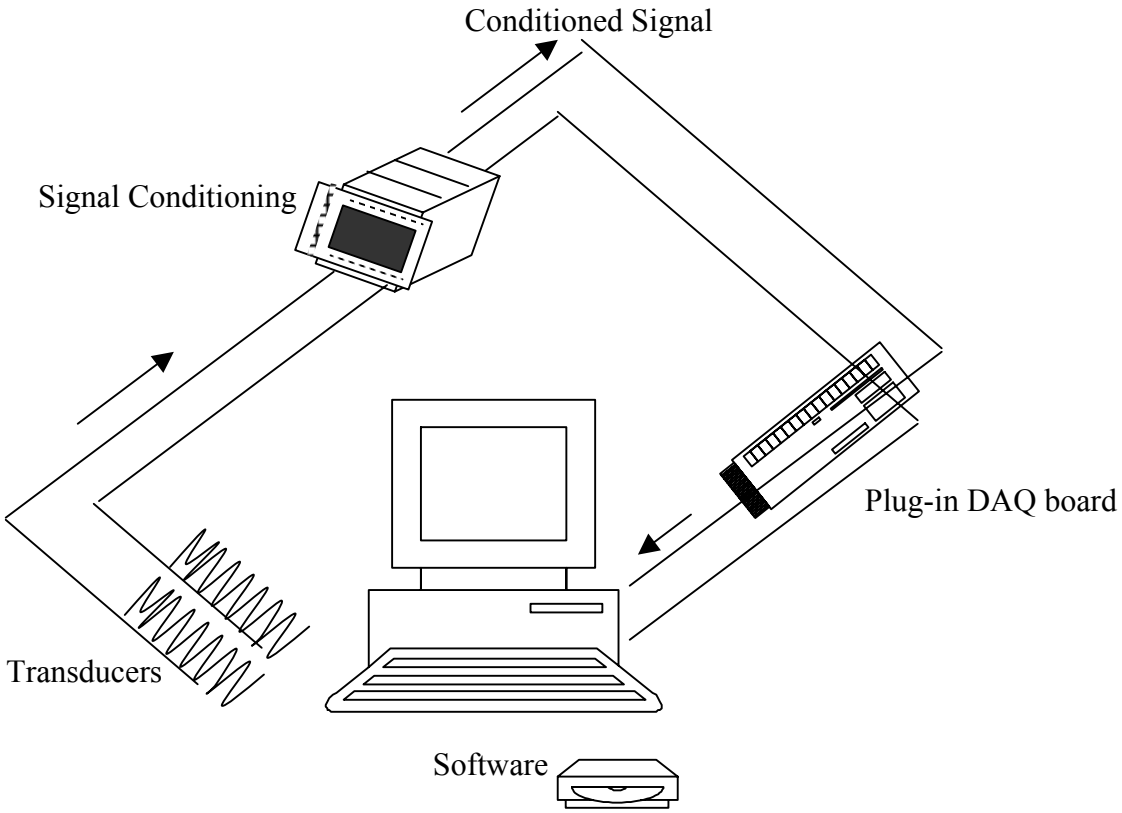

Figure 4.4. DAQ System Components

Application software (in our case LabVIEW) sends the commands to the drivers, such as acquire a transducer reading and return the reading, then displays and analyzes the data acquired. Lab VIEW includes a set of Vis that let us configure, acquire data from and send data to DAQ devices. LabVIEW DAQ Vis makes calls to the NI-DAQ Application Program Interface (API). The NI-DAQ API contains the tools and basic functions that interface to DAQ hardware. Lab VIEW instrument drivers simplify instrument programming to high-level commands, so there is no need to learn the low-level instrument-specific syntax needed to control the instrument. Figure 4.5 shows the relationship between LabVIEW, driver software, and measurement hardware.

In general, the ultrasonic measurement system works as follows. A piezoelectric-based ultrasonic transducers are placed on the tunnel in a diagonal mode. The transducer-transmitter is electrically excited by a voltage from a pulser and transforms the voltage into a high frequency mechanical wave (vibration). The wave is transmitted through the air in the tunnel to the second transducer-receiver, where it is converted from mechanical back to electrical form. The received signals are sent to a PC-based 1 GHz analog-to-digital (A/D) converter for digitization. The digitized waveform is output from the A/D converter for digital processing and display.

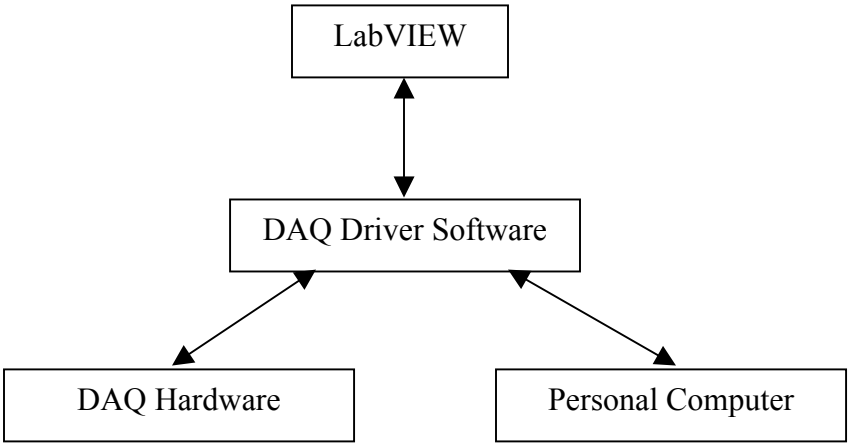

Figure 4.5. Relationship between LabVIEW, Driver Software, and Measurement Hardware

The LabVIEW program performs the major functions necessary to control the A/D converter (via a custom software driver). In addition, the software is responsible for analyzing the measurement data generated by the experiment, as well as displaying and storing the results of the analysis.

In our application an ultrasonic measurement system consisted of the following parts:

Hewlett-Packard programmable signal generator, model 3314A, power amplifier, model 50A15, Panametrix Low Frequency Narrowband Transducers, National Instrument PCI/PXI-6711/6713 Analog Voltage Output Device for PCI/PXI (NI DAQ), LabVIEW Software, CompuScope 82G Analog Input DAQ (CS DAQ). Ultrasonic bursts were generated using a programmable signal generator, and a power amplifier. Received signals were amplified and sampled using high-speed data acquisition equipment. A transmit/receive switch protected the receiver from transmitted signal. The enabling pulse is started by the first positive voltage step in the four-pulse burst of square waves. The burst was $100\,kHz$ frequency and had $50\,mV$ amplitude produced by a function generator, which, in turn, was driven by NI DAQ. The four-pulse burst was sent to the transducer-transmitter through the amplifier. Figure 4.6 demonstrates a four-pulse burst coming out of the transducer-transmitter.

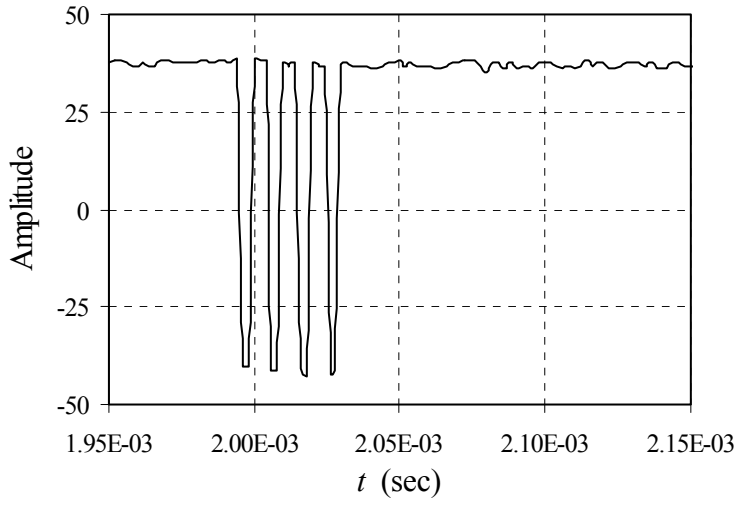

Figure 4.6. Four-pulse burst of square shape waves.

The NI DAQ allows one to detect the burst departure time extremely accurately. The pulse was generated with a repetition frequency of 500 cycles/second. The ultrasound beam, send by the first transducer was received by the second one. The main problem was to measure travel time t_n with a high precision. The analog data, then, from the second transducer was connected to a CSDAQ with a large acquisition memory and wide analog bandwidth that transformed analog data to digital data and transferred data from CS DAQ card to the PC memory with the resolution of $5 \cdot 10^{-9} s$. Both DAQ cards were installed inside the PC. Digital representation of the experimental data, provided by the DAQs allowed determination of the travel time t_n very precisely. Figure 4.7 demonstrates a typical data representation obtained from CS DAQ, transferred to the PC and processed in Excel. The acquisition rate was 50000000 samples/s. Two signals shown in Figure 4.7 are received signal e_1 and transmitted signal e_2.

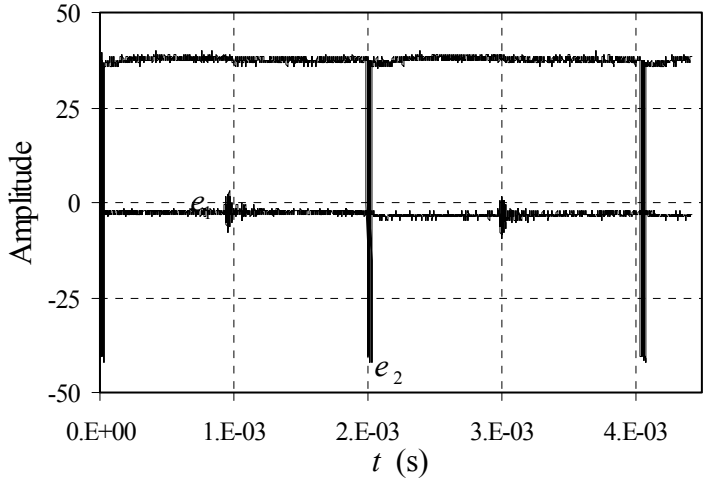

Figure 4.7. Typical data representation obtained from CompuScope 82G DAQ, transferred to the PC and processed in Excel. Signals e_1 and e_2 are received and transmitted signals respectively.

For this case, the ultrasonic signal traversed the flow perpendicular to the mean flow. Approximately 0.9 ms was required. A magnification of the transmitted and received bursts is shown in Figure 4.8. The block diagram of analog and digital processing is shown in Figure 4.9.The OSCOPE subVI module is the heart of the ultrasonic measurement system. When the main VI is started, waveform acquisition begins immediately in the background and the waveforms are placed in a queue. The block diagram of the OSCOPE module is presented in Appendix A.

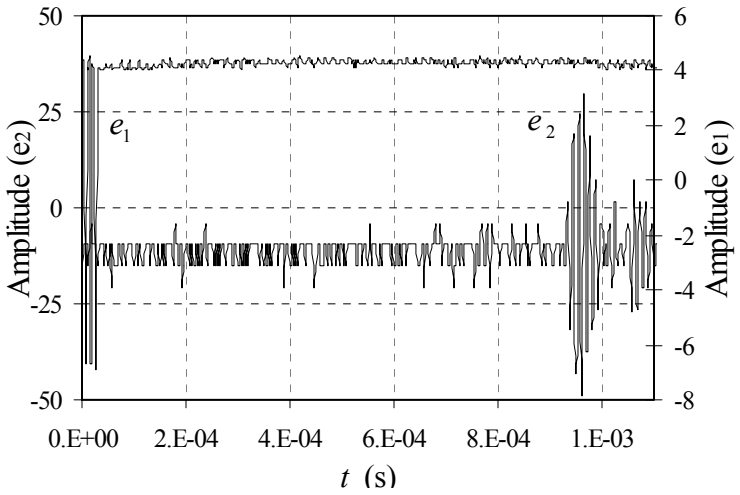

Figure 4.8. Magnification of received signal e_1 and transmitted signal e_2, obtained from the digital data acquisition system CompuScope 82, shown in Figure 4.6.

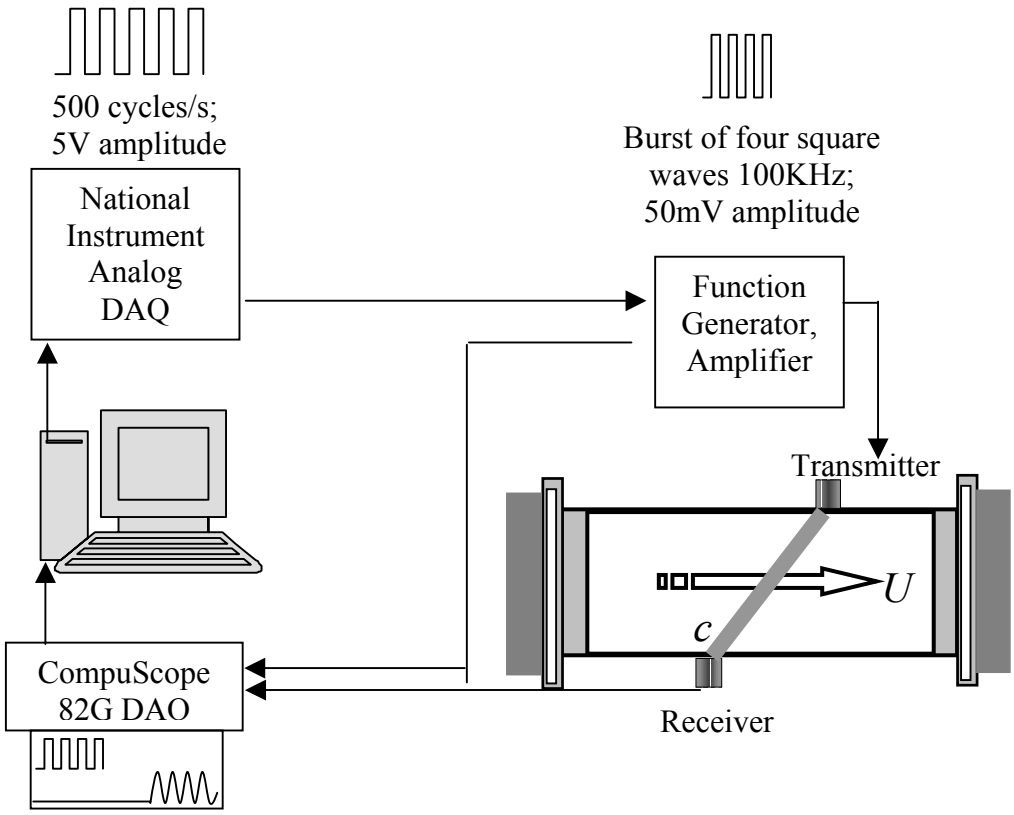

Figure 4.9. Block diagram of analog and digital processing.

Chapter 5. Experimental Results and Discussion

In this chapter we present the most important aspect of the dissertation: application of the travel-time ultrasonic technique for data acquisition in a grid-generated turbulence and analysis of the experimental data.

5.1 Application of Travel-time Ultrasonic Techniques for Data Acquisition

We consider here a locally isotropic turbulent flow, which can be approximately generated by introducing a grid into a uniform flow. At a sufficient distance downstream from the grid the flow becomes locally isotropic and a power law spectral representation is applicable. Studies that permit identification of the downstream position where the flow be considered nearly homogeneous and locally isotropic are described in detail by *G Corrsin*; *Uberoi and Wallis* [1967], *Comte-Bellot and Corrsin* [1971] *Mohamed and LaRue* [1990]. In order to collect experimental data in nearly isotropic and homogeneous portions of flow, the locations of transducers as well as mean flow speed were chosen using the criteria established by Mohamed and LaRue. Specifically, experimental data were collected in the $25" - 42"$ portion of the test section. The specific grid structure as well as the tunnel geometry were essentially the experimental setups used by previous investigators to insure that turbulence level and other statistical characteristics of the turbulence were the same as measured by Yeh and van Atta [1973], Sepri [1976],

Sreenivasan et al, (and references therein) [1980]. In the present study we assume, that the basic characteristics of ultrasound propagation in the turbulence are determined by slow changes in the state of medium (mean speed, temperature, and density of the air). It seems reasonable to assume that ultrasonic pulses have negligible effect on the turbulence because they are at very high frequency, low power, and propagate in very short bursts. Under these conditions, it is expedient to use the method of ray acoustics. However, as shown in Chapter 2, the method of ray acoustics has a limitation in terms of the length of the travel path. When diffraction effects are of importance the parabolic equation along with the Rytov approximation method is very powerful for describing waves propagation. This approach allows investigation of the effect of turbulence in terms of travel time and log-amplitude variance.

An important contribution of the present work is the recognition of the effect of turbulent fluctuations on acoustic wave propagation. Specifically, in Chapter 2 we reformulated the original flowmeter equation in order to account for both velocity and sound speed fluctuations. Experimental data obtained from heated- and non-heated grids supplements the theory of the Chapter 2, which together formulate a methodology for determination of the correlation functions and spectra of turbulent velocity and sound speed fluctuations.

In the experimental apparatus each transducer acted both as a transmitter and as a receiver. The difference in transit times along the path were measured and more than 700 realizations achieved. For each mean velocity and separation distance data were collected for 45 sec. The data file for each measurement sequence was about 15Mb. The transit time for the ultrasound pulse was determined from the correlation function

$$K_{12}(t) = \overline{e_1(t+\tau)e_2(t)}, \qquad (5.1)$$

where $K_{12}(t)$ is a cross correlation function of received and transmitted waves e_1 and e_2 shown in Figure 4.7. By definition

$$K_{12}(t) = \int_0^\infty e_1(t+\tau)e_2(t)p(e_1,e_2,t)\,dt, \qquad (5.2)$$

where $p(e_1,e_2,t)$ is a probability density function. However, assuming the process to be ergodic, spatial averaging may be replaced by averaging over the time:

$$K_{12}(t) = \frac{1}{T}\int_0^T e_1(t+\tau)e_2(t)dt. \qquad (5.3)$$

Hence, the travel time t_n may be determined as

$$\max K_{12}(t) = K_{12}(t_n). \qquad (5.4)$$

The numerical computation of the cross correlation function involves the computation of average products among the sample data values [*Bendat and Piersol*, 1971]. Namely, we consider N data values $\{x_n\}, n = 1,2,...,N$ sampled at equally spaced time intervals dt from a transformed record $x(t) = x(ndt)$. The cross correlation function of $x(t)$ can be estimated from the sample values at the time delay rdt by

$$K_{12}(rdt) = \frac{1}{N-r}\sum_{n=1}^{N-r} x_n x_{n+r}, r = 0,1,2,...,m. \qquad (5.5)$$

The number of real multiply-add operations required to compute the cross correlation estimate is approximately Nm, assuming $N << m$. The numerical code, which was used to calculate the cross correlation function K_{12} included module *CCF* from IMSL Fortran

library. Module *CCF* serves to compute the sample cross correlation functions of two stationary time series. The text of the numerical code is presented in the Appendix B.

5.2 Ray Acoustics Approach

In this chapter the analysis of the effects that turbulence have on acoustic signals developed in the contest of ray acoustics. Structure constant entering Kolmogorov's law is determined using statistics of the travel time [*Andreeva and Durgin*, 2003(a), 2003(b)].

5.2.1 Travel time fluctuations as a function of a separation distance L.

Figure 5.1 represents a schematic diagram of the experimental setup. Nine cases of different distances *L* were studied. Geometrical parameters are listed in the Table 5.1 and it can be seen, that the angle with respect to the mean flow varied so, that the mean flow component along the path also varied. The mean velocity during the experiment was $U = 3.5m/\sec$, which corresponded to a Reynolds number based on the mesh size of $\mathrm{Re} \cong 7000$. The signal was sent in a direction opposite to the inlet flow. From theoretical point of view, one may expect that the travel time will increase with distance. In Figure 5.2 the travel time data in disturbed medium is plotted along with data collected in

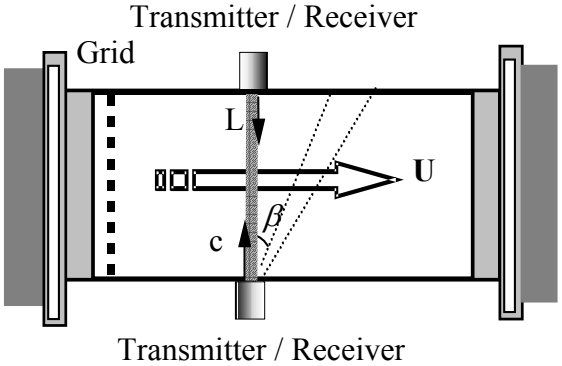

Figure 5.1. Sketch of wind-tunnel test section

undisturbed medium and compared with theoretical estimation of the travel time without taking into account the effect of turbulence, namely, $t_{theoretical} = L/(c - U\sin\beta)$. Figure 5.3 demonstrates well-expected result of significant decrease of mean travel time in presence

β (deg)	0	5	10	15	20	25	30	35	40
L (m)	0.33	0.3335	0.3395	0.3483	0.3603	0.3758	0.3955	0.42	0.45

Table 5.1. Geometrical parameters.

of turbulence. The decrease due to turbulence is 5% or greater. The uncertainty in measurements of the ambient temperature is at most 3.5%, which would introduce an uncertainty in the mean travel time determination of only 0.2%. Similarly, the uncertainty in measurements of the travel distance 0.3%, which would introduce an uncertainty in the measurement of the travel time of approximately 0.3%. Figure 5.3 demonstrates the travel time standard deviation as a function of traveled distance. The result obtained by *Kolmogorov* and *Obukhov* predicts that the standard deviation should increase in proportion to the square root of a distance, which is depicted by the solid line. Therefore, the experimental data is plotted together with $L^{1/2}$ curve in order to verify that the standard deviation obtained experimentally is indeed proportional to $L^{1/2}$. Although the standard deviation is increasing with distance, the scattering of the data can be clearly seen. The scattered data must be interpreted with some caution and may not be inconsistent with the theoretical analysis, but rather may be due to the uncertainty of the measurements, which were found to be around 20%.

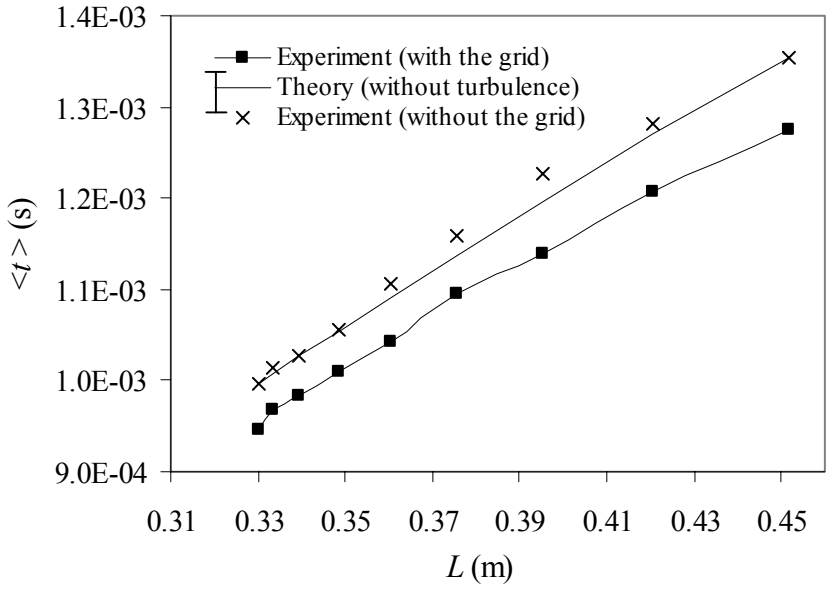

Figure 5.2. Average travel time versus a path length, $U = 3.5\text{m/s}$.

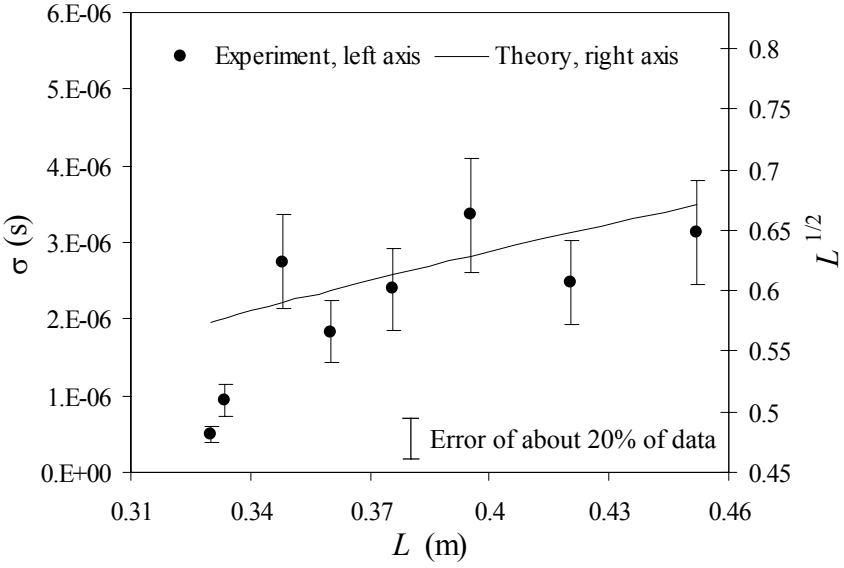

Figure 5.3. Standard deviation of the travel time versus the travel distance, $U = 3.5\text{m/s}$.

5.2.2 Transit Time Fluctuations as a Function of the Mean Velocity U .

For this case we used two transducers placed at a distance L from each other with the direction of mean flow perpendicular to *L*. The Reynolds number based on the mesh size M varied from 4016 to 20080. Following the procedure described in the foregoing section the cross correlation function K_{12} of two signals e_1, e_2 for $U = 4$ (m/sec) was obtained and is shown in Figure 5.4. After calculation of the travel time t for each sample using formula we calculated the averaged travel time $< t >$ and deviation of the transit time σ for each velocity.

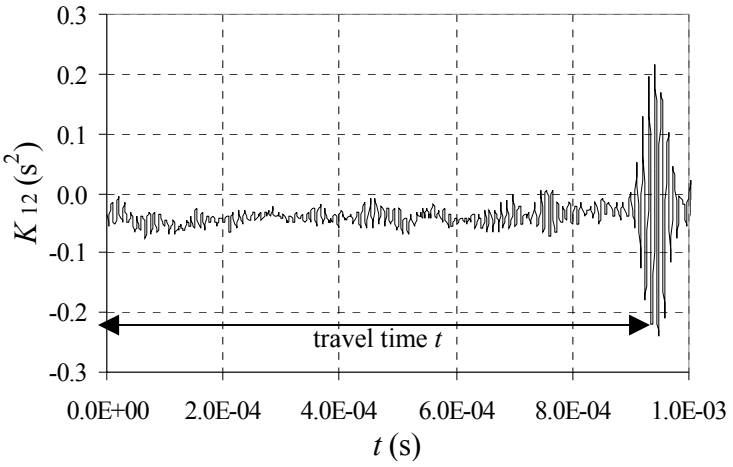

Figure 5.4. Correlation function $K_{12}(t)$ of two waves. Maximum value of the correlation function corresponds to the travel time t .

Averaged travel time and deviation of the travel time are two crucial parameters that carry the most information about experimental data. As expected, Figure 5.5 shows substantial decrease in $\langle t \rangle$ as mean velocity increases. As it was stated in the section 3.5, for a standard deviation, σ, theory predicts a dependence of $(U < t >)^{5/6}$. Figure 5.6

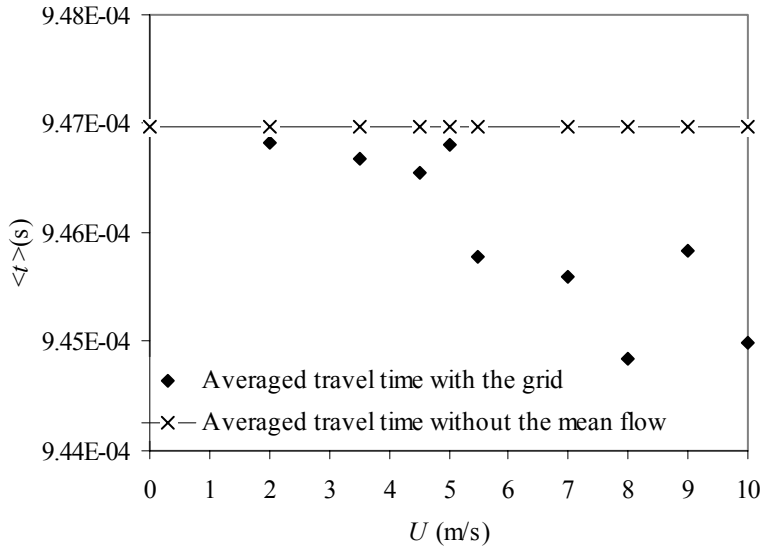

Figure 5.5. Averaged travel time as a function of the mean velocity, $L = 0.33\text{m}, \beta = 0$.

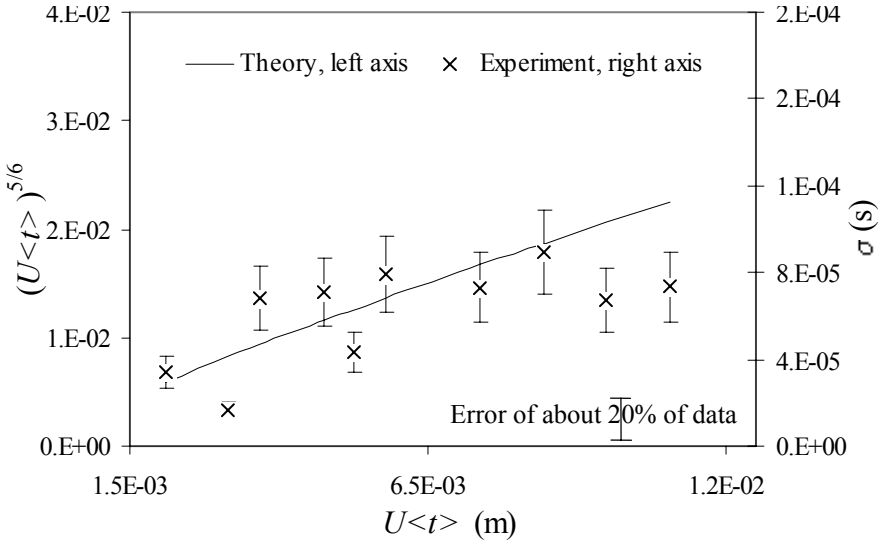

Figure 5.6. Standard deviation of the travel time versus mean velocity, $L = 0.33\text{m}, \beta = 0$.

illustrates that experimental results are in fairly good accordance with theoretical predictions, namely, standard deviation is proportional to $\left(U < t >\right)^{5/6}$. After validation of our experimental results we may determine the turbulent constant C from equation (3.85)

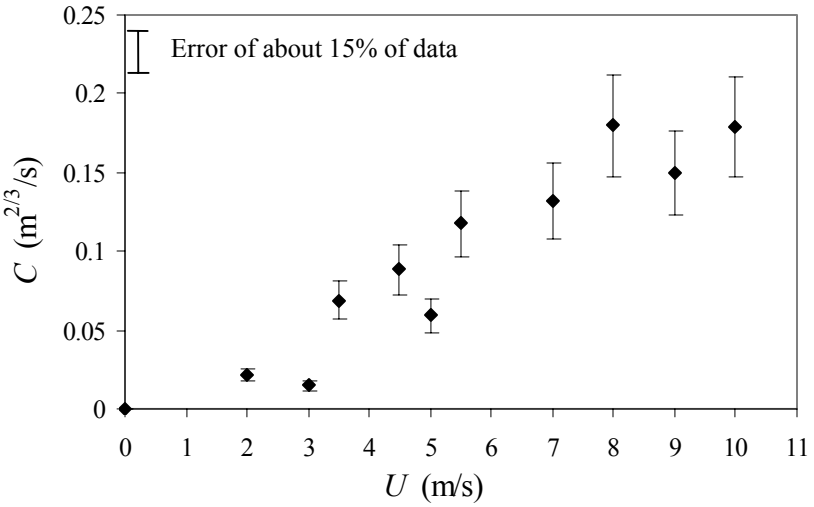

Figure 5.7. Variation of the structure constant C versus mean velocity, $L = 0.33\text{m}, \beta = 0$.

$$\overline{\Delta t^2} = C^2 L \left(\frac{1}{c^2} \right)^2 \delta^{5/3} const \qquad (5.6)$$

In accordance with equation (5.6) with the quantities entering into this formula obtained from experiment one can determine the value of turbulent characteristic C. Figure 5.7 shows the variation of the structure parameter C as a function of a velocity. Evidently, the constant C increases with mean flow. This result is consistent with results obtained earlier by *Krasil'nikov* [1947, 1949, 1953, 1963] and *Oboukhov* [1951].

5.3 Parabolic Equation and Perturbation Method (Rytov's Method)

The effect of turbulence on acoustic waves in terms of the travel time is studied for various mean velocities and for different angular orientations of the acoustic waves with respect to the mean flow. The effect of the time shift between the travel times in turbulent and undisturbed media, associated with Fermat's principle is observed experimentally.

This chapter discusses the situation when mathematical conditions for ray acoustics

are violated and ray acoustics approach is no longer valid. Rytov's approach is used to study the influence of turbulence on acoustic wave propagation in terms of second moments of travel time and log-amplitude fluctuations. Statistical moments obtained experimentally are compared with theoretical results from literature [*Andreeva and Durgin*, 2003].

5.3.1 Travel Time Fluctuations as a Function of Mean Velocity and Travel Distance.

We consider a locally isotropic turbulent flow generated by a grid at room temperature. The experimental setup shown in Figure 5.8 serves for investigation of the averaged travel time as a function of a mean velocity U, that changes from 1m/s to 10m/s, so that the Re number based on the grid space size changes from 4016 to 20080. The path length stayed unchanged. Acoustic waves were sent upstream and downstream with respect to the mean flow. Travel time for both cases is plotted in Figure 5.9 along with the theoretical estimates for the travel times in the undisturbed medium. The effect of the travel-time shift Δt between $\langle t \rangle$ and t_0, where t_0 is travel time in undisturbed media is observed.

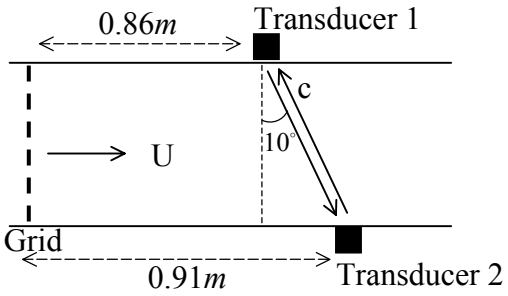

Figure 5.8. Diagrams of the experimental setup that serves to investigate the average travel time as a function of a mean velocity U

Due to the fast path effect, the effective velocity is higher than the mean velocity of the medium. Indeed, $\langle t \rangle \le t_0$ and $\frac{X}{\langle t \rangle} \ge \frac{X}{t_0}$ [*Iooss*, 2000]. The experimental setup shown in Figure 5.10 serves to illustrate the influence of the travel distance varying from 0.33m to 0.45m. The mean velocity was unchanged, 3.5 m/s. Another interesting effect of acoustic wave propagation is the linear increase of travel time variance with distance [*Chernov*, 1960]. Nonlinear effects become apparent at a certain propagation distances both in the numerical experiments by *Karweit et al*, [1991] and in the work by *Iooss et al*, [2000].

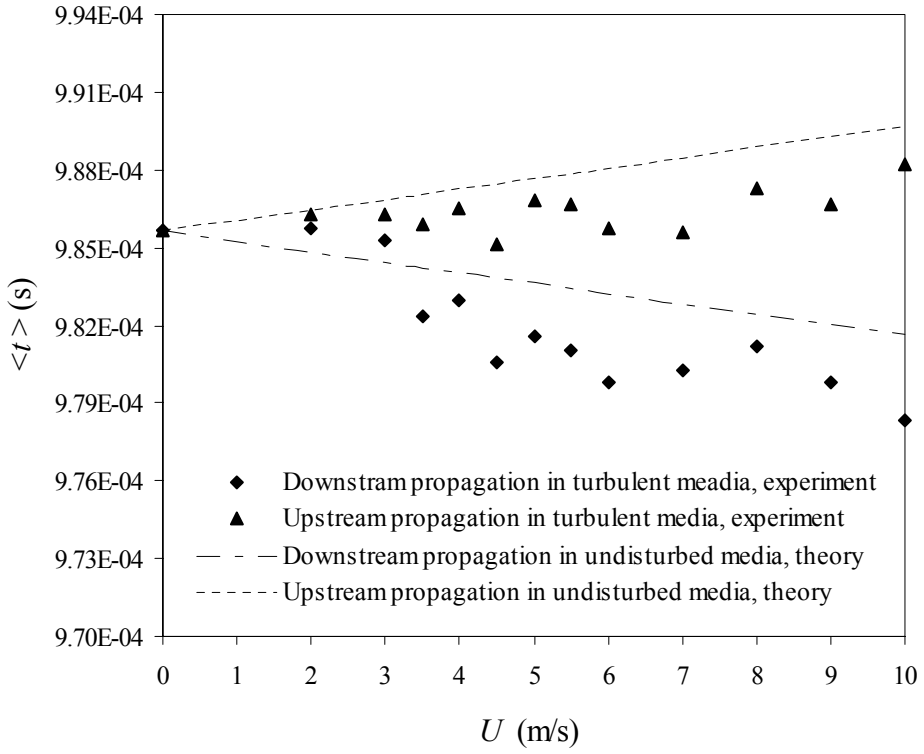

Figure 5.9. Experimental data for mean travel time as a function of mean velocity for upstream and downstream propagation plotted along with theoretical estimates for the travel times in undisturbed medium.

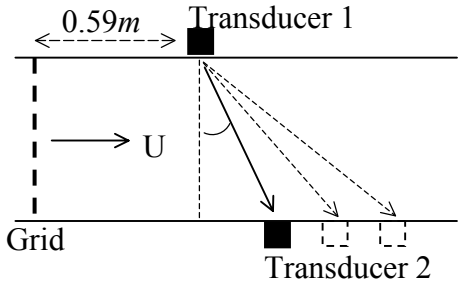

Figure 5.10. Diagram of he experimental setup that serves to study the influence of the travel distance, L.

In our experiment due to the limited size of the wind tunnel we did not reach the distances where these nonlinear effects could be observed. In Figure 5.11 we compare our experimental data firstly with theoretical results obtained by *Iooss et al* [2000]. In their work, the authors were investigating travel time using a geometrical optics approach, which neglects all diffraction phenomena. They developed a theoretical model for the second order travel time variance for the plane waves. Secondly, we compare our results with solution of the parabolic equation for the travel time variance of a plane wave in a moving random media, derived by means of the Rytov method and Markov approximation for the Gaussian spectrum of medium inhomogeneities, modified Equation (3.109), derived in Chapter 3.7

$$\left\langle \phi^2 \right\rangle = \frac{\pi^2 k^2 l x}{8}\left[\left(1+\frac{\arctan D}{D}\right)\sigma_\varepsilon^2 + \left(1+\frac{\arctan D}{D}\right)\frac{4\sigma_v^2}{c_0^2}\right],\ D = 4x/\left(kl^2\right) \qquad (5.7)$$

During the experiment we did not have the ability to measure all flow parameters appearing in the Equation (5.7). Consequently, for the comparison, we simply reproduce the arctangent behavior of the travel time variance, namely,

$\left\langle \tau^2 \right\rangle \equiv \left\langle \left(t - \langle t \rangle\right)^2 \right\rangle \sim \left(x - \arctan x\right)$. For demonstration purposes, all the analytical lines start from the same point. We observe that nonlinear effects of second order travel

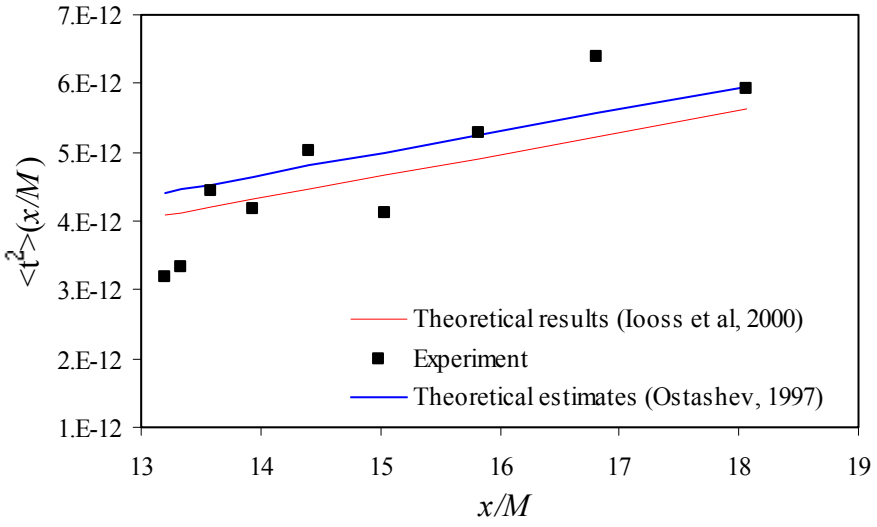

Figure 5.11. Experimental data for the travel time variance versus normalized travel distance x/M. Rytov solution and theoretical model by Iooss et al. 2000 are plotted for comparison.

time variance do not appear at such short distances. Moreover, comparison of the travel time variance obtained using the Rytov method and ray acoustic approach reveals, that some of the results of geometric acoustics are acceptable even beyond the area of the validity of the approach. It has been shown by *Rytov* [1987] that ray acoustics is accurate enough for phase difference calculations, since the account for diffraction effects matters only in numerical coefficients.

5.3.2 Travel-time and Log-Amplitude Variances

The large-scale, energetic motions drive acoustic phase fluctuations, while

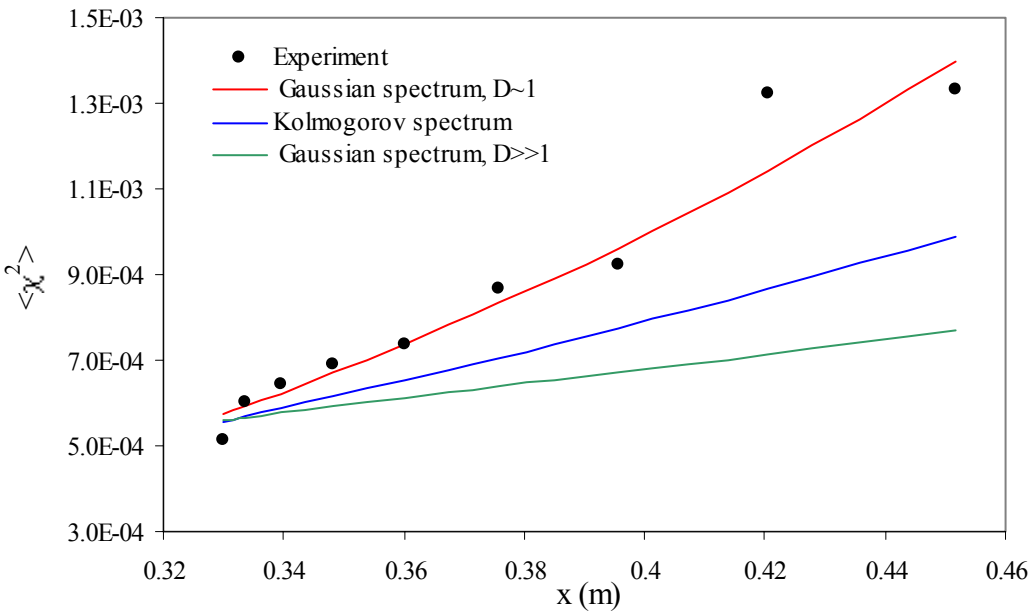

Figure 5.12. Experimental data for the log-amplitude variance as a function of travel distance. Rytov solution for Kolmogorov spectra, Gaussian spectra and Frauhofer diffraction are plotted for comparison.

smaller-scale motions drive the amplitude fluctuations [*Wilson*, 2000]. The energy-containing subrange play the primary role in the experiment reported here. For our experimental conditions the smallest, Kolmogorov, scale is $l_0 \approx 5.6 \cdot 10^{-4} m$, while the largest, integral scale has a size of the grid spacing, $L_0 = 0.025m$. The diffraction region is approximately defined as $l_0^2 / \lambda < L < L_0^2 / \lambda$, so that according to the geometry of the experiment our experimental domain falls into the diffraction region. Figure 5.12 shows experimental data for log-amplitude variations plotted along with theoretical results, Equation (3.108), derived in Chapter 3.7 for Kolmogorov spectra, Gaussian spectra and its limiting case, Frauhofer diffraction for $D >> 1$

$$\left\langle \chi^2 \right\rangle = \frac{\pi^2 k^2 lx}{8}\left[\left(1-\frac{\arctan D}{D}\right)\sigma_\varepsilon^2 + \left(1-\frac{\arctan D}{D}\right)\frac{4\sigma_v^2}{c_0^2}\right],\ D = 4x/\left(kl^2\right) \qquad (5.8)$$

In case of D close to 1, which is the case in our experiment, the non-linearity due to arctangent is well established. The general form of the log-amplitude variance in the case of Gaussian spectra, which takes into consideration small diffraction effects, is the best fit for our data. For demonstration purposes, all the analytical lines start from the same point.

5.4 Methodology for Determination of Statistical Characteristics of Grid Generated Turbulence

Experimental data were obtained for ultrasonic wave propagation downstream of a non-heated and heated grid in a wind tunnel for different angular orientations of the acoustic waves with respect to the mean flow. Since travel time fluctuations contain information about the turbulence the developed methodology suggests using statistics of travel time fluctuations for recovering of the correlation functions and spectra of turbulent velocity and sound speed fluctuations [*Andreeva and Durgin*, 2001, 2002,2003 (c)].

5.4.1 Methodology for Determination of Correlation Functions of Velocity and Acoustic Waves Fluctuations

The velocity and temperature fluctuations were generated simultaneously using a heated grid. Nine cases of different distances L for two different temperatures $\mathrm{T} = 59^\circ F$ and $\mathrm{T} = 159^\circ F$, are studied. The defined temperatures correspond to the

temperature of aluminum rods of the grid. The angle β in Figure 5.1 is changed from 0 to 40 degrees with 5-degree step. It was experimentally demonstrated that for an open loop tunnel thermal stratification is not significant even for low-speed flows, and also that the mean air temperature is independent of downstream location within the range considered [*Yeh and van Atta*, 1973; *Sepri*, 1976]. In the earlier works [*Yeh and van Atta*, 1973; Sepri, 1976] it was found that near the grid the wall temperature is higher than that of the fluid because of the radiation from the hot grid. Therefore, the measurements were collected at $x/M = 25" \div 45"$, where radiation effects are negligible.

The mean flow velocity was $U = 3.5$ m/s. During the recording of turbulent data the low velocity was chosen in favor of higher velocity in order to maximize the effect of temperature fluctuations. The Reynolds number Re_M based on M and U was about 6000 and the corresponding Péclet number $Pe_M = \mathrm{Pr}\,\mathrm{Re}_M \sim 4350$; $\mathrm{Pr} = 0.725$ for the working fluid air. Following the strategy described in the Section 3.6 we first use flowmeter integral equation for the case of temperature of $59^\circ F$,

$$K_t^{F59}(s,s') = \frac{1}{c^4}\int_0^s\int_0^{s'} K_{u'}(x,x')\,dxdx'. \qquad (5.9)$$

In many practical problems, the form of the correlation function is not known. However, its general shape is often approximated by a Gaussian function. It is very convenient for analytical studies of wave propagation in random media, and, besides, it allows taking into consideration the effect of the largest inhomogeneities in a medium on the statistical moments of a sound field [*Ostashev*, 1997]. In addition, the combination of numerical simulations and analytical approximations confirmed that a sound pulse tend to

effectively obey Gaussian statistics [*Dacol*, 2001]. We represent the correlation function in equation (5.9) by

$$K_t^{59F}(s,s') = \sigma_t^2\big|_{F59} \exp\left(-(s-s')^2 / l^2\right) = \sigma_t^2\big|_{F59} \exp\left(-\tau^2 / l^2\right). \qquad (5.10)$$

Here σ_t^2 is a variance of travel time fluctuations. Selection of l is problematic. In some applications l is chosen to be equivalent to a Taylor microscale. A better procedure is to choose l on the basis of the integral length scale of the turbulence [*Ostashev*, 1997]. Since we are considering travel time fluctuations in, rigorously speaking, diffractive media in the approximation of ray acoustics, we should realize that there is some uncertainty up to some numerical coefficient [*Rytov* et al, 1978]. Figure 5.13 demonstrates correlation function of travel time obtained using experimental data as a function of separation distance compared with Gaussian curve providing the best fit. The experimental data allow us to determine the unknown coefficients, $\sigma_t^2 = 9.85e-15$ and $l^2 = 0.0036$. Integration of equation (5.10) with known σ_t^2 and l^2 leads to the following form of correlation function of turbulent velocity

$$K_{u'}^{F59^\circ}(\tau) = c^4\left[2\frac{\sigma_t^2\big|_{F59^\circ}}{l^2}\exp\left(-\tau^2/l^2\right)\right] - c^4\left[4\frac{\sigma_t^2\big|_{F59^\circ}}{l^4}\tau^2\exp\left(-\tau^2/l^2\right)\right]. \qquad (5.11)$$

It is apparent that the correlation function of turbulent velocity is no longer Gaussian, although a Gaussian part is present in the first term in equation (5.11) and the second term vanishes rapidly with distance. Figure 5.14 shows the correlation function of turbulent velocity for our particular experimental data. The variance of velocity fluctuations is $\sigma_{u'}^2 = 2c^4\frac{\sigma_t^2}{l^2} = 0.0801$. At the same time we know, that $\sigma_{u'} = \left\langle u'^2 \right\rangle^{0.5}$,

meaning that for our experimental conditions we have very small values of $u'^2/c^2 \sim 6.9\cdot 10^{-7}$, which is in a very good correspondence with data [*Sepri*, 1976]. The ratio of a turbulent velocity to the mean velocity is $\alpha = u'/U \cdot 100\% \sim 6\%$, which is typical for experiments performed in grid turbulence. Figure 5.15 shows the cross correlation function of travel time at temperature 159F, again along with Gaussian function providing the best fit

$$K_t^{F159}(s,s') = \sigma_t^2\big|_{F159} \exp\left(-\tau^2/l^2\right). \qquad (5.12)$$

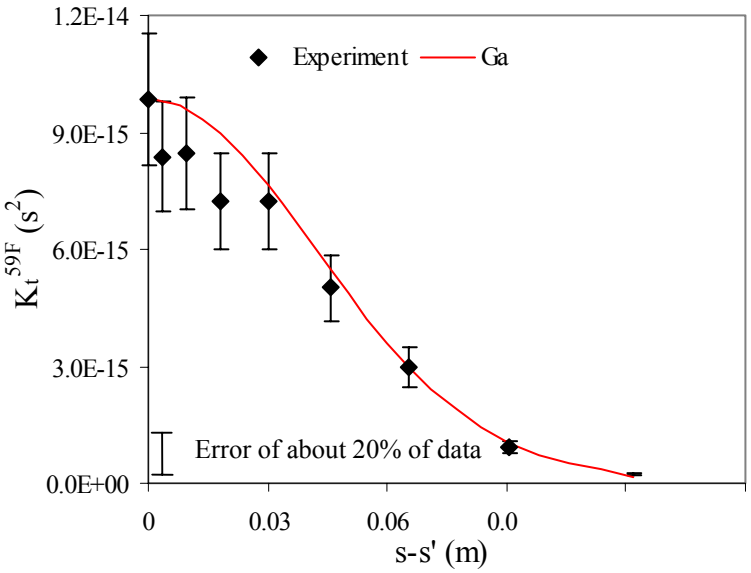

Figure 5.13. Correlation function of travel time obtained from experimental data collected at temperature of $59^\circ F$ along with Gaussian function providing the best fit. The mean flow velocity is U = 3.5 m/s.

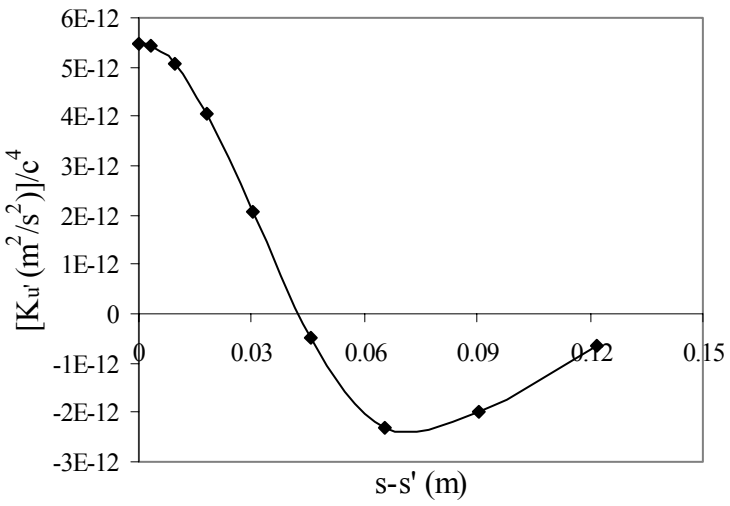

Figure 5.14. Experimentally obtained correlation function of turbulent velocity.

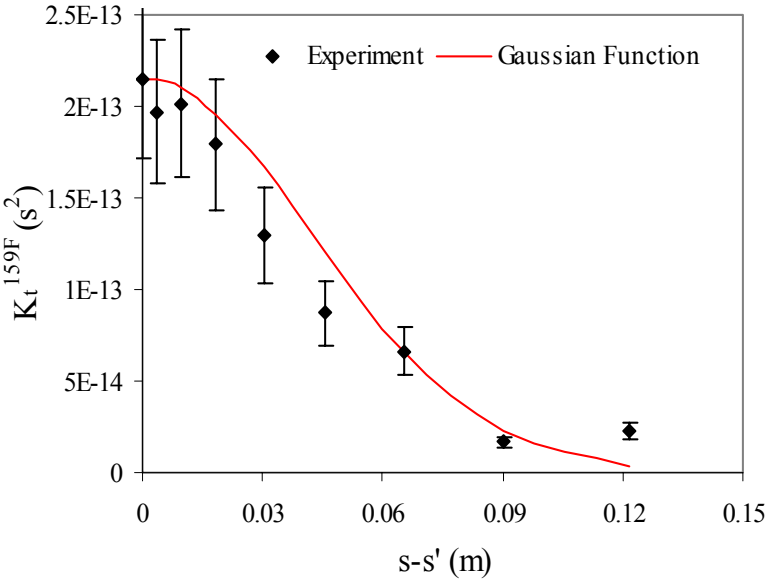

Figure 5.15. Correlation function of travel time obtained from experimental data collected at temperature of $159^{\circ}F$ along with Gaussian function providing the best fit. The mean flow velocity is $U = 3.5$ m/s.

The unknown coefficient is determined to be $\sigma_t^2\big|_{F159} = 2.05\text{E-}13$. In accordance with the methodology, the next step is to find the correlation function of sound speed fluctuations. Correlation function of sound speed fluctuations can be found from the following equation

$$K_t^{F159^\circ}(s,s') - K_t^{F59^\circ}(s,s') = \frac{1}{c^4}\int_s\int_{s'} K_{c'}(x,x')dxdx', \qquad (5.13)$$

where

$$K_t^{F159^\circ}(s,s') - K_t^{F59^\circ}(s,s') = \left(\sigma_t^2\big|_{F159^\circ} - \sigma_t^2\big|_{F59^\circ}\right)\exp\left(-(s-s')^2/l^2\right) = \\ = \Delta\sigma_t^2\exp\left(-\tau^2/l^2\right) \qquad (5.14)$$

Figure 5.16 shows the difference in correlation functions that appear in equation (5.14).

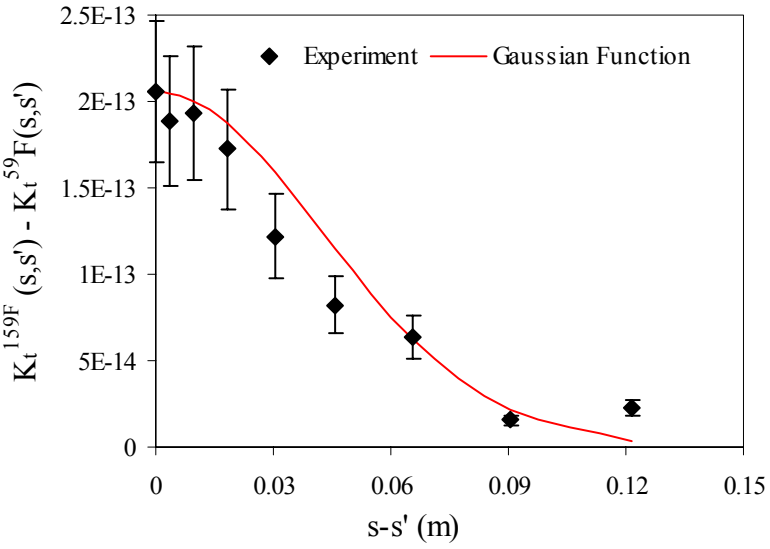

Figure 5.16. Difference in travel time correlation functions corresponding to temperatures and $159^\circ F$.

Substitution of equation (5.13) into equation (5.14) yelds

$$K_{c'}(s,s') = c^4\left[2\frac{\Delta\sigma_t^2}{l^2}\exp\left(-\tau^2/l^2\right)\right] - c^4\left[4\frac{\Delta\sigma_t^2}{l^4}\tau^2\exp\left(-\tau^2/l^2\right)\right]. \quad (5.15)$$

Figure 5.17 shows the correlation function of sound speed fluctuations. The variance of the sound speed fluctuations is $\sigma_{c'}^2 = c^4 2\Delta\sigma_t^2/l^2 \sim 1m^2/s^2$. Neglecting humidity fluctuations, a speed of sound fluctuation is given to the first order by $\langle c'^2\rangle^{0.5} = (c_0/2T_0)\langle T'^2\rangle^{0.5}$ [*Wilson*, 2000], where T_0 is a representative value of the temperature. Turbulence-level measurements made with heating the grid are consistent with results of *Yeh and Van Atta* [1973], namely

$$\beta\langle u'^2\rangle^{0.5}/C_p\,\mathrm{Re} \sim 10^{-9};\ \beta\langle T'^2\rangle^{0.5}/\mathrm{Re}\,\mathrm{Pr} \sim 10^{-5}. \quad (5.16)$$

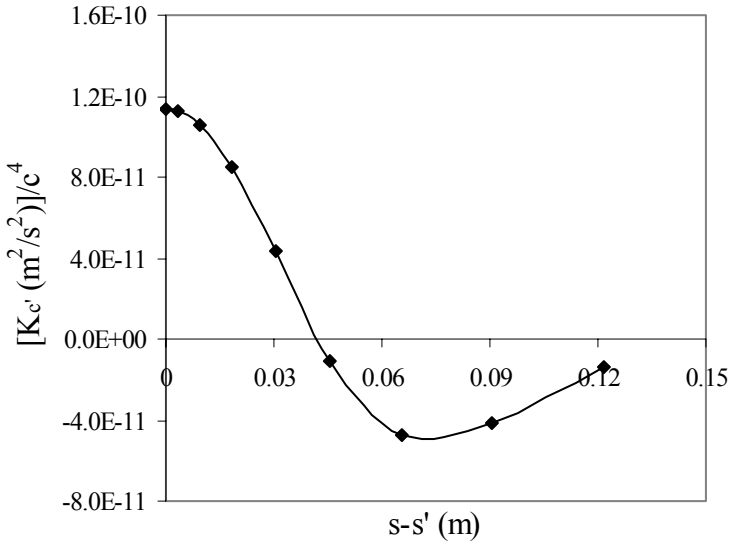

Figure 5.17. Correlation function of sound speed fluctuations.

where β is a coefficient of thermal expansion for air, C_p is a specific heat and R is a universal gas constant.

In the Table 5.1 we compare the basic flow parameters of the flow conditions such as standard deviation of velocity fluctuations σ_u, rate of dissipation ε_u, Kolmogorov length scale l_k, with corresponding wave number k_k, time scale τ_k, velocity scale v_k, Taylor microscale λ_T with corresponding Reynolds number Re_λ, and Reynolds number based on the mesh size *M* and mean velocity *U*. Standard deviation of turbulent velocity is recovered from travel time measurements, consequently it is extremely important to measure the length of a travel path precisely, otherwise small inconsistency in measuring the travel distance results in considerable errors in determination other flow parameters. Standard deviation of velocity fluctuations is almost three times as higher as it was experimentally measured by *Yeh and van Atta* [1973]. Exceedingly high Reynolds number $R_\lambda \sim 400$ is a consequence of a rough approximation of the standard deviation of turbulent velocity.

5.4.2 Spectrum of Grid-Generated Turbulent Flow.

Early works on wave propagation in random media were based on 3-D Gaussian turbulence models [*Wilson*, 2000]. As it was mentioned above, the model has an advantage of analytical convenience. However, one range of turbulence structure it does not capture is the inertial subrange, where energy is proportional to the wave number raised to the $-5/3$ power, which exists in high Reynolds number flows, such as atmosphere [*Wilson*, 2000]. For the present experimental conditions an inertial subrange is not expected in the power spectrum. Under similar conditions *Van Atta and Chen* [1968] reported the absence of an inertial subrange in their velocity spectra for unheated grids. *Yeh and Van Atta* [1973], *Sepri* [1976] observed no inertial subrange in the velocity

Experiment		Yeh and van Atta [1973]	
U	3.5 m/s	U	4.0 m/s
M	$2.54 \cdot 10^{-2} m$	M	$4 \cdot 10^{-2} m$
D	$6.35 \cdot 10^{-3} m$	D	$8.0 \cdot 10^{-3} m$ m
$\sigma_u = \langle u'^2 \rangle^{0.5}$	0.28 m/s	$\sigma_u = \langle u'^2 \rangle^{0.5}$	0.09 m/s
ν	$1.55 \cdot 10^{-5} m^2/s$	ν	$1.55 \cdot 10^{-5} m^2/s$
ε_u	$3.5 \cdot 10^{-2} m^2/s^3$	ε_u	$4.56 \cdot 10^{-2} m^2/s^3$
$k_k = (\varepsilon_u / \nu^3)^{0.25}$	$1771\,\mathrm{m}^{-1}$	$k_k = (\varepsilon_u / \nu^3)^{0.25}$	$1872 m^{-1}$
$\eta = l_0 = 1/k_k$	$5.6 \cdot 10^{-4} m$	$l_k = 1/k_k$	$5.34 \cdot 10^{-4} m$
$\tau_k = (\nu / \varepsilon_u)^{0.5}$	$2.1 \cdot 10^{-2}\,\mathrm{s}^{-1}$	$\tau_k = (\nu / \varepsilon_u)^{0.5}$	$1.87 \cdot 10^{-2}\,\mathrm{s}^{-1}$
$v_k = (\varepsilon_u \tau_k)^{0.5}$	$2.7 \cdot 10^{-2}$ m/s	$v_k = (\varepsilon_u \tau_k)^{0.5}$	$2.88 \cdot 10^{-2}$ m/s
$\lambda_T = (15\nu / \varepsilon_u)^{\frac{1}{2}} \sigma_u$	$2.28 \cdot 10^{-2}$ m/s	$\lambda_T = (15\nu / \varepsilon_u)^{\frac{1}{2}} u'$	$6.25 \cdot 10^{-3} m$
$\mathrm{Re}_M = UM/\nu$	~6000	$\mathrm{Re}_M = UM/\nu$	~10500
$\mathrm{R}_\lambda = \sigma_u \lambda_T / \nu$	~400	$\mathrm{R}_\lambda = u' \lambda_T / \nu$	35.2

Table 5.2 Basic Parameters of the Flow Conditions for Heated Grid Turbulence at x/M=30. (Comparison with Yeh and Van Atta, 1973).

spectrum, however temperature spectra unexpectedly exhibited $-5/3$ slope for a short range of wavenumbers, although authors noted that there were no satisfactory physical

explanation for the appearance of the temperature spectrum.

The one-dimensional energy spectra were directly calculated from analytical expressions of cross-correlation function of turbulent velocity and sound speed fluctuations.

$$\Phi_t = \frac{1}{2\pi}\int_{-\infty}^{+\infty} K_t(\tau)\exp(-ik\tau)d\tau = \frac{1}{\pi}\int_{0}^{+\infty} K_t(\tau)\cos(k\tau)d\tau\,. \tag{5.17}$$

The PSD of the travel time at the room temperature is

$$\Phi_t^{RT} = \frac{1}{2\pi} A\sqrt{\pi a}\exp\left(-k^2 a / A\right). \tag{5.18}$$

The PSD of the turbulent velocity is

$$\begin{aligned}\Phi_{u'}(k) = {} & \frac{c^4}{\pi}\int_0^{+\infty}\frac{\sigma_t^2\big|_{F59^\circ}}{a}\exp\left(-\tau^2/l^2\right)\cos\left(k\tau\right)d\tau - \\ & -\frac{c^4}{\pi}\int_0^{+\infty}\frac{\sigma_t^2\big|_{F59^\circ}}{l^4}\tau^2\exp\left(-\tau^2/l^2\right)\cos\left(k\tau\right)d\tau\end{aligned}\,. \tag{5.19}$$

Integration of Equation (5.16) yields to the final expression for the PSD of turbulent velocity

$$\Phi_{u'}(\omega) = \frac{c^4 k^2}{4\sqrt{\pi}}\sigma_t^2\big|_{F59^\circ}\, l\exp\left(-k^2 l^2/4\right)\left(\frac{1}{l^2}+\frac{k^2}{2}\right). \tag{5.20}$$

As expected, the PSD of sound speed fluctuations will have the same form, the only difference will be in the numerical coefficient, $\Delta\sigma_t^2$ instead of $\sigma_t^2\big|_{F59^\circ}$. Figure 5.18 shows typical spectra for turbulent velocity and sound speed fluctuations. It is remarkable that the spectral shapes appear unchanged at each of the locations, but that they appear to be shifted uniformly in magnitude. The appearance of such difference was observed in experiments by Sepri [1971, 1976], who studied velocity and temperature spectra under

similar conditions. In Figure 5.19 we compare 1-D velocity spectra is compared with one obtained experimentally by Yeh and van Atta. Experiments by Yeh and van Atta were carried out in the 0.76*m* x 0.76*m* 9*m* test section of the low turbulence wind tunnel. The grid mesh size was *M* was 0.04*m,* with tubular rods of diameter of 0.008*m.* Comparison reveals good correspondence between the velocity spectra recovered from travel time measurements and the one, measured experimentally for the wave number up to $k = 100m^{-1}$. For the larger wave numbers the present velocity spectra is different from the measured velocity spectra. There are several aspects that may explain this difference. First, our velocity spectra are recovered from experimental data for travel time, modeled by the Gaussian function. Apriori, we did not expect to observe -5/3 slope corresponding to the inertial subrange exhibited by the velocity spectra data by *Yeh and van Atta* [1973]. Secondly, due to the fact that turbulent velocity spectra as well as the sound speed fluctuations spectra were drawn directly from travel time data, uncertainty in determination of a length of the travel path leads to considerable errors in modeling of the velocity spectra.

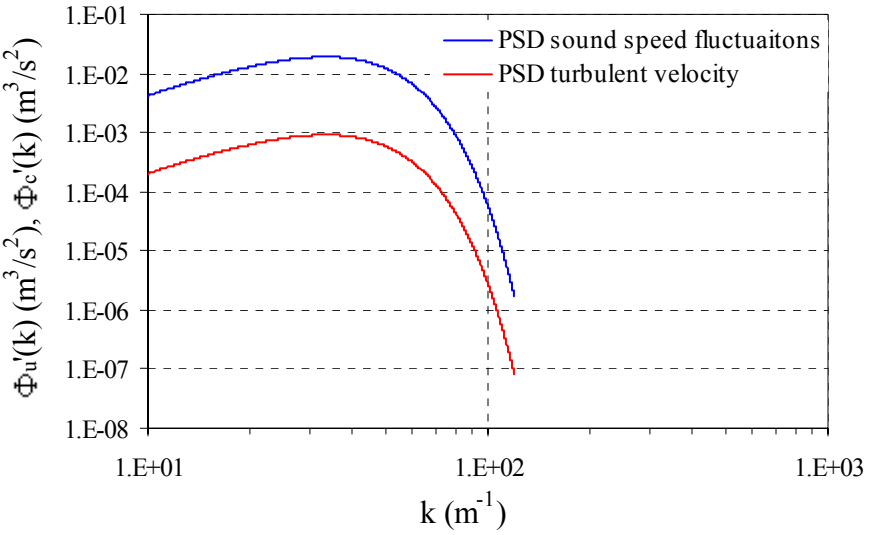

Figure 5.18. 1-D energy spectra of turbulent velocity and sound speed fluctuations

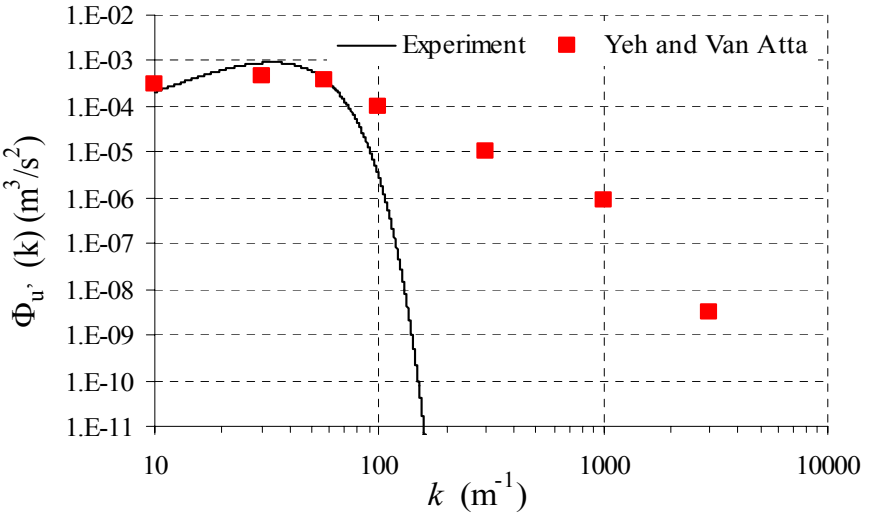

Figure 5.19. Comparison of 1-D energy spectrum of turbulent velocity recovered from experimentally measured travel time statistics with 1-D energy spectrum measured by Yeh and van Atta [1973]

Chapter 6. Summary, Conclusions, Recommendations

In this work we have presented the development of a methodology based on ultrasonic technique for determination of turbulent flow characteristics from statistics of travel time variations. Several experimental results have been presented for the case of heated and non-heated grid experiments. In general these results appear as initially expected, and are in agreement with the conclusions of other investigators. The dissertation is a combination of theoretical and experimental work. Significant effort was put into the development of the methodology for determination of correlation functions and spectra of turbulent velocity and sound speed fluctuations based on the measurements of the travel time. Below we will summarize findings and outline possible directions for future research.

6.1 Summary and Conclusions

In Chapter 1 the motivations for this research work were outlined. The review of classical and recent work in all, theoretical, experimental and numerical areas relevant to this dissertation was presented. The primary goals of the dissertation, objectives and methodology were formulated.

In the Chapter 2 a brief exposition of several topics from the theory of random fields and turbulent theory related to the following experimental and theoretical analysis were

given.

Theoretical model

Chapter 3 was devoted to the derivation and analysis of the equations describing the propagation of acoustical waves in inhomogeneous moving media. Two well known approximate theories of wave propagation, namely ray acoustics and the Rytov method were presented. Statistical moments of a sound field were calculated using these two approaches following the reviews of published works. The theory of travel time fluctuations of sound waves due to the turbulence in the atmosphere based on the Kolmogorov's "2/3" law was presented and the physical and mathematical issues related to the basic flowmeter equation were addressed. Special attention was put into the reformulation of the classical flowmeter equation in the form that includes turbulent velocity and sound speed fluctuations. The resulting integral equation in terms of correlation functions for the travel time, turbulent velocity and sound speed fluctuations is novel and important not only in the perspective of development of the methodology for spectral analysis of isotropic homogeneous turbulence but also as an important issue in achieving of a higher accuracy of ultrasonic devices.

Experimental model

The ultrasonic technique was employed for diagnostics and determination of the statistics of grid-generated turbulence. Chapter 4 was devoted to the description of the experimental apparatus. The major steps of the performance of ultrasonic measurement system with a discussion of each component of the system, namely, ultrasonic flowmeter, Data Acquisition Cards, LabVIEW software and characteristics of each component were summarized in this chapter.

Chapter 5 was devoted to the key aspect of the dissertation: application of the travel-time ultrasonic technique for data acquisition in the grid-generated turbulence and analysis of the experimental data. The difficulty of obtaining laboratory measurements of phase or time of flight variance, as well as amplitude variance is indicated by the dearth of data. The chapter was opened with an overview of ultrasonic technique. The effect of turbulence on acoustic waves in terms of the travel time was studied for various mean velocities and for different angular orientations of the acoustic waves with respect to the mean flow. The overview was followed by the analysis of the effects that turbulence has on acoustic signals developed in the context of ray acoustic approach. Further, the situation when mathematical conditions for ray acoustics are violated and ray acoustic approach is no longer valid was discussed. Rytov's approach was used to study the influence of turbulence in terms of second moments of the travel time and log-amplitude fluctuations. Comparison with theoretical results provided in literature was performed. In the second half of Chapter 5 experimental data were obtained for ultrasonic wave propagation downstream of a heated and non-heated grid for different angular orientations of the acoustic waves with respect to the mean flow. A new methodology for determination of correlation functions and spectra of turbulent velocity and sound speed fluctuations has been proposed. The travel time statistics are approximated by a Gaussian function. The coefficients and decay exponent of Gaussian function are determined by the experimental data. Originally meant for ideal flow ultrasonic flowmeter equation has been reformulated in terms of correlation functionsin order to account for turbulent velocity and sound speed fluctuations.

.

1. It has been experimentally demonstrated that an ultrasonic travel-time method can be efficiently utilized for determination of turbulent flow statistical characteristics in laboratory conditions.

2. Simple methodology using the ultrasonic technique together with Kolmogorov's 2/3 law was implemented for diagnostic of the grid-generated turbulent flow.

    a. Methodology was validated using analytical estimates obtained from ray acoustic theory.

    b. In the experiment with different values of mean velocity, the experimental results have indicated that there is strong dependence on the former.

    c. The experimental results have shown that the ultrasonic method along with ray acoustic approach can be efficiently utilized for measuring characteristics of turbulent flow in laboratory scale, such as structure coefficient, C ($m^{2/3}/s$).

3. From the travel time measurements performed in both turbulent and non-turbulent media, Fermat's principle is demonstrated.

4. Using experimental data of travel time effect of turbulence on acoustic wave propagation has been demonstrated in terms of travel time variation and log-amplitude variation. The experimental data have been interpreted using the ray acoustic method and diffraction theory, or Rytov's method.

    a. It is clear from experimental results for travel time variance that in the presence of small diffraction effects, the ray acoustic approach is valid, so area of ray acoustic

approach is broader than the rigorous sufficient conditions defined, at least for travel-time fluctuations.

b. The experimental data confirm the Rytov theory in that amplitude variation is greatly influenced by diffraction effects.

5. Experimental data for the case of both, velocity and thermal turbulence interpreted using updated version of flowmeter equation, reveal a significant effect due to sound speed fluctuations, thus, sound speed fluctuations may not be neglected in the flowmeter equation as has often been supposed previously both in experiments and theory.

6. The results provided by the methodology appear to be consistent with the wealth of experimental data provided.

7. Updated flowmeter technology has a great potential for flow metering in industrial facilities for various flow types, including non-ideal flows, thus reducing errors caused by disturbances of the flow profile.

8. The combination of the proposed methodology together with ultrasonic technique benefits not only from high accuracy provided by high-tech equipment, but also offers a portable, simple in installation and use apparatus that can be used for turbulent flow diagnostic in commercial and non-commercial applications.

6.2 Recommendations

1. The experimental data presented as well as their interpretation, are a subject to re-examination in improved experimental conditions. Namely,

- Well-controlled mean temperature
- Stable wind tunnel flow at low speeds
- Extremely accurate determination and control of a travel distance
- Accurate determination of the temperature far downstream the grid, since small errors in temperature determination may lead to large errors in sound speed fluctuations

2. In situ characterization of the turbulence as well as a good source of data for a comparison ultrasonic measurements could be combined probe studies (hot, cold wire anemometry).

3. Along theoretical lines it would be useful to examine the von Karman spectrum for travel time experimental data approximation since the von Karman in many case, especially in a grid-generated turbulent flow it provides a fairly good approximation to the spectrum of turbulence [*Ostashev*, 1997; *Wilson*, 2000].

4. The methodology developed based on the measurements of the travel time fluctuations at the receiver can be used to reconstruct not only velocity but also temperature field.

5. The basic theory of wave propagation in turbulent media demonstrates the linear

increase of travel-time variance with the propagation distance [*Chernov*, 1960]. However, recent numerical and theoretical studies exhibit an almost quadratic growth of travel time variance with travel distance [*Karweit et al*, 1991; *Iooss et al*, 2001]. The reason for this behavior is not entirely understood yet, but it proved to be closely related to the occurrence of first caustics [*Kulkarny and White*, 1982; *Blanc-Benon et al*, 1991, *Klyatskin*, 1993]. It would be useful to perform similar experiments for larger travel distances in order to detect nonlinear behavior of travel time variance [*Durgin, et al*., 2004 (accepted)].

Bibliography

Andreeva, T.A., Durgin, W.W., Weber, F.J., Johari, H, "Determination of Statistical Characteristics of Isotropic Turbulence," *Proceedings of ASME FEDSM'01, ASME Fluids Engineering Division Summer Meeting*, New Orleans, Louisiana, May 29-June 1, 2001.

Andreeva T.A and Durgin, "Ultrasonic Technique in Characterization of the Grid-Generated Turbulent Flow," *Advanced Problems in Mechanics, XXX International Conference*, Russia, St.-Petersburg, June 22-July 2, 2002.

Andreeva T.A. and Durgin, W.W., "Ultrasonic Technique for Investigation of the Effect of Grid-generated Turbulence on Sound Wave Propagation, "*AIAA Paper 2003-1090, 41st Aerospace Science Meeting and Exhibit*, Reno, Nevada, 2003 (a).

Andreeva T.A. and Durgin, W.W., "Ultrasound Technique for Prediction of Statistical Characteristics of Grid-Generated Turbulence," *AIAA Journal*, Vol. 41(8), 2003, pp.1438-1443 (b).

Andreeva T.A. and Durgin, "Some Theoretical and Experimental Aspects in Ultrasonic Travel Time Method for Diagnostic of Grid-generated Turbulence," *World Congress on Ultrasonics* , Paris, France, September 7-10, 2003 (c).

Andreeva, T.A, and Durgin, W.W., "Experimental Investigation of Ultrasound Propagation in Turbulent, Diffractive Media," *The Journal of the Acoustical Society of America*, accepted for publication, 2003 (d).

Bass, H.E., Bolen, L.N., Raspet, R., McBride, W. and Noble, J., "Acoustic propagation through a turbulent atmosphere: Experimental characterization," *Journal of Acoustical Society of America,* Vol. 90 (96), 1991, pp.3307-3313.

Batchelor, G.K., The Theory of Homogeneous Turbulence, Cambridge University Press., 1953.

Bergman L., and Schaefer, C., Optics of Waves and Particles., Berlin ; New York : W. de Gruyter, 1999.

Bendat, J. S. and Piersol, A.G., Random data; analysis and measurement procedures, New York, Wiley-Interscience, 1971.

Blanc-Benon, Ph., Juvé, D. and Comte-Bellot, G., "Occurrence of caustics for high-frequency caustic waves propagating through turbulent field," *Theoretical and Computational Fluid Dynamics* Vol. 2, 1991, pp. 271-278.

Blanc-Benon, Ph., Juvé, D. and Chevret, P., "On the influence of the turbulence modeling for atmospheric sound propagation," *Journal of Acoustical Society of America,*

Vol. 98, 1995, p. 2924.

Blokhintzev, D., The Acoustics of an Inhomogeneous Moving Medium, 1953

Boyse, W.E., "Wave Propagation and the Inversion in Slightly Inhomogeneous Media," Ph.D. Dissertation, Stanford University, 1986.

Boyse, W.E., and Keller, J.B., "Short Acoustic, Electromagentic, and Elastic Waves in Random Media," *Journal of Optical Society of America A*, Vol. 12, 1994, pp. 380-389.

Brassier, P., Hosten.B., Vulovic, F., "High-frequency Transducers and Correlation Method to Enchance Ultrasonic Gas Flow Metering," *Flow Measurement and Instrumentation,* Vol. 12, 2001, pp. 201-211.

Brown, E.H. and Hall, F.F., "Advances in atmospheric acoustics," *Rev. Geophys. Space Phys.***16**, 47-110 (1978).

Chernov, L.A. Wave Propagation in a Random Medium, McGraw-Hill Book Company, Inc, 1960.

Chevret, P., Blanc-Benon, Ph. and Juvé, D., "A numerical model for sound propagation through a turbulent atmosphere near the ground," *Journal of Acousitcal Society of America,* Vol. 100(6), 1996, pp. 3587-3599.

Clifford, S.F. and Lataitis, R.J., "Turbulence Effects on Acoustic Wave Propagation over a Smooth Surface," *Journal of Acoustical Society of America,* Vol. 73(5), 1983, pp. 1545-1550.

Comte-Bellot, G. and Corrsin, S., "Simple Eulerian Time Correlation of Full- and Narrow- Band Velocity Signals in Grid-Generated "Isotropic" Turbulence," *Journal of Fluid Mechanics*, Vol. 48, 1971, pp. 273-336.

Corrsin, S., "Encyclopedia of Physics," Vol. 8(2), 1963, p.568.

Daigle, G.A., J.E. Piercy, J.E. and Embleton, T.F., "Effect of atmopspheric turbulence on the interference of sound waves near a hard boundary," *Journal of Acousitcal Society of America,* Vol. 64, 1978, pp. 622-630.

Daigle, G.A., Piercy, J.E. and Embleton, T.F. "Line-of-site propagation through atmospheric turbulence near the ground," *Journal of Acoustical Society of America*, Vol. 74, 1983, pp.1505-1513.

Daigle, G.A., Embleton, T.F.W. and Piercy, J.E., "Propagation of sound in the presence of gradients and turbulence near the ground," *Journal of Acoustical Society of America,* Vol. 79, 1986, pp. 613-627.

Dacol, D.K., "Pulse Propagation in Randomly Fluctuating Media," *Journal of Acoustical Society of America*, Vol. 109 (6), 2001, pp.2581-2586.

Di Iorio, D.D. and Farmer, D.M., "Separation of current and sound speed in the effective refractive index for a turbulent environment using reciprocal acoustic transmission," *The Journal of the Acoustical Society of America,* Vol. 103(1), 1981, pp. 321-329.

Di Iorio, D.D. and Farmer, D.M., "Two-Dimensional Angle of Arrival Fluctuations," *The Journal of the Acoustical Society of America,* Vol. 100(2) (Part1), 1996, pp.814-824.

Durgin, W.W., Meleschi, S.B. and Andreeva, T.A., "Experimental Investigation of Statistical Moments of Travel Time in Grid-Generated Turbulence," *42nd AIAA Aerospace Sciences Meeting and Exhibit*, 5-8 January, 2004, Reno, Nevada. (Accepted)

Ewart, T.E. and Percival, D.B., "Forward Scattered Waves in Rnadom Media: The Probability Distribution of Intensity," *The Journal of the Acoustical Society of America*, Vol. 80, 1986, pp.1745-1753.

Godin, O.A., "Wave Equation for Sound in a Medium with Slow Current," *Trans. Acad. Sci. USSR Earth Science,* Vol. 293 (1), 1987, pp.63-67.

Ho, C.M. and Kovasznay, L.S.G., "Modulation of an acoustic wave by turbulent shear flow," *U.S. Air Force Office of Scient. Res., Interim Tech. Rep.*, F44-620-69-C-0023, 1974.

Högström, U, "Review of some basic characteristics of the atmospheric surface layer," *Boundary- Layer Meteorology*, Vol. 78**,** 1996, pp. 215-246.

Iooss, B., Blanc-Benon, Ph. and Lhuillier, C., "Statistical moments of travel times at second order in isotropic and anisotropic *random* media," *Waves in Random Media* Vol. 10, 2000, pp. 381-394.

Iooss, B. and Galli, A., "Statistical tomography for seismic reflection data," Proceedings of the 6th International Geostatistics Congress, Cape Town, South Africa, April 2000.

Ishimaru, A., Wave Propagation and Scattering in Random Media, Academic, New York, 1978.

Johari, H. and Durgin, W.W., "Direct Measurements of Circulation using Ultrasound," *Experiments in Fluids*, Vol. 25, 1998, pp.445-454.

Jojnson, M.A., Raspet, R. and Bobak, M.T., "A Turbulence Model for Sound Propagation from an Elevated Above Level Ground," *The Journal of the Acoustical Society of America,* Vol.81(3), 1987, pp. 638-646.

Karweit, M., Blanc-Benon, Ph., Juvé, D. and Comte-Bellot, G., Simulation of the Propagation of an Acoustic Wave through a Turbulent Velocity Field: a Study of Phase Variance," *The Journal of the Acoustical Society of America,* Vol. 89(1), 1991, pp. 52-62.

Kistler, A.L., O'Brien, V. and Corrsin, S., "Preliminary Measurements of Turbulence and Temperature Fluctuations Behind a Heated Grid," *N.A.S.A.* RM 54D19, 1954.

Kits, A.H. van Heyningen, "Solid State Doppler Wind Sensor," *Abstracts, SBIR* Topic No. N85-181, 1987

Klyatskin, V.I., "Caustics in Random Media," *Waves in Random Media*, Vol. 3, 1993, pp. 93-100.

Kolmogorov, A., "The Local Structure of Turbulence in Incompressible Viscous Fluid for Very Large Reynolds Numbers, *C.R. Akad. Sci. SSSR*, Vol. 30, 1941, pp. 301-305.

Kolmogorov, A.N., "Energy Dissipation with Locally Isotropic Turbulence," *DAN SSSR*, Vol. 32(1), 1941, p.19

Kolmogorov, A., "A Refinement of Previous Hypothesis Concerning the local Structure in a Viscous Incompressible Fluid in High Reynolds Number," Journal of Fluid Mechanics, Vol. 13, 1963, p.82.

Krasil'nikov, V.A., "Propagation of Sound in a Turbulent Atmosphere," *Doklady Acadenii Nauk SSSR* (in Russian), Vol. 47, 1945, pp.486-489.

Krasil'nikov, V.A. "Phase Fluctuations in Ultrasonic Waves During Propagation of Sound in the Atmosphere," Doklady Academii Nauk SSR (in Russian), Vol. 88, 1953, pp. 657-660.

Krasil'nikov, V.A., Sound and Ultrasound Waves in Air, Water and Solid Bodies, Jerusalem, 1963.

Krasil'nikov, V.A., "The Effect of Refractive Index Fluctuations in the Atmosphere on Propagation of Ultrashort Radio Waves," Izvestiya AN SSSR, Seria Geograficheskaya I Geofizicheskaya, vol. 13(1), 1949, p.33

Kristensen, L., Lenschow, D. H., Kirkegaard, P. and Courtney, M., ''The spectral velocity tensor for homogeneous boundary-layer turbulence,'' *Boundary-Layer Meteorology*. Vol. 47, 1989, pp. 149–193.

Kulkarny, V.A. and White, B.S., "Focusing of Waves in Turbulent Inhomogeneous Media," *Journal of Physics of Fluids*, Vol. 25 (10), 1982, pp. 1779-1784.

Landau, L.D. and Lifshitz, E.M., Course of Theoretical Physics, Fluid Mechanics, Volume 6, 2nd edition, Institute of Physical Problems, USSR Academy of Science, Moscow.

Leontovich, M.A., Journal of Experimental Physics, Vol. 6, 1936, p.561. In Russian

Loitsianskii, L.G., "Some Basic Laws of Isotropic Turbulent Flow," *Cent. Aero. Hydrodyn. Inst. Moscow, Rept. 440. (Trans. NACA TM 1079.)* 1939.

Lawrence, R.S. and Strohbehn, J.W., "A survey of clear-air propagation effects relevant to optical communications," *Proceedings IEEE,* Vol. 58, 1970, pp. 1523-1545.

Lynnworth, L.C., "Ultrasonic Measurements for Process Control," Academic Press, San Diego, CA, 1989.

Mann, J., "The spatial structure of neutral atmospheric surface layer turbulence," *Journal of Fluid Mechanics*, Vol. 273, 1994, pp. 141–168.

Mills, R.R. and Kistler, A.L., O'Brien, V. and Corrsin, S., "Turbulence and Temperature Fluctuations Behind a Heated Grid," *N.A.S.A. Technical Note* 4288, 1958.

Mohamed, M.S. and LaRue J.C., "The Decay Power Law in Grid-generated Turbulence," *Journal of Fluid Mechanics*, Vol. 219, 1990, pp. 195-214.

Monin, A.S. and Yaglom, A. M., Statistical Fluid Mechanics, Cambridge, MA: MIT Press, 1981.

Mydlarskii, L. and Warhaft, Z., "Passive Scalar Statistics in High_Péclet-number Grid Turbulence," *Journal of Fluid Mechanics*, Vol. 358, 1998, pp. 135-175.

Nelkin, M., "Universality and Scaling in Fully Developed Turbulence," *Advanced Physics,* Vol. 43, 1991, pp.143-181.

Nghiem-Phu, L. and Tappert, F., "Parabolic Equation Modeling of the Effects of Ocean Currents on Sound Transmission and Reciprocity in the Time Domain," *Journal of Acoustical Society of America,"* Vol. 78(2), 1985, pp. 642-648.

Noble, J. M., Bass, H. E. and Raspet, R., "The Effect of Large-scale Atmospheric Inhomogeneities on Acoustic Aropagation," *Journal of Acoustical Society of America*, Vol. 92, 1992, pp.1040–1046.

Obukhov, A.M., "Scattering of Sound in Turbulent Flow," *DAN SSSR*, Vol. 30(7), 1941, pp. 611

Obukhov, A.M., "Characteristics of wind microstructures in the atmosphere near the surface," *Izv. Acad. Sci. USSR Atmos. Ocean. Phys.*, Vol. 3, 1951, p.49.

Obukhov, A.M., " Energy Distribution in the Spectrum of Turbulent Flow," Izvestiya AN SSSR, Seriya Geograficheskaya I Geofizichaskaya, Vol. 5(4/5), 1941, pp.453.

Ostashev, V.E. Acoustics in Moving Inhomogeneous Media, E & FN SPON, London, UK, 1997.

Ostashev, V.E., Salomons, E.M., Clifford, S.F., Lataitis, R.J., Wilson, D.K., Blanc-Benon, Ph., Juvé, D., "Sound propagation in a turbulent atmosphere near the ground: A parabolic equation approach," *Journal of Acoustical Society of America,* Vol. 109(5), 2001, pp. 1894-1906.

Ostashev, V.E. and G. H. Goedecke, ''Interference of direct and ground reflected waves in a turbulent atmosphere,'' *Proceedings of the 8th International Symposium on Long*

Range Sound Propagation, Penn State University,1998, pp. 313–325.

Peltier, L. J., Wyngaard, J. C., Khanna, S. and Brasseur, J. G., ‘‘Spectra in the unstable surface layer,’’ Journal of atmospheric Science, Vol. 53, 1996, pp. 49–61.

Pierce, A.D., Acoustics: An Introduction to Its Physical Principles and Applications, McGraw-Hill, New York, 1981.

Pierce, A.D., “Wave Equation for Sound in Fluids with Unsteady Inhomogeneous Flow,” The Journal of the Acoustical Society of America, Vol. 87(6), 1990, pp. 2292-2299.

Robertson, J.S., Siegmann, W.L. and Jacobson, M.J., “Current and Current Shear Effects in the Parabolic Approximation for Underwater Sound Channel,” *Journal of Acoustical Society of America,* Vol. 77(5), 1985, pp. 1768-1780.

Roth, S.D., Acoustic Propagation in the Surface Layer under Convectively Unstable Conditions, Ph.D. Dissertation in Acoustics, The Pennsylvania State University, University Park, Pennsylvania, 1983.

Roth, M., Müller, G. and Snieder, R., “Velocity Shift in Random Media,” *Geophysical Journal Internationa,* Vol 115, 1993, pp. 552-563.

Rytov, S.M., Kravcov, Yu.A., Tatarskii, V.I., Elements of Random Process Theory: Principles of Statistical Radiophysics, Springer-Verlag, Berlin, 1987, Vol. 4.

Samuelides, Y., “Velocity shift using the Rytov approximation,” *Journal of Acoustical Society of America*, Vol. 104, 1998, pp. 2596-2603.

Schmidt, D.W., “Acoustical Method for Fast Detection and Measurement of Vortices in Wind Tunnels,”*ICIASF’75 Record”*, pp.216-228.

Schmidt, D.W., Tilmann, P.M., “Experimental Study of Sound-wave Phase Fluctuations caused by Turbylant Wakes,” *Journal of Acoustical Society of America,* Vol. 47, 1970, pp.1310-1324.

Sepri, P., “Two-point Turbulence Measurements Downstream of a Heated Grid,” *The Physics of Fluids,* Vol. 19 (12), 1976, pp. 1876-1884.

Snieder, T., and Aldridge, D.F., “Perturbation Theory for Travel Times,” *Journal of Acoustical Society of America*, Vol. 98, 1995, pp. 1565-1569

Sreenivasan, K.R. and Antonia, R.A., “The phenomenology of Small-Scale Turbulence,” *Annual Review of Fluid Mechanics*, Vol. 29, 1997, pp. 435-472.

Sreenivasan, K.R., Tavoularis, S., Henry, R. and Corrsin, S., “Temperature Fluctuations and Scales in Grid-generated Turbulence,” *Journal of Fluid Mechanics*, Vol. 100(3), 1980, pp. 597-621.

Stratonovich, R.L., Selected Topics in the Theory of Fluctuations in Radio Engineering, Sovetskoe Radio, 1961.

Tatarskii, V.I., Wave Propagation in a Turbulent Medium, McGraw-Hill, New York, 1961.

Tatarski, V.I., The Effect of the Turbulent Atmosphere on Waves Propagation, Israel Program for Scientific Translation, Jerusalem, 1971.

Tatarskii, V.I., Wave Propagation in Turbulent Media, (Nauka, Moscow, 1967, in Russian).

Tennekes, H. and Lumley, J.L., First Course in Turbulence, The MIT Press, 1972.

M.S. Uberoi and S. Wallis, "Effect of Grid Geometry on Turbulence Decay, "*Journal of Physics of Fluids,* Vol. 10, 1967, pp. 1216-1230.

Van W. Atta and Chen, W.Y., *Journal of Fluid Mechanics*, Vol. 34, 1968, p.497.

Warhaft, Z., "Passive Scalars in Turbulent Flows," *Annual Review of Fluid Mechanics,* Vol. 32, 2000, pp. 203-240.

Warhaft, Z., and Lumley, J.L., "The Decay of Temperature Fluctuations and Heat Flux in Grid-Generated Turbulence,"*Structure and Mechanism of Turbulence*, Vol. 2, Lectures Notes in Physycs, Vol. 76, 1978(a).

Warhaft, Z., and Lumley, J.L., "An Experimental Study of the Decay of Temperature Fluctuations in Grid-generated Turbulence," *Journal of Fluid Mechanics*, Vol. 88 (4), 1978 (b), pp.659-684.

Wielandt, E., "On the Validity of the Ray Approximation for Interpreting Delay Times," *in Seismic Tomography,* edited by G. Nolet (Reidel, Dordrecht, 1987), pp.85-98.

Weber, F.J., Ultrasonic Circulation-meter for Determining the Magnitude of Circulation about a Rapidly Pitching Airfoil, Master Thesis, Worcester Polytechnic Institute, 1994.

Wilken, W., ''Experimental study of the influence of varying atmospheric conditions on sound propagation close to the ground'' *Acustica*, Vol. 62, 1986, pp. 55–65.

Wilson, D.K., Acoustic Tomographic Monitoring of the Atmospheric Boundary Layer, Ph.D. Dissertation, The Pennsylvania State University, 1992.

Wilson, D.K., Brasseur, J.G., Gilbert, K.E., "Acoustic scattering and the spectrum of atmospheric turbulence," *The Journal of the Acoustic Society of America*, Vol. 105(1), 1999, pp.30-34.

Wilson, D. K., "A turbulence spectral model for sound propagation in the atmosphere that incorporates shear and buoyancy forcing," *Journal of Acoustical Society of America*,

Vol. 108 (5), 2000, pp.2021-2038.

Wilson, D. K. and Thomson, D. W., ‘‘Acoustic propagation through anisotropic, surface-layer turbulence,’’ *The Journal of the Acousitcal Society of America,* Vol. 96, 1994, pp. 1080–1095.

Yeh, T.T. and van Atta, C.W., “Spectral Transfer of Scalar and Velocity Fields in Heated-grid Turbulence,” *Journal of Fluid Mechanics,* Vol. 58, 1973, pp. 233-261.

Yeh, T.T. and Espina, P.I., “Special Ultrasonic Flowmeters for In-situ Diagnosis of Swirl and Cross Flow,” *Proceedings of ASME Fluids Engineering Division Summer Meeting*, FEDSM 2001-18037, 2001.

Yeh, T.T. and Mattingly, G.E., “Ultrasonic Technology: Prospects for Improving Flow Measurements and Standards,” *Proceedings of the 4th International Symposium on Fluid Flow Measurements*, Denver, Co, *NAFFMC* 1999 and *Proceedings FLOMEKO* 2000.

Yeh, T.T. and Espina P.I., Osella, S.A., “An Intelligent Ultrasonic Flow Meter for Improved Flow Measurements and Flow Calibration Facility,” *IEEE Instrumentation and Measurement technology Conference*, Budapest, Hungary, May 21-23, 2001.

Appendix A

The CS_SCOPE. VI is the actual interface to any version of the CompuScope high-speed data acquisition hardware. CS_SCOPE is the main interface between the CompuScope hardware installed in the computer and LabVIEW

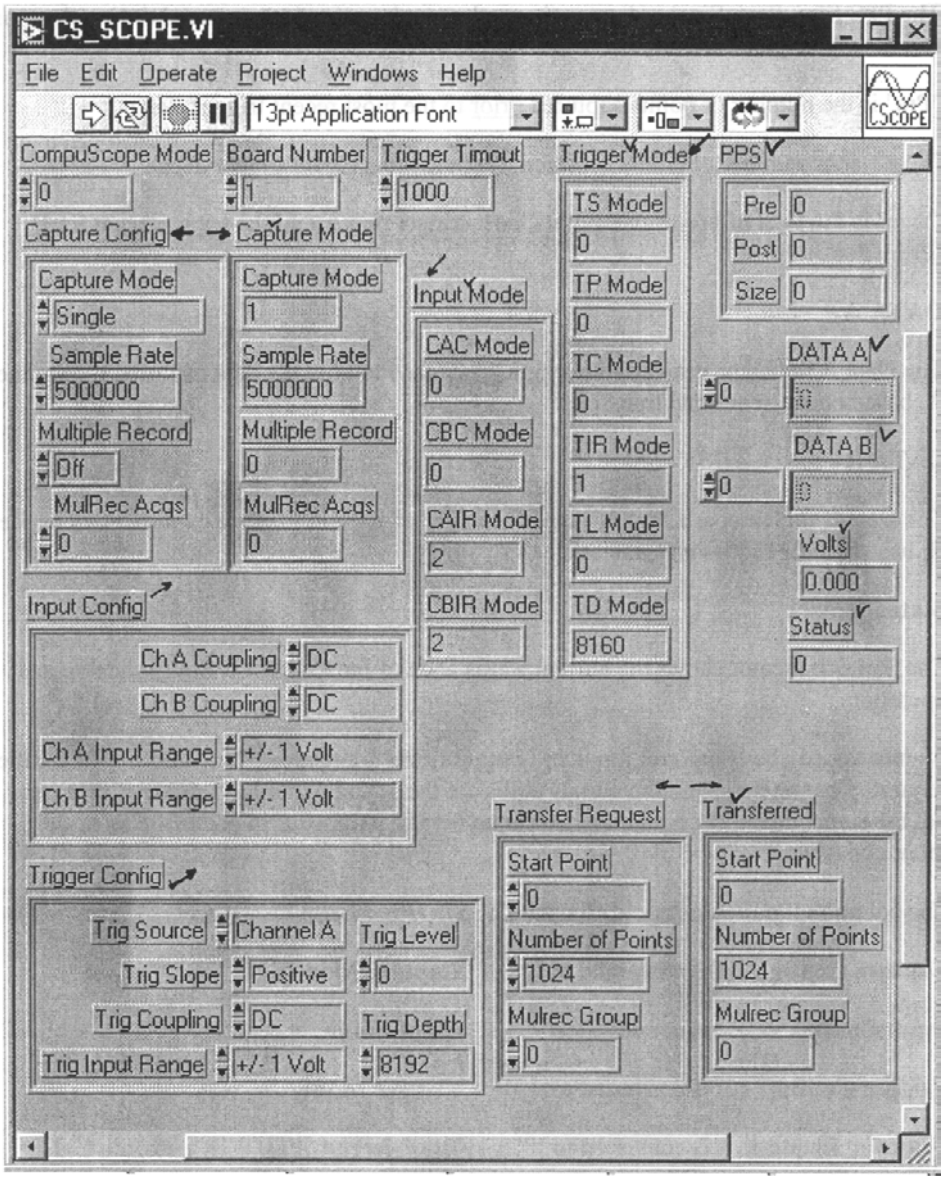

Figure 6.1 The CS_SCOPE. VI Front Panel.

The Gage Oscilloscope.VI is a program that uses the CompuScope modes to capture, transfer and display data acquired from CompuScope board.

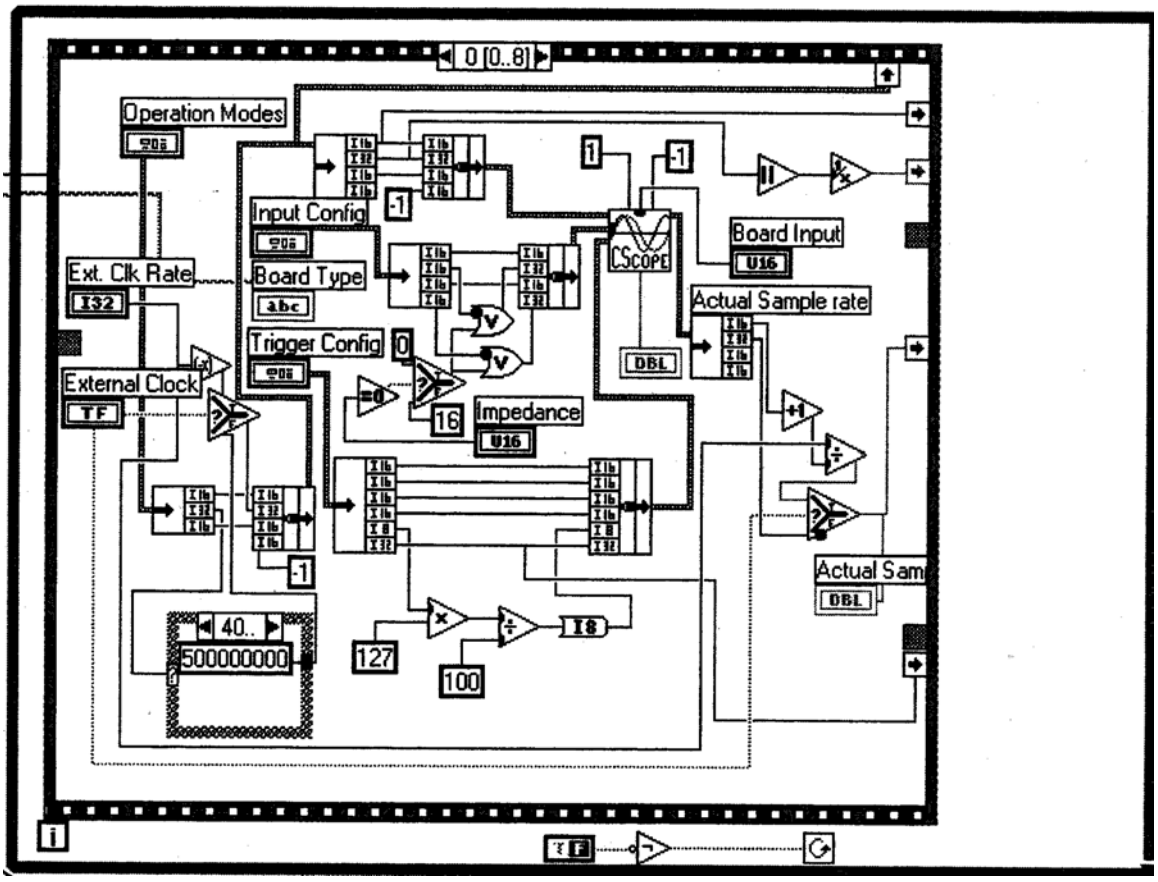

Figure 6.2. Gage Oscilloscope Sequence 0.

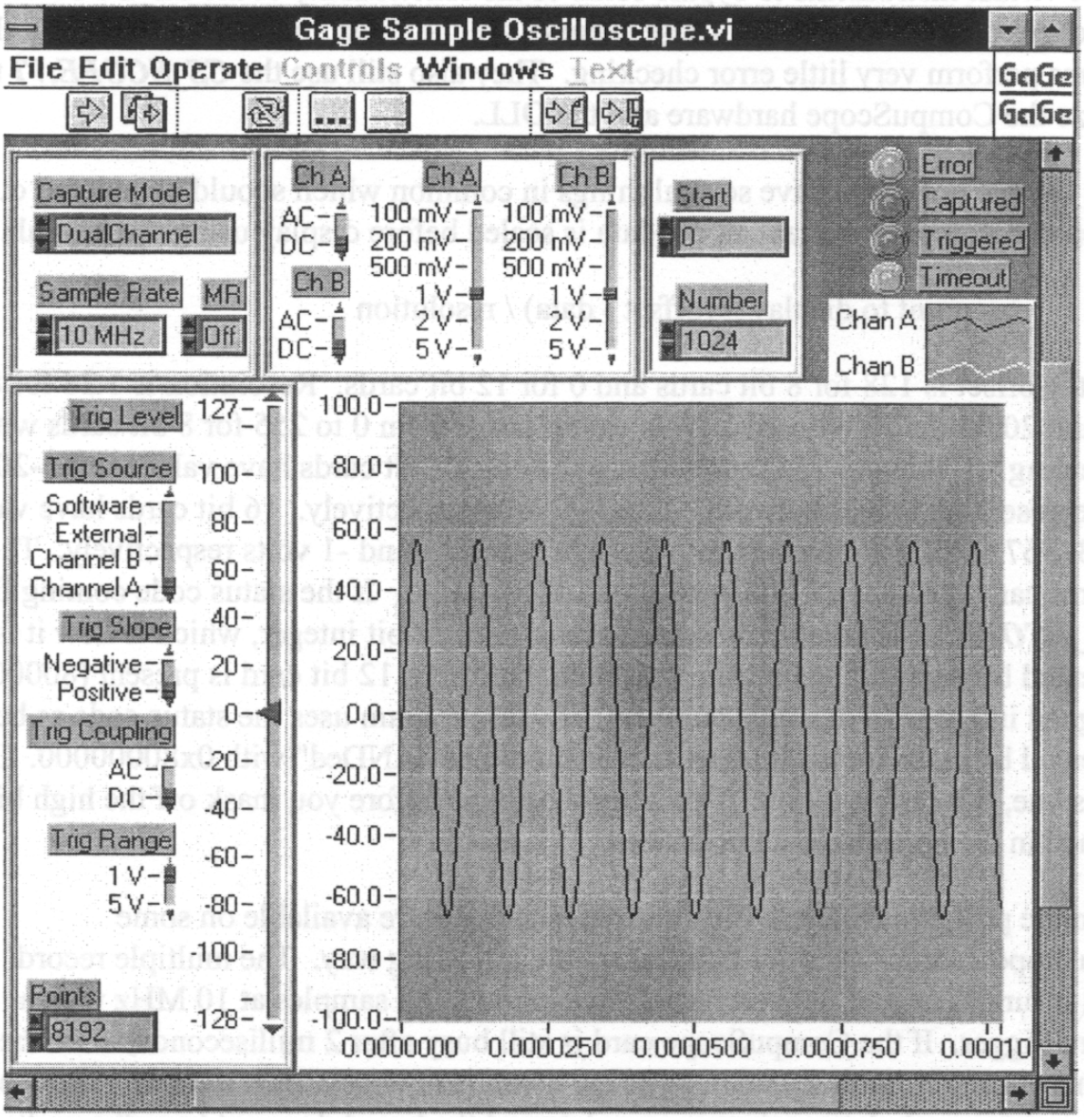

Figure 6.3. Gage Sample Oscilloscope. VI (demonstration mode).

Appendix B

```
!The program calculates correlation function to find
! the time interval between the sent and arrived signals

          include '../Input/param.txt'

        INTEGER    IPRINT, MAXLAG, K, NF, LL
     PARAMETER  (IPRINT=0, MAXLAG=1000, NOBS=1024)
     INTEGER    IMEAN, ISEOPT, NCOL, NROW
        REAL                CC(-MAXLAG:MAXLAG),   CCV(-MAXLAG:MAXLAG),
Y(NOBS),
    &        RDATA(1000,2), SECC(-MAXLAG:MAXLAG),XMEAN,
    &        XVAR, YMEAN, YVAR, X(NOBS)
     double precision XX(N),YY(N),TT(N)
        EXTERNAL   CCF

        kk=1
        ikl=1
!This part of the program opens two files, reads data, makes one file with
!a proper time interval and calculates length of each vectors

!FILE NAMES HAVE TO BE CHANGED/\/\/\/\/\/\/\/\/\/\/\/\/\/\/\/\/\/\/\/\/\/\/\/\/
c          open(unit=3,file='../INPUT/TRDPR/DATA/
c    +A_10.txt',status='old')
c          open(unit=5,file='../INPUT/TRDPR/DATA/
c    +B_10.txt',status='old')

c        if (ikl.eq.1) then
c          open(unit=6,file='../INPUT/TRDPR/COM/
c    +AB_10.txt', status='unknown')
           open(unit=7,file='
    +corel.txt', status='unknown')
c        endif
**********************************************************
c        ____________________________________________________________________
c        if (kk.eq.1) then
c          open(unit=9,file='../INPUT/RoomTemp/
c    +/Correlation/realcor_10.txt', status='unknown')
c        endif
c        ____________________________________________________________________

c          open(unit=10, file='../INPUT/Dt(v)500/
c    +Amplitude/MAX_Amp_35.txt', status='unknown')
c        write(10,*)'   Max_Send           Max_Received '
```

!THE LAST FILE IS THE ONE WITH PROPER TIME AND TWO COLUMNS OF DATA

```
!/\/\/\/\/\/\/\/\/\/\/\/\/\/\/\/\/\/\/\/\/\/\/\/\/\/\/\/\/\/\/\/\/\/\/\/\/\/\


c          do i=1,N
c          read(3,*,end=2) TT(i),YY(i)
c          end do
c  2       continue
c          do i=1,N
c          read(5,*,end=4) TT(i),XX(i)
c          end do
c  4       continue

c          do j=1,N
c          TT(j)=TT(2)*(j-1)
********************************
c         print*,'TT=',TT(2),TT(j)
c         if (TT(2).GT.1.e-5) then
c         print*,'j=',j
c         endif
********************************

c         if (ikl.eq.1) then
c          write(6,8)TT(j),XX(j),YY(j)
c  8       format(3x,3(E15.6,3x))
c         endif
c          enddo
c          close(3)
c          close(5)
c          close(6)
!/\/\/\/\/\/\/\/\/\/\/\/\/\/\/\/\/\/\/\/\/\/\/\/\/\/\/\/\/\/\/\/\/\/\/\/\/\/
!/\/\/\/\/\/\/\/\/\/\/\/\/\/\/\/\/\/\/\/\/\/\/\/\/\/\/\/\/\/\\/\/\/\\/\/\/\/
          PI = 4.*atan(1.)
          IMEAN = 1
   ISEOPT = 0
!==============================================================
======
! This block selects a data interval from all data
c         NF=N/NOBS
c         do LL=1,NF

!==============================================================
=======
c         do J=NOBS*(LL-1)+1,LL*NOBS
c          X(-NOBS*(LL-1)+J)=1.*XX(J)
```

```
c          Y(-NOBS*(LL-1)+J)=1.*YY(J)
c         end do

          CALL CCF (NOBS, X, Y, MAXLAG, IPRINT, ISEOPT, IMEAN, XMEAN,
     &         YMEAN, XVAR, YVAR, CCV, CC, SECC)

c         S=0.
          print*,XMEAN, YMEAN
          do I=1,2*MAXLAG+1
c
c         if (CC(I).GE.S) then
c                   S=CC(I)
c                   K=I
c         endif
c         if (kk.eq.1) then
          write(7,*)(I-1)*0.1*PI,CC(I)
c         endif
          end do
c         write(7,*)'delta_T',K*TT(2)

          sum=0
          do I=1,1024
          sum=sum+Y(I)
          enddo
          averageY=sum/1024.

          smaxX=0.
          smaxY=0.

          do I=1, 1024
          if (abs (X(I)).GT.smaxX) then
          smaxX=abs(X(I))
          endif
          if (abs  (Y(I)-averageY).GT.smaxY) then
          smaxY=abs(Y(I)-averageY)
          endif
          end do
          write (10,*)smaxX,smaxY
c         end do
          end


Make sure your input files are in ../Input/*.* directory!
!=========================================================

           open(unit=3,file='../INPUT/TRDPR/DATA/
```

```
     +A_10.txt',status='old')
           open(unit=5,file='../INPUT/TRDPR/DATA/
     +B_10.txt',status='old')
           open(unit=4,file='../INPUT/param.txt', status='unknown')

           i=1
1          read(3,*,end=10) t,t
           i=i+1
           goto 1
10         N1=i
           j=1
2          read(5,*,end=20) t,t
           j=j+1
           goto 2
20         N2=j
           if (N1.lt.N2) then
           N=N1
           else
           N=N2
           endif
           Print*,'N=',N
           write(4,5)N-1
5          format('       PARAMETER (N=',I8,')')

           write(*,*)'File "param.txt" has been successfully created'
           close(3)
           close(4)
           close(5)
           end
```